Table of contents:

Table of tables:

Table of figures:

CHAPTER 1: INTRODUCTION

1.1 Introduction

In recent times all big utilities have been confronted by major power issues. These issues range from penalties for power quality to interference with sensitive equipment supplied from the same grid. Power penalties are incurred when the delivered waveform from the supplier, ESKOM, is distorted. The source of this distortion is commonly referred to as harmonics and harmonics are formed by non linear loads. The term non linear refers to a load that is ***not*** considered as having a sinusoidal waveform that only consists of one frequency. In South Africa the fundamental frequency is measured at 50 Hz. The area where most of these harmonic related problems occur is when AC is converted to DC and vice versa.

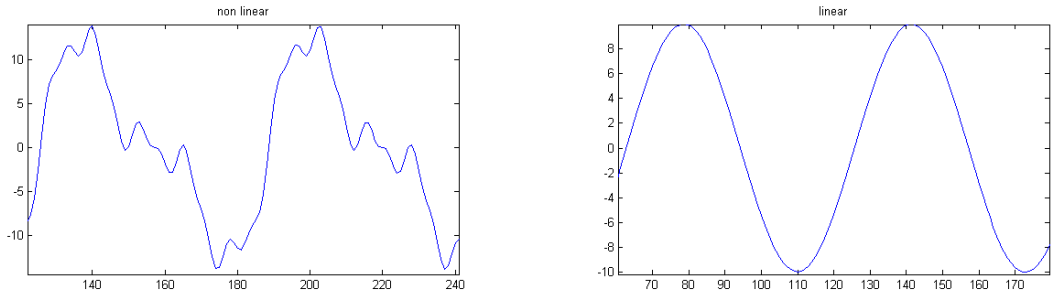

Figure 1.1 - An example of a waveform caused by a non linear load (left) and a waveform caused by a linear load (right), the x-axis represents time in seconds and the y-axis represents amplitude in Volts and the data was generated manually

The question might be raised why these penalties have become such a big issue in recent years and the simple answer is that utilities overload supplies and modern electronic control circuitry has inherent harmonics that are formed during operation. Some of these sources are controlled and un-controlled rectifiers and transformers operating in saturation.

There are basically two types of loads of interest for harmonics:

- Linear loads can be analysed using Ohm's Law

$$V = I \times R \qquad (1.1)$$

- Non-linear loads that does not consist of a single sinusoidal frequency

The DC sub station currently used by Transnet is built up of various sub systems and can be shown in **figure 1.2**:

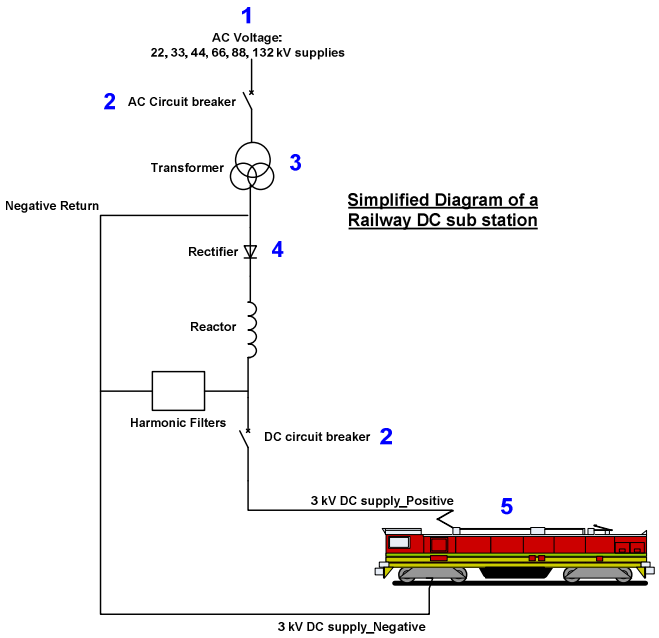

Figure 1.2 – The component break-up of the DC sub-station

The DC sub-station consists of various harmonic sources as numbered in **figure 1.2**:

1. In many cases the assumption is made that the three phase supply to the utility is balanced [2]. This means that the three phases have been shifted 120 ° from each other and that the amplitudes of the phases are the same. The 120 ° shift ensures that the three phases share a full rotation of 360 ° equally. Above mentioned is very seldom true and the un-balance in the loads can be caused by various things such as only one phase being loaded on the supply grid.

2. Circuit breakers are known to generate high frequency harmonics (MHz to GHz range) due to the arcing between contacts when opening or closing occurs. Currently SF6 filled circuit breakers are installed.

3. When the transformer is operated outside its voltage and VA range, thus in saturation, it is responsible for “distortion” of the waveform due to the flux linkage of the transformer not being linear. Transformer topologies are used in practice to eliminate certain harmonics from being generated. The current configurations employed by Transnet are the star/delta and the extended-delta topologies on secondary windings.

4. The rectifier, due to its inherent operation, causes harmonics to be generated. The order harmonics are dependant on the amount of diodes used and the configuration it is used in.

5. Transnet uses new train fleets that have active inverter/converter combinations but the DC sub stations were not designed to compensate for the generated frequency bands. The frequency bands are often encountered at the “chopping” frequency of the inverter/converter. In many cases the harmonics generated are in the audio range. The older generation locomotives used DC machines where the speed of the locomotive was controlled by controlling the amplitude of the supplied waveform using resistor banks.

In the case of Transnet, the generated harmonics cause various problems apart from the penalties incurred for a distorted waveform. Certain harmonics generated in specific frequency bands cause track side equipment to malfunction and even fail. In the case of DC locomotives these harmonics cause the motor-sets to overheat and this decreases the life span of the equipment. The monitoring of these harmonics and the influence it has on the equipment it supplies have become increasingly important.

Transnet currently employs passive AC to DC rectification. The sub-stations are equipped with 12 pulse rectifiers with passive filters for the generated rectifier harmonics. The filters are used to filter the 12^{th}, 24^{th}, 36^{th} etc. harmonics [39]. If the sub-station receives a symmetric three phase supply from ESKOM, the diode rectifier will produce harmonics with multiples of ***12xn*** on the secondary side of the ESKOM/Transnet step-down transformer, where ***n*** is the fundamental frequency and the ***12*** originates from the 12 pulse rectification. Another way of rectification is by using active rectifiers to convert AC to DC [12]. Active rectification has not been implemented on the main DC supply bus at Transnet.

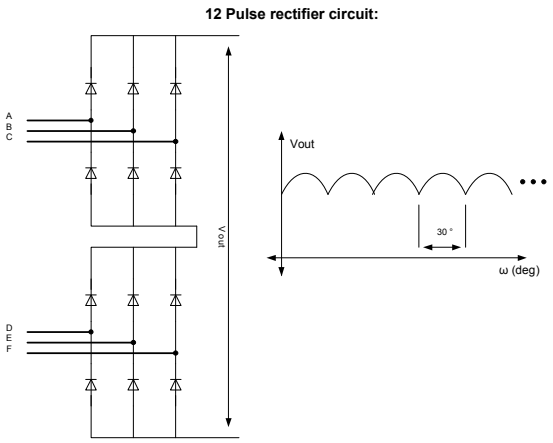

Figure 1.3 – The representation of the 12 pulse diode rectifier, there are 2 6 pulse rectifiers in series

From a power quality point of view, the filters that filter the rectifier harmonics are very important. The filters used for the purpose of attenuating the harmonics of interest, 12^{th} and 24^{th}, is made up of inductors and capacitors. The passive filter components realise a band–reject topology for the harmonics. The reason for filtering out only the 12^{th} and 24^{th} harmonics is that they are in the operating frequency band of sensitive trackside equipment and due to their amplitudes they can cause heating problems in transformers and locomotive motors. The proper operation of the filters will ensure less interference with trackside equipment and the more effective operation of the rolling fleet. From the maintenance point of view the passive filters used in sub stations has never been monitored from outside the sub station. Monitoring the passive harmonic filters in terms of frequency cut-off, efficiency and the availability in the frequency domain without disrupting the installation has not been done by Transnet.

The reasons for the need to monitor the passive filters are the following:

- The aging passive components, especially capacitors, have deviated from the values it originally started with. Capacitor values deviated due to aging of dielectric materials between the capacitor plates. Corrosion and moisture also influence the values of various components, due to the breakdown of dielectric strength of the insulation of the components.

- Due to the passive components´ aging, the cut-off band of the passive filters shift. The deviated capacitor values cause new cut-off frequencies. The shifted cut-off frequency causes the filter to fail in suppressing the harmonics effectively.

- Another problem Transnet currently experiences is that the filters installed to suppress the problem harmonics are vandalised and stolen.

From an interference and preventative maintenance perspective it is thus critical that the condition of the harmonic filters are monitored to ensure a clean energy supply to trackside equipment as well as locomotives.

1.2 Problem Statement

The condition monitoring of the harmonic filters in sub-stations have become increasingly important due to increasing amounts of interference with trackside equipment and locomotives.

In practise, when the passive filters are inspected, the sub-station must be entered and occupation must be taken and the sub station must be switched off. The components are then measured independently and compared to the original component value. The tolerance of the component is calculated and it determines whether the component is still acceptable. The disadvantage of this method is that the measurement method is time consuming and the technician must take occupation of the sub station to enter it. This implies the station to be switched off and that might influence train operation.

A better method of the capture of detailed data and methods for quick and easy analysis have to be researched and developed.

1.3 Aim and Objectives of the study

The aims and objectives of the study are summarised in the following figure:

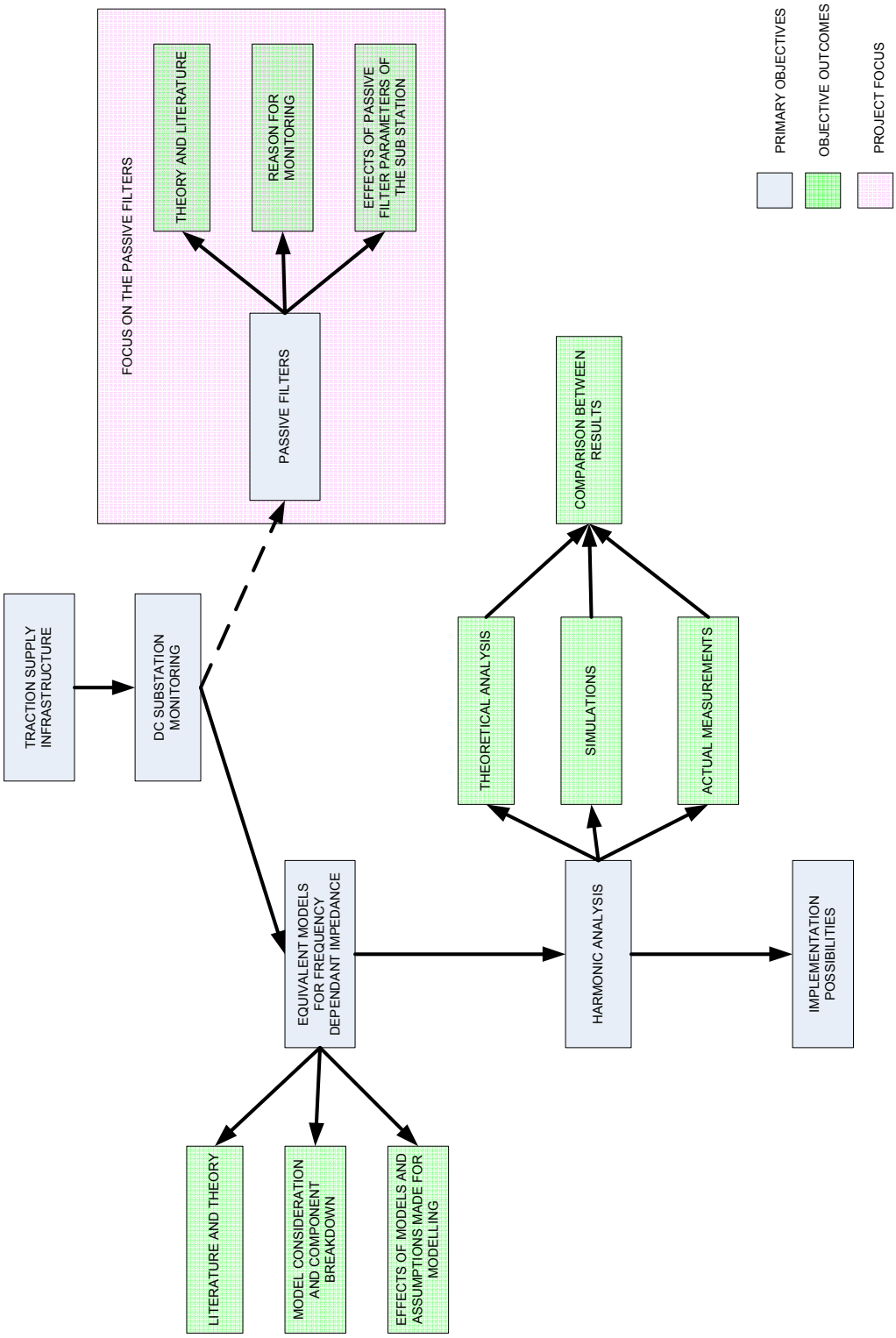

Figure 1.4 – The representation of the aim and objectives of the study

From **Figure 1.4** the aim and the objectives of the project can be broken into ***primary objectives***, ***objective outcomes*** and the ***project focus***.

1.3.1 Primary objectives and objective outcomes

The primary objective and the objective outcomes from Figure **1.4** for the project can expressed as the following:

1. Modelling of the sub station to obtain generated harmonics due to operating circumstances.
2. Harmonic analysis of the sub station under load and without a load
3. Possible implementation strategy for the condition monitoring of passive filters

Modelling of the sub station to obtain generated harmonics

The aim of the modelling of the substation is to get an understanding of the influence that passive filter components have on the voltage harmonic amplitudes of the sub station under load and no-load conditions. The modelling of periodic sub station harmonics will serve as a reference for the measured data. Looking for appropriate modelling strategies for the DC supply grid entails doing detailed research and potential development of models specific to the problem at hand.

To successfully analyse the efficiency of the passive harmonic filters, a model for the DC supply grid must be obtained and simulated. The objective with the literature and theory survey of the modelling of the DC supply grid will aid in simplifying the model with regard to simulation speed and mathematical complexity while still being effective.

Harmonic analysis of the sub-station under load and without a load

The harmonic analysis of the DC supply grid implemented by Transnet spans over three disciplines, namely:

1. Theoretical analysis (model development)
2. Simulations
3. Actual measurements

The aim of using all three above mentioned disciplines is to evaluate and re-evaluate and finally to confirm whether the proposed harmonic measurement techniques would work or not. The aim of confirming the measurement techniques is to propose a proven method for doing condition monitoring of passive harmonic filters in sub stations and improving on old measurement techniques.

1.3.2 Project focus

The main focus of the project is the monitoring of the harmonic filters in the sub-station. Referring to Figure 4, the region of interest for the focus of the project is the pink region. The following three parameters will for the basis of the project focus:

1. Theory and literature study
2. Reason for monitoring the condition of the filters
3. The effects of the passive filter operation on the sub-station and the Transnet DC supply grid.

Theory and literature study

To better understand the operation of passive filters, a detailed analysis of the current topologies used by Transnet must be done. The aim of the literature and theory is to focus on the ageing mechanisms involved in passive filter components, especially oil/paper capacitors.
Modelling and graphing of the filters will give a better understanding of what is to be expected when the project reaches the field measurement phase.

Reason for monitoring

The aim of obtaining and assessing the reasons for monitoring is that the project can possibly address some of the mentioned or known issues surrounding the monitoring of the passive filters in sub stations. The main aim of this section is the development of easier and non-invasive measurement techniques for the DC sub stations, with potential implementation of such techniques.

The effects of the passive filter operation on the DC supply grid

The influence of the passive filter operation on the DC supply grid will play a critical role in establishing the condition and efficiency of the passive filter. The types of loads the DC sub station supplies varies from amplitude controlled DC motors to modern induction motors with variable speed drives implemented using IGBT's. The aim is to simulate and to measure as many as possible operating scenarios that would serve as a reference library for the condition monitoring of passive filters.

1.4 Research Design and Methodology

The aim of the document is to establish if condition monitoring of passive wave filters for the 12^{th} and 24^{th} harmonics are possible in DC sub stations employing 12 pulse passive rectifiers. The research approach taken was to identify the main harmonic generating components. After the identification, the components are isolated and the research focuses on the inherent properties of the components responsible for the generation of harmonics in the range of the 12^{th} and 24^{th} harmonics. The research of the generation of harmonics also focuses on the influence of passive components on each other.

The research portion of the document looks at what other railways around the world have done as well as surveys done by other people to identify the passive DC sub station components responsible for the generation of the harmonics of interest. Apart from the non-linear characteristics of the components the ageing of components shall also be investigated.

The DC sub station will then be modelled; simulated and actual measurements will be taken. The conducted research will then serve as the basis to make assumptions to simplify the models and simulation without loosing relevant information. The aim off simulating and modelling the DC sub station is to verify the assumptions made and to verify the obtained results. The simulation of the sub station will be done using MATLAB SIMULINK software. The modelling of the DC sub station will be a paper exercise and the graphing of the data will be done in MATLAB.

The simulation will be used to gather data that can serve as the reference for actual measured conditions, because the actual sub station cannot be modified to measure fault conditions. The actual measurement of the sub station involves measuring the DC bus voltage (output of the sub station) with a parallel voltage divider. A National Instruments LABVIEW program will be written to capture and save the data on a computer. The actual measurement will thus serve the purpose of calibrating the simulation results, and then the simulation results can be used as the "actual reference".

Once all the results are combined the aim is to obtain thresholds for identifying fault conditions where the harmonic filters are:

- Out off service
- Within specification
- Working properly

Between the thresholds, the simulated scenarios are summarised which might give a good indication of faulty equipment that is generating harmonics at 600 and 1200 Hz.

The thresholds must be calibrated/obtained from as mush as possible data based on realistic and actual operating conditions. Obtaining data for most of the operating conditions will be restricted to simulations due to the safety and operation implications the conditions might have on actual DC sub stations.

1.5 Chapter Outline

The document consists of the following chapters:

Chapter 1 - The chapter serves as the introduction to the problem, the environment the problem occurs in and the effects the problems have on the system as a whole. The chapter is also used to quantify the problem and the proposed methodology to solve the problem.

Chapter 2 - The chapter serves as the literature study. The chapter's aim is to investigate the work that has been done in the field and to quantify and understand the problem at hand. The investigation includes theoretical work done, actual measurements and various modelling approaches to obtain results in various disciplines. These disciplines range from passive rectification of AC to DC, harmonic mitigation in passive complex networks and the ageing mechanisms of passive components.

Chapter3 - The Chapter aims to model a DC sub station based on various quantified assumptions. The aim of the model is to generate a simplified formula to easily obtain results pertaining to the problem at hand in terms of steady state operation of DC substations. The aim of the model is also to verify assumptions made and simulation results. The modelling approach investigates the differences between time and frequency domain modelling and reasons for choosing either. The model is an adoption and completion in terms of this problem based on previous work done by other researchers.

Chapter 4 - This chapter summarises the simulation of the DC sub station based on quantified assumptions in an attempt to simplify the simulation without losing relevant information. The aim of the chapter is to simulate actual operating conditions in order to obtain a good reference for actual measurements. The results obtained in the chapter will form the basis of the condition monitoring criteria used to evaluate the condition of sub station passive harmonic filters.

Chapter 5 - The actual measurements on DC sub stations is summarised in this chapter. The aim of this chapter is to obtain actual data that will serve to calibrate simulated data in order to obtain realistic simulation data. The actual data thus validates the assumptions made in Chapter 4.

Chapter 6 - The concluding chapter summarises the findings made during the investigation, the validity of the solution and future implementation of the solution as well and further work that can be done in the field of DC sub station condition monitoring.

1.6 Conclusion

The condition monitoring of the passive 12^{th} and 24^{th} harmonic filters in the DC sub station employing 12 pulse passive rectification plays the vital role of suppressing the harmonics that cause ageing of components.

The railway service of South Africa (Transnet) is confronted by the introduction of variable speed drives and complex loads the sub stations were never designed for. In recent years the suppression of harmonics has become increasingly important due to penalties incurred from the energy supplier.

The condition monitoring of harmonic filters can thus be used to control harmonic energy. Due to the fact that these filters are passive they have to be monitored to ensure efficiency. The efficiency of the filter is dependant on the filter components being within specification to ensure accurate attenuation of generated harmonics. The investigation of the document aims to address the condition monitoring of the passive filter components for various operating conditions to establish whether these components are still operating in an efficient manner.

In the short term the proper functioning of the harmonic filters will reduce power factor quality penalties and in the long term the life expectancy of systems supplied by the DC grid will be prolonged.

CHAPTER 2: LITERATURE STUDY

2.1 Introduction

The approach taken for the literature study looks as follows:

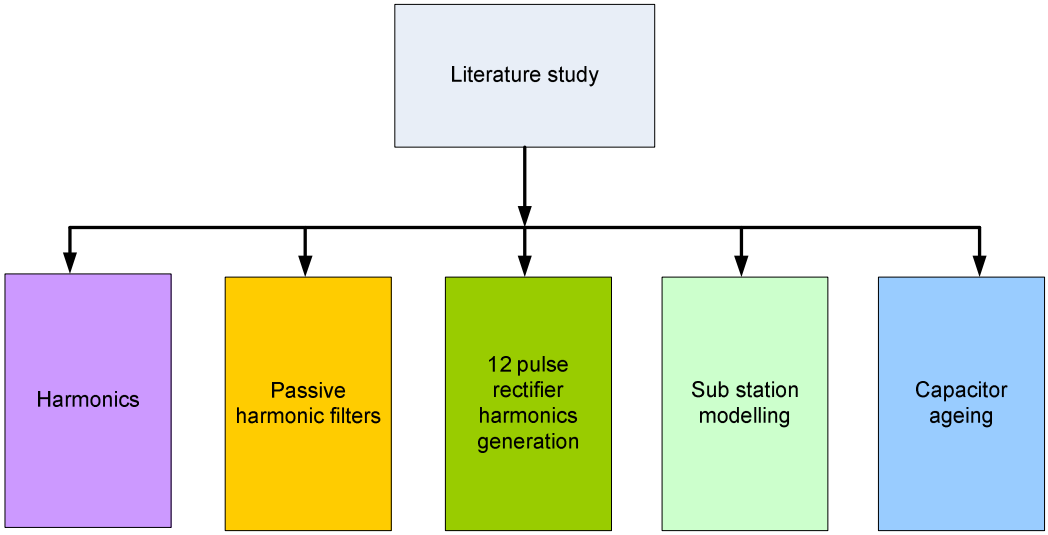

Figure 2.1.1 – The approach taken for the literature study

2.2 Harmonics

2.2.1 Introduction

Power utilities strive to limit voltage harmonics found on the grid by limiting the current harmonics generated by the equipment supplied by the utilities [1].Harmonics does not necessarily mean that equipment will not function: it means that equipment sensitive to interference might not function properly [3]. Harmonics in general are not like transient events such as lightning that only lasts a few seconds. Harmonics is a steady state periodic phenomenon that produces continuous distortion of the waveform [8].

Voltage and current harmonics are produced by nonlinear loads that increase power losses, thus having a negative impact on the power distribution and the systems operating on the grid [5], [7]. Harmonics in power systems are considered as being current and voltage waveforms that consist of a fundamental frequency and multiples of the fundamental frequency [4]. For a 50Hz fundamental frequency the harmonics generated are multiples of the 50 Hz [7], [8].

Harmonics are generated when non linear loads generate non-sinusoidal currents. These harmonic currents then generate harmonics voltages due to frequency specific impedances [4], [8]. The types and severity of harmonics encountered on the grid is dependant on the utility supply configuration, other loads being supplied from the same grid and background harmonics from the supply grid. The energy supplier is responsible for suppressing the background harmonics introduced to the loads from other utilities on the same grid [1].

With an increase of supply side induction, the generated voltage harmonics increases with a linear fashion [1]. Distortion of sinusoidal voltage and current waveforms caused by harmonics is one of the biggest concerns of the supplied power quality of the energy supplier [2]. Standards for the control of harmonics have been established [2].

In order to analyse distorted waveform a number of mathematical methods can be used, of which the most popular method is the Fourier Transformation. The Fourier transformation is used to analyse periodic waveforms, where the sources of harmonics does not change over time [3], [8]. To ensure that enough data is sampled, the harmonic frequency band must be half the sampling frequency. This sampling criterion is referred to as the Nyquist sampling criteria [3].

The modelling of harmonics consists of the periodic steady state distortion of voltage and current waveforms. One of the methods of analysing harmonics is by doing a Fourier analysis on the distorted waveform. The Fourier representation for a periodic function ***f (t)*** with a period of ***T*** seconds and a fundamental frequency of ***f=1/T*** can be written as:

$$f(t) = C_0 + \sum_{n=1}^{\infty} C_n \cos(n\omega t + \theta_n)$$

where C_0 is the DC value

where C_n is the peak value of the n^{th} harmonic

where θ_n is the phase angle of the harmonic component

Devices that produce distorted waveforms exhibit non-linear characteristics between the current and voltage waveforms [2].There are four types of waveform distortion [2]:

1. The Fourier analysis can be done of a periodic waveform where the fundamental frequency of the waveform is the same as the fundamental frequency of the supplied grid waveform, for example 50 Hz

2. Distorted waveform exists where the fundamental frequency of the distorted waveform is a sub-multiple of the supplied grid waveform. There are cases where the harmonics generated are lower in frequency than the fundamental frequency. These harmonics are referred to as sub-harmonics.

3. Some components in the Fourier series can not be expressed as multiples of the fundamental frequency. These harmonics are referred to as non-integer harmonics.

4. Fourier series is approximated when a-periodic distorted waveforms are analysed.

In most cases number **1** from above is encountered. The advantage is that the individual harmonic components can be isolated and compared using Ohm's law. The harmonics of interest can be isolated from the frequency spectrum [2]. In certain cases where modulated or pulsed loads exist, harmonics of type 2 is generated [2]. Pulse width modulated loads can lead to harmonics of the third kind [2]. The harmonics of the fourth kind can be generated by the arc furnaces and the inrush current of transformers [2].

Harmonics originate from: [2]

1. Devices that employ switching techniques like inverters and active motor drives.

2. Devices with non-linear current and voltage relationships like saturated transformers and saturated motors

A clean waveform is one where the waveform comprises of only one harmonic, the fundamental frequency [3]. When looking at harmonics, it is possible to get inter-harmonics, where the harmonic source is not part of the fundamental frequency and multiples of it, for example:

- A 50 Hz and 120 Hz combined waveform exist where the fundamental frequency is 50 Hz and the multiples are 100, 150, 200 Hz etc. but the energy content of the other harmonic is at 120 Hz. It is then possible for the harmonics of 100 Hz and 150 Hz, when measured, to wrongfully include the energy content of the 120 Hz harmonic [3].

2.2.2 Quantifying harmonics

Rectifiers and other non linear elements in a DC sub station cause the distortion of system currents, harmonics, inter harmonics, the consumption of reactive power, the unbalance of supply voltage and flicker [23], [24]. The need arose in industry to quantify the efficiency of current consumption from the grid by the load. Power Factor is referred to as the measure for consumption efficiency [5]. Power Factor has traditionally been measured as the cosine of the phase difference between the voltage and current waveforms [8]. Power Factor can be expressed as the ratio between average power consumption and apparent power consumption [5]. [8].

$$pf_{true} = \frac{P_{average}}{S} = \frac{P_{average}}{I_{rms}.V_{rms}}$$

When looking at the project the assumption is made that nonlinear loads are present that will cause a distortion in the supply waveform. When looking at the generation of harmonics for the project, the focus is on the passive (uncontrolled) rectifier. When steady state harmonics are present the voltage and current harmonics can be presented by a Fourier series [5].

$$v(t) = \sum_{k=1}^{\infty} V_k \sin(k\omega_0 t + \delta_k)$$

$$i(t) = \sum_{k=1}^{\infty} I_k \sin(k\omega_0 t + \theta_k)$$

k is the harmonic number

ω_0 is the fundamental frequency in radians

δ is the phase angle of the specific voltage harmonic

θ is the phase angle of the specific current harmonic

The **root mean square (RMS)** values of the specific harmonics can then be calculated [5].

$$V_{rms} = \sqrt{\sum_{k=1}^{\infty} \frac{V_k^2}{2}} = \sqrt{\sum_{k=1}^{\infty} V_{krms}^2}$$

$$I_{rms} = \sqrt{\sum_{k=1}^{\infty} \frac{I_k^2}{2}} = \sqrt{\sum_{k=1}^{\infty} I_{krms}^2}$$

k is the harmonic number

Looking at the formulae, when addressing a single harmonic at a time, the sinusoidal RMS characteristics apply because a single harmonic is nothing more than a sinusoidal waveform.

The average power can then be calculated.

$$P_{average} = \sum_{k=1}^{\infty} V_{krms} I_{krms} . \cos(\delta_k - \theta_k) = P_{1average} + P_{2average} + P_{3average} + ...$$

k is the harmonic number

δ is the phase angle of the specific voltage harmonic

θ is the phase angle of the specific current harmonic

Other means of quantifying the amount of distortion the original waveform has undergone is to measure the **Total Harmonic Distortion** or **THD** [5].

$$THD_{voltage} = \frac{\sqrt{\sum_{k=2}^{\infty} V_k^2}}{V_1} .100\%$$

k is the specific harmonic number

The THD measurement is thus expressed as a percentage of distortion the waveform has undergone. The lower the THD the better the system is in terms of distortion.

2.2.3 Harmonics in balanced and unbalanced three phase systems

For balanced systems the harmonics have specific phase relationships with regard to the three phases and the system impedances for the specific harmonics must be included in the modelling of a system. Systems are very sensitive to small unbalances in the supply phases, especially the phase angles of the current and voltage waveforms [2], [8].

When positive and negative half cycles of the power voltage and current waveforms have symmetry about the x-axis only odd harmonics are generated [8]. There is a traditional belief that balanced power systems can not generate zero-sequence or negative harmonics, but this is not always the case when harmonics are generated or present in the system [8]. Three phase power electronic converters can generate non-characteristic harmonics when supplied by un-balanced three phase supplies [2].

When looking at harmonics in balanced three phase systems, harmonics have various effects on the operation of equipment based on the specific harmonic:

Harmonic number	**fundamental**	**2nd**	**3rd**	**4th**	**5th**	**6th**
Sequence	**+**	**-**	**0**	**+**	**-**	**0**

The sequence of the harmonic describes the effect the harmonic energy has on the system. For example, when a motor is supplied by the 4^{th} harmonic it wants to turn in the direction of operation, when the 2^{nd} harmonic energy is supplied to a motor it wants to turn the motor in the opposite direction of operation [3].

The sequence of the harmonics can be equated by means of the following [3]:

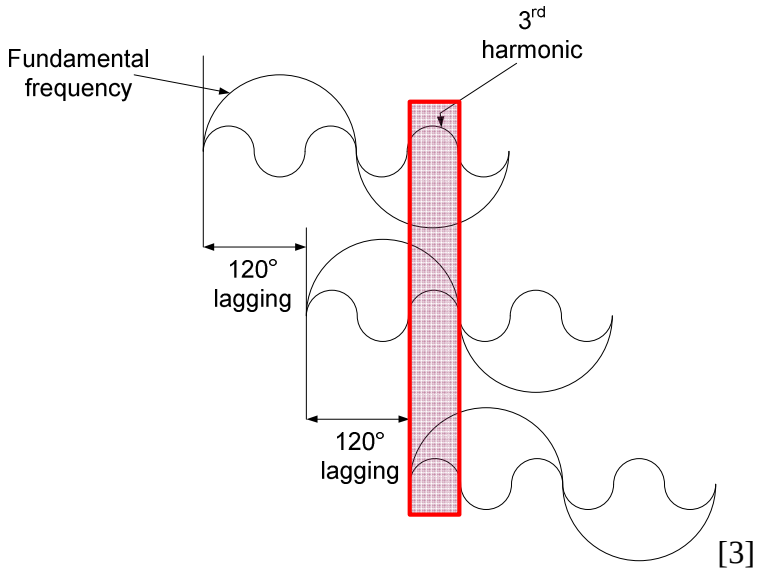

[3]

Figure 2.2.3.1 – The illustration of zero sequence harmonics [3]

The region in red shows that, in terms of the fundamental frequency, the result of the three waveforms within the red region is equal to zero, thus a zero sequence. But looking at the 3rd harmonic, if the three harmonic energies are added it superposes and becomes three times more than the original energy. The energy content in the sequence causes heating of equipment such as motors and transformers [3]. Triplen (zero sequence) harmonics are responsible for neutral conductor overheating [8]. The unbalance of three phase supply to the system has zero sequence harmonics flowing in the power networks. For the zero sequence harmonics there must be a path to flow in the network in the form of ground wires and shunt capacitors [7].

2.2.4 Harmonic modelling and simulation

The simulation of harmonics can identify potential resonant conditions [2]. The analysis of harmonics can be divided into three steps [2]:

1. The various harmonic generating sources must be identified and relevant modelling of the sources must be done

2. After the modelling for the sources are complete a model for the complete system must be obtained to simulate the system as a whole

3. Simulations for various scenarios must then be run

Harmonic models

The most common model for harmonic analysis is by modelling the harmonic sources as current sources, specified by its magnitude and phase spectrum [2], [7]. Data for this type of modelling can be obtained by actual measurements or theoretical models. When a system contains a dominant harmonic source the phase spectrum is not important.

For unbalanced or severely distorted voltage waveforms the modelling of the harmonic sources becomes complex. These models are dependant on the operational modes of devices, operating states might have to be broken up in smaller parts and added together and finally time domain analysis of the data might be considered [2]. Harmonics can have time varying characteristics, to avoid missing these varying harmonics it must be included to ensure a more realistic interpretation of the distorted waveform [2].

Time domain analysis of the system of interest can be done. The disadvantage is that the simulation has to run until steady state has been reached before analysis. There are problems associated with this method, identifying when the system has reached steady state and in some cases techniques have to be used to obtain steady state in a reasonable time. This applies to lightly damped systems that take very long to reach steady state [2].

Frequency domain analysis is the other method available to analyse the system [7]. The frequency domain waveforms generated in the DC sub-station used by Transnet can be broken into various sinusoidal waveforms that are added together.

In 1882 Joseph Fourier, a French physicist and mathematician published a document called “analytic theory of heat” [41]. In this document Fourier described how a waveform can be broken up into its fundamental frequency and a combination of multiples of the fundamental frequency. The fundamental frequency and its’ multiples became known as harmonics. Doing the Fourier analysis of a time domain waveforms gives a “component” like representation of the waveform in the frequency domain. A seemingly distorted waveform can thus be broken up in a fundamental sinusoid and multiples of that fundamental, where the fundamental will have the largest amplitude. The amplitude will decrease as the multiples of the fundamental frequency increases.

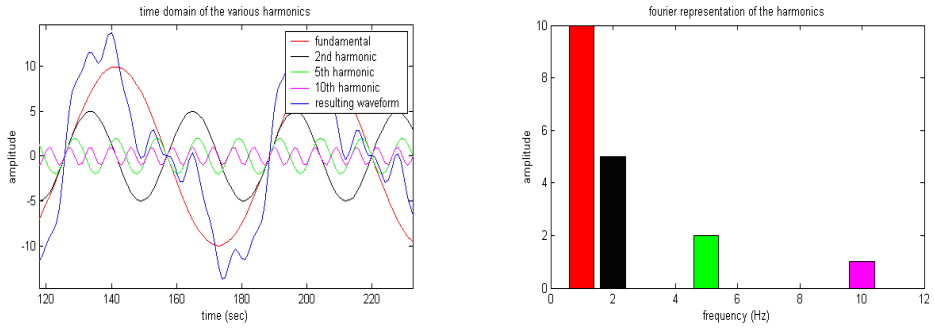

Figure 2.2.4.1 - the time domain (left) in comparison to the frequency domain analysis (right) of the resulting waveform, the waveform data was arbitrarily generated with a 50 Hz fundamental frequency

From figure 2.2.4.1 it is evident that a Fourier frequency domain analysis will give more information regarding the harmonic components of a waveform than its equivalent time domain representation. For frequency domain analysis the waveforms must be linear and time invariant. If the system does not comply, methods can be used to still decompose the waveforms. Piecewise linear modelling can be done. The process is then repeated until the waveform is decomposed. The Fourier method for frequency domain analysis can thus be used for non-linear time varying systems by isolating parts of the waveform and adding the results to analyse the entire waveform [7]. When analysing harmonics, each harmonic can be represented by a two port admittance model [7].

DQ modelling

The DQ modelling approach is a method developed to put the instantaneous values of, in our case, three phase transformers onto an active and reactive axis. The main aim thus is to have space orientated or shifted axis, like in the case of three phase transformers on one set of axis (x and y) in an attempt to compare them [10], [11].

The main advantage of DQ modelling is that the model helps to eliminate switching action, like the zero crossings of the three phase transformer AC supply, in an attempt to establish time invariant models [12]. The ideal would be to calculate the DC voltages and currents generated by rectifier circuits without having the influence of switching phenomena such as commutation and conduction [13].

2.2.5 Nonlinear Voltage and Current sources

The best example of nonlinear current and voltage relationships are transformers, due to their nonlinear magnetization characteristics [2]. These devices, due to their waveforms being affected by voltage peaks, can not be modelled just as current sources. The modelling of these devices must include both the current and voltage characteristics. These devices include power electronic converters and rotating machines, the distortion characteristic of motors are greatly affected by over-voltage and saturation operation of the device [2].

2.2.6 Network and load modelling

In most cases, the identifying and modelling of harmonic sources in a system model has to be carefully considered. The trade-off between too many components against too few components usually affects the accuracy of the models with regard to actual measurements [2]. In most cases the assumption can be made that the transformer impedance is dominant in a model and for distribution cables shorter than 500 feet the capacitance of the cable can be neglected [2]. The modelling of the entire feeder line must be done in regions where the sub-station under test is not supplied with an unbalanced supply [2].

In many cases the modelling of harmonic sources on the same grid can be modelled as frequency dependant impedances to simplify calculations, due to the current and voltage harmonics having linear relationships when looking at only one harmonic at a time [2].

For balanced three phase systems the models can be simplified by converting the three phase systems into PI- or T-circuits. These models are dependant on the length of line present in the system [2]. A few things must be kept in mind when looking at modelling systems with long transmission lines [2]:

1. Cable capacitance can usually be neglected except where long cable stretches are available.

2. Rule of thumb estimations for including cable parameters in the model is when the length of cable available in the system exceeds **150/n** miles for overhead cables and **90/n** miles for underground cables. Where **n** is the harmonic number [2].
   For example, the system has 10 miles of overhead cables and the 12 harmonic is looked at, thus the ratio 150/12 gives us 12.5 miles is the maximum length before line parameters should be included in the modelling. The system only has 10 miles of overhead lines, thus the parameters do not need to be included.

3. For high voltage modelling, higher than the Transnet supply voltage, the skin effect of the conductors must be taken into account due to the fact that the skin resistance plays an important role in the damping mechanism of the line [2].

Many models do not include the effect of the change of resistance with regard to frequency. Due to the skin effect, resistance goes up as frequency increases. If the same harmonic current, 1A for example, flows, the losses in the higher harmonics will be more compared to the fundamental loss due to the increased skin resistance [5]. The dielectric stress in cables is increased due to harmonic voltages and the life span of the cables decreased [7], [29].

Apart from the pollution introduced by harmonics and losses in terms of heat, harmonics also have the following disadvantages [29]:

Motors	Harmonics causes a decrease in efficiency and torque of motors
Capacitors	Harmonics causes a decrease of efficiency and the accelerated failure of dielectric materials
Circuit Breakers	Harmonics causes false tripping of breakers
Transformers	Harmonics causes noise levels to increase due to saturation and a reduction in efficiency
Meters	Harmonics causes measurement errors that may lead to excessive billing

Transformers

As early as 1916 the 3rd harmonic was identified as being a point of concern. The saturated iron in transformers and machines generates the 3rd harmonic, delta winding topologies was proposed in 1916 to prevent the 3rd harmonic from flowing due to the absence of a neutral conductor in delta configurations [8]. The following things must be considered for transformers [2]:

1. The transformer configuration and space orientation of the winding must be kept in mind when modelling the system when looking at phase shifts.

2. Transformers have nonlinear characteristics when modelling the core loss resistance. The dominant parameter for harmonic effects is the nonlinear inductance of the transformer.

3. There are stray capacitances between the windings and the core of the transformer saturates at some stage. The effect of the stray capacitance is only noticeable for frequencies higher than 4 kHz.

When a transformer is supplied by an unbalanced three phase input or the winding parameters per phase such as winding resistance is not equal, the transformer will be a source of harmonics. When a transformer is driven into saturation it also becomes a source of harmonics [3]. The resistance increase posed with the increase of frequency due to the skin effect must be taken into account for transformer design [5]. Harmonics thus manifest themselves as power losses and in turn as generated heat in the transformer due to the skin effect.

Harmonics inherently cause reduced life spans of insulation, reduced power factors and efficiency, increases in operating temperature and a lack of system performance [30]. Transformers are usually produced to make optimal use of their magnetic core materials, thus having a peak magnetic flux density in its steady state [8]. During large disturbances harmonics can considerably increase the harmonics generated [7]. When peaks occur the core materials are subjected to large magnetic flux density, thus saturation of the core materials [7], [31].

The magnetizing current associated with the core saturation of transformers produce only odd harmonics. Transformers can be designed to utilise different topologies to eliminate some of the odd harmonics. Due to inherent properties of the star-delta transformer design the triplen (zero sequence) harmonics can be absorbed by the secondary delta windings due to the absence of a neutral wire on the secondary delta windings [7], [8]. Transformers produce harmonics whether the load coupled to it is nonlinear or not and the harmonics produced are odd. Balanced excitation is the product of symmetric sinusoidal voltage supply to the transformer. When a load consumes or draws direct current from the transformer the excitation becomes unbalanced, then an average flux exists and the transformer excitation current contains even and odd harmonics [7].

Large rotating Loads

For induction motors the resistance normally increases in the form of **n^a** where **n** is the harmonic and **a** is a factor between **0.5-1.5**. Most motors have delta winding topologies, thus the zero sequence harmonics do not have a path to propagate [2].

For a machine to not generate harmonics the magnetic flux in the machine must have a perfect sinusoidal distribution. This means that the machine does not operate in saturation. Harmonics are also generated due to the imperfection of the distribution of the windings in the motor [7].

Harmonics can cause a decrease in the torque of induction machines as well as vibration. Positive sequence harmonics causes the development of shaft torque in the direction of the motor rotation; negative sequence harmonics causes the inverse [7].

Converters

The variable speed drives employed by Transnet for induction motors use converters. Converters are responsible for distortion of the waveform, these current and voltage harmonics can be seen on the DC and AC side. The harmonics generated are dependant on the amount of "switches" or devices used in the topology. The following harmonics are generated: [7], [14], [22], [34]

$np \pm 1$ on the AC side
np on the DC side
n is the harmonic integer
p is the number of devices

Converters can have characteristic and non-characteristic harmonics. Characteristic harmonics occur when the control of the firing of devices/switches is kept constant and the converter is supplied by a balanced three phase supply. Un-characteristic harmonics occurs when the converter is supplied by unbalanced three phase supplies, the control of the converter is active and changes the whole time like motor drives trying to control the speed of the motor [7].

2.2.7 Passive rectifier harmonics

Passive diode rectifier operation has instances where phases are shorted with each other, the process is called commutation. When the phases are shorted it causes large current transients [3]. For a 12 pulse rectifier, the harmonics created is ***12.n*** and multiples of it where ***n*** is the fundamental frequency [3], [33]. Various rectifier topologies generate different harmonics that can be summarised as follows:

type of diode device	**number of diode (pulses)**	**generated AC harmonics**
half wave rectifier	**1**	**2, 3, 4, 5, 6….**
full wave rectifier	**2**	**3, 5, 7, 9, 11…**
three phase full wave	**6**	**5, 7, 11, 13, 17, 19…**
three phase full wave	**12**	**11, 13, 23, 25, 35, 37…..**

Apart from the single pulse half wave rectifier, most of the other loads produce symmetric current harmonics on the AC side of the rectifier.

The harmonics generated can serve the purpose of finding harmonic sources. Harmonics can also indicate faulty diodes in the rectifier if harmonics are generated that are uncharacteristic of the rectifier topology [3].

The operation of passive rectifiers is based on some assumptions, where the AC supply is assumed to be ideal, the main transformer is ideal and the conduction of the diode is assumed not to overlap [35].

2.2.8 Harmonic suppression

Various methods exist to reduce harmonics and their energy content [3]:

1. Passive filters tuned for specific harmonics: these filters are used to clamp specific harmonics, thus periodic harmonics.

2. Active filters: these filters are used to firstly measure harmonics and on the next cycle produce currents to reduce the energy content.

The advantage of passive filters over active filters is the price of the passive components used. The advantage of the active filter is that it can “track” specific harmonic frequencies and adapt accordingly, thus the active filter is more dynamic and efficient [23]. In some cases hybrid filters are employed to save money and to have an active nature for some frequency bands, thus combining the advantages of both filter topologies [23].

Another method of reducing the harmonic energy is to increase the rectifier pulses; the harmonics shift up in order. The amplitude for harmonics can be obtained by taking the fundamental amplitude or DC amplitude in the case of the rectifier and dividing it by the harmonic order [3].

Most power systems have capacitance and inductance components, therefore resonance between the components are likely. When a nonlinear load produces a harmonic at the resonant frequency, resonance of that component will occur [8], [23]. Resonant states have two disadvantages: it causes the waveform to distort even further and nuisance tripping of sensitive electronic devices might occur [8]. Careful consideration must be taken when trying to compensate for harmonics. The inclusion of shunt capacitors might lead to resonance at higher frequencies [7], [8].

For **parallel resonance** the harmonics sources are seen as current sources, the voltage drop across capacitors and inductors are experienced. The result is that the insulation of capacitors and inductors are severely stressed [7], [8]. For parallel resonance the voltage peaks generated are at the nonlinear load responsible for the harmonics.

Series resonance occurs when the majority of inductance and capacitance components are in series with the nonlinear load. For series resonance the voltage peak generated by the nonlinear source is only present at the feed transformer/sub station, but it can potentially be far away [8]. Harmonic voltages cause excessive currents in capacitors, due to the relationship [8]:

$$I = C.\frac{dv}{dt}$$

I is the current

C is the capacitance

$\frac{\mathrm{dv}}{\mathrm{dt}}$ is the voltage harmonic content over a specified time

Most nonlinear loads are inductive and the inclusion of shunt capacitors can worsen harmonic performance due to potential resonances. A good alternative is utilizing active or passive filters to suppress harmonics [5]. In terms of passive filters, the suppressed harmonic energy is absorbed in the form of generated heat. Reactors can be added in power systems to move resonance frequencies away from generated harmonic frequencies [8].

IEEE 519 recommends the maximum allowed voltage and currents relating to the amount of waveform distortion present [2]. The philosophy for IEEE 519 is that [8]:

1. Users of the grid control the current harmonics generated by controlling the nonlinear loads

2. Power system utilities should limit the voltage harmonic limits by controlling the system impedances

3. The power system users plus the suppliers are responsible for keeping harmonic levels in check.

The IEEE 519 is just a recommended guideline for users and not a legal document [8].

2.3 Passive filters

2.3.1 Introduction

Passive filters are used as a cheap and moderately effective way to suppress harmonics generated by passive rectifiers. The reason for suppressing harmonics can be summarised as follows [27]:

- Harmonics are undesirable because they "consume" part of the transformer, cable and electric motor electric capacity, influencing performance and efficiency of the mentioned components. The generated harmonics, in most cases, tend to flow back toward the source of the energy.

The common belief is that passive components such as capacitors and inductors are linear under normal circumstances, but when the supplied voltage is not sinusoidal the driven current is not sinusoidal. The result: when non sinusoidal voltages are applied to complex loads harmonics are going to be generated and have to be compensated for [27]. The purpose of harmonic filters is to absorb currents generated in a circuit in an effort to stop the circulation of the unwanted currents generated by components in a circuit [29].

Passive filters are used for specific frequencies. In the case of Transnet, filters are used for 600 Hz (12^{th} harmonic) and 1200 Hz (24^{th} harmonic), these frequencies are the dominant harmonics created by the passive 12 pulse diode rectifiers. When looking at the harmonic filters Transnet employs, acceptor filters are used. These filters have an inductor and capacitor in series and the result is that the voltage drop across the capacitor is 180° out of phase with the voltage drop across the inductor and the resulting voltage drop across the series L and C is zero. The series L and C circuit thus acts as a "short" or very low impedance path for the tuned frequency current flowing [27], [29]. A critical design characteristic that influences the performance of passive filters are the fact that the filter impedance at the frequency of interest must be lower than the equivalent short circuit impedance presented by the source of the circuit the filter is employed in [27]. Filter characteristics is thus dependant on the ratio of the filter impedance to the total impedance of the source, effectively making the path of least resistance the filter and not the source. The ratio has a fundamental flaw. The flaw is the fact that the impedance of the complex system changes continuously [28].

To improve the quality of the passive components and efficiency, due to losses due to generated heat while absorbing harmonic energy, filters have to be of a very good quality in terms of tolerance, materials used and cross section/ area of component conduction materials. The tolerance of the components plays a critical role in the sharpness of the filter cut-off and the centre frequency of the filter, thus effectively absorbing the filter properly. Passive filter components in the total circuit may result in unwanted resonance [27]. When looking at passive filters, up to 60% of the filter amount can be spent on capacitors [29].

The disadvantage of passive filters is that changes in the power frequency changes the harmonic frequencies accordingly, the passive filter thus being less effective [29]. Traction filters along with the physical traction line (catenary) present frequency specific impedances and the presence of these frequency dependant components might lead to resonance of the system components [19].

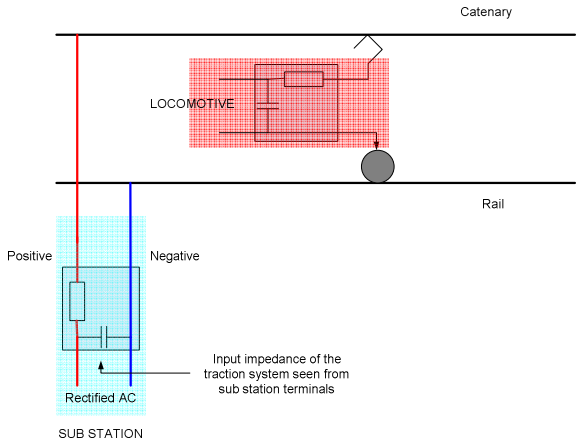

Figure 2.3.1.1 – The illustration of the various components in the traction supply system that might have an influence with resonance [19]

When locomotives decelerate they inject energy back into the traction system and the motors become generators. The process is called regeneration. During regeneration harmonics are injected into the grid, thus locomotive line filters are needed to suppress generated harmonics [19]. In railway traction systems the sub station and locomotive can generate or absorb harmonics depending on the operation of the locomotive [19]. The sub station harmonics filters are only used to protect the sub station AC to DC converter from over voltage due to harmonics [19].

2.3.2 System impedance

During motoring, the locomotive and the sub station is responsible for the generation of harmonics [19]. Passive filters, having combinations of inductance and capacitance, are used to suppress harmonics or whole bands of frequency. The passive filter operates on the principle that the filter must present lower impedance to the harmonic than the rest of the system/load on the DC side [23].

Substation terminals

The sub station will be responsible for the generation of characteristic and non-characteristic DC side harmonics. These harmonics will propagate to the rest of the traction system. The system impedance will comprise of a sub station output filter, a locomotive input filter and the catenary connecting the system. For a given frequency the impedance presented by the system to the source will be zero, during this state over currents will be experienced in the system [19].

2.3.3 Sub station equivalent model and filters

DC sub stations employ two types of filters for the suppression of harmonics: a simple low pass filter may be used or more complex filter tuned specifically to suppress generated characteristic harmonics [19]. DC sub stations have 12 pulse rectifiers. The advantage 12 pulse has over six pulse is that the harmonics generated are of a higher order, thus reduced energy content [19]. The harmonic filter must be able to absorb the energy present in the harmonics it has to suppress.

The AC equivalent model for the sub station can be considered as being a short at 50 Hz. This can be verified by the low inductance of the secondary winding of the transformer, the inductance is generally in the 0.1 mH range [19].

$$X_L = 2.\pi.f.L$$

X_L is the impedance

f is the frequency

L is the iductance

Thus the equivalent impedance for AC is 0.031Ω; this can be considered a short.

Modelling of the traction system is thus dependant on the secondary impedance of the transformer at 50 Hz. The model does not hold when the equivalent line impedance at 50 Hz is the same or smaller. The equivalent line impedance is represented by 63 m of track, thus the model accuracy is lost as soon as the train is closer than 63 m to the sub station [19]. There are two commonly used filters [19]:

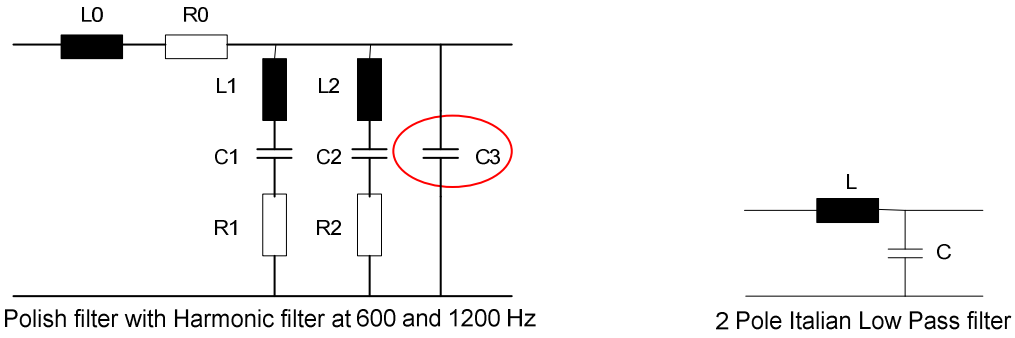

Figure 2.3.3.1 – The types of passive filters commonly used [19]

The filter on the left in figure **2.3.3.1** is used to suppress specific harmonics, the 12th and 24th harmonic generated by the 12 pulse rectifier. The output capacitor C3 (red circled region) is responsible for increasing the trap frequency [19]. The low pass sub station filter is responsible for clearing traction line oscillations [19].

2.4 12 Pulse rectifiers

2.4.1 Introduction

Passive twelve pulse rectifier operation is critical in terms of harmonic generation. These generated harmonics are repetitive, when supplied by balanced three phase supplies. DC sub stations employ transformers with more than one secondary three phase output. In Transnet the transformer secondary is a six phase system. Passive diode rectifiers are well known for the injection of current harmonics into the power grid, these injected current harmonics are responsible for the overloading of shunt capacitors and the interference of the DC bus voltage at points of common coupling [26].
The railway service in Poland also consists of two sets of three phase secondary outputs from a three phase system [25]. The idea with increasing the secondary windings to six phases is because the rectifier converting AC to DC will now consist of more pulses. More phases entail lower ripple and higher harmonics, thus the energy content of the harmonics is reduced.

Various factors are known for influencing diode rectifier operation and the generation of harmonics [25]:

- Transformer construction symmetry
- Supply voltage symmetry
- Harmonic content of the supplied waveforms
- Transformer operation in saturation
- Finally, the characteristics of commutation between the transformer and the rectifier circuit

The final bullet regarding the commutation of the rectifier circuit will form the centre of the discussion. The basis of the modelling of the rectifier is the fact that every switching cycle of the rectifier experiences commutation [25], [32].

2.4.2 Commutation

Commutation is the process where one conducting diode branch is still conducting when the next branch has started conducting [25]. When two diodes are involved in commutation it is referred to as simple commutation. When multiple diodes are involved in commutation, the process is referred to as complex commutation [25].

Commutation is responsible for current decay in the rectifier circuit. Decay takes place when various voltages interact with each other during commutation. The one voltage is the phase voltage from the transformer windings and the other voltage is self-induced due to inductance in the commutation circuit. The self induced voltage is responsible for decreasing the phase voltage across the rectifier and consequently the rectified voltage suffers as well, thus a voltage dip [25].

2.5 DC sub station modelling

2.5.1 Introduction

It is very important to identify power harmonics in the DC traction environment. These harmonics originate from traction controllers and sub station rectifiers. The generated harmonics poses the threat of interfering with sensitive signalling and communication equipment. Over-voltage and over-current is also a possibility at the pantograph of the locomotive due to harmonics [15], [18], [19]. DC traction systems are considered as being large harmonic sources due to the fact that most locomotives are seen as non linear loads. Most of the demand on a DC sub station comes from non linear loads and the AC/DC converter of the sub station is non linear [22].

Railway traction system frequency dependence is dependant on the impedance presented by sub station line filters, locomotive line filters and the traction line [19]. Harmonics with frequency content in the power and audio band have to be suppressed [18]. The introduction of new generation controlled traction loads or motor drives have seen the increase of current harmonics introduced in the grid. The new drives have caused the degradation of power quality and network safety [16].

The DC traction system consists of various passive components, such as filters, inductance and capacitance of motors, overhead lines and transformers. The complex configuration of all these passive components is at risk of having resonant frequency points that are the same as harmonics being generated. The result is over current and over voltage [15]. In terms of rectifier circuitry, the harmonics that are generated are due to the electrical switching properties of the switching devices (diodes) [17].

Passive rectifier topologies consist of 12 diodes making up the AC to DC rectifier. Twelve pulse rectifiers are made up of two six pulse rectifiers being in series or parallel. The advantage of a twelve pulse rectifier over the six pulse rectifier is its ripple rejection, the generated harmonics are less severe, better utilization of the transformer and better voltage regulation [21]. The main difference between 6, 12 and 18 pulse rectifiers are the order harmonics generated and the magnitude of the generated harmonics.

The 18 pulse rectifiers have the smallest voltage ripple (compared to 6 and 12 pulse rectifiers) on the DC voltage due to it having the most pulses, the result is the reduction in the harmonic distortion [9]. The main traction supply transformer can be illustrated as follows [21]:

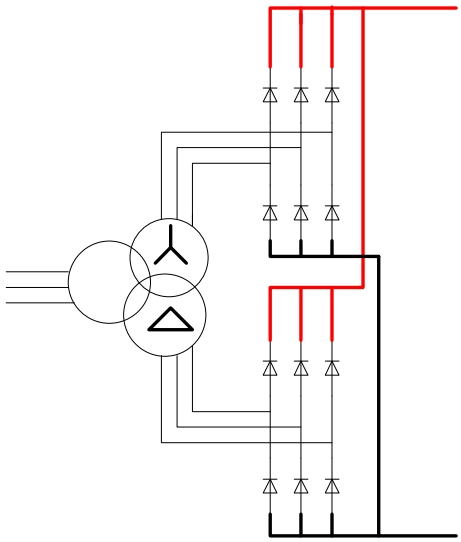

Figure 2.5.1.1 – The main traction supply configuration, two six pulse passive rectifiers are in parallel with each other [21]

The topology as seen from the above (figure 2.5.1.1) shows two six pulse rectifier configurations in parallel. The secondary consists of a ***delta*** and ***wye*** connection where the reactance of the two windings are assumed to be equal, but they seldom are due to construction flaws and the attempt to realise a ratio of √3 between the two windings. Reactance evaluation is usually done by doing short circuit tests on the transformer [21].

DC substations employ filters to suppress harmonics in the DC sub station. Typical filter installations suppress the following harmonics [17]:

For a passive 12 pulse rectifier system	
AC side	**DC side**
11,13 23, 25	12 24

The above table represents the harmonics generated and for every harmonic a filter is employed to suppress the harmonic. In some cases high pass filters are employed in sub stations as well [17].

2.5.2 Modelling

Investigation has been done to model DC traction systems supplied by 12 pulse rectifiers and controlled traction drives using time domain simulations [15]. Simulation of complete power systems are very complex due to interaction of power sources and the frequency dependence of the feeder lines [18]. The frequency dependence of traction lines must be taken into account [15], [19].

The parameters of interest for modelling sub stations is the impedance per frequency presented by the system under test and the influence it has on the system as a whole per frequency [15]. It is very difficult to make detailed measurements of harmonics in the rail environment and the result is that most information regarding DC traction systems for railways are made by simulations [15].

The traction system can be modelled using a two port modelling approach [16].

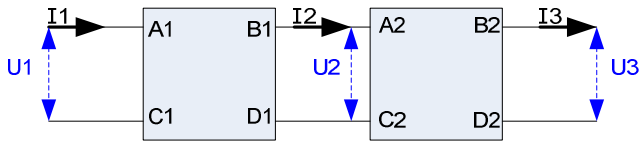

Figure 2.5.2.1 – The two port modelling approach can be used to model whole systems based on the inputs and outputs [16]

Every two port model represents components of the traction system. In the case of the referred literature every **N** locomotives in the traction system is represented by **N+1** two port models [16].

When the AC supply to the sub station is assumed balanced and the devices such as transformers and rectifiers are linear, all the sub station components can be analysed in terms of frequency. These components can be expressed as Norton equivalent (current source) circuits for every frequency. The analysis of the power system then entails doing nodal analysis per frequency of the power system [17].

Track Modelling

Rail lines or better known as tracks have two purposes, the rails are used for conducting traction current and signalling currents. For the modelling both cases of current conduction must be taken into account due to the various propagation frequencies [15]. Signalling systems propagate in the low kHz region and traction current propagates at 50 Hz.

Line modelling

Traction line modelling, consisting of the overhead catenary with rail return, has to take the frequency dependence of the transmission line in consideration [19]. Traction system lines can be modelled as mutually connected parallel conductors, where the conductors can be seen as the following [18]:

- Power cables (catenary)
- Auxiliary cables (feeder cables)
- Earth wires
- Communication wires

The capacitance can be assumed constant with frequency, but the resistance and inductance of the line will change with frequency due to the skin effect in the rails and the ground. The constant capacitance value is set at **11.4 nF / km** [19].

The track can be modelled in terms of an admittance and impedance matrix where that is dependant on the distance from the source, the sub station [15], [18].

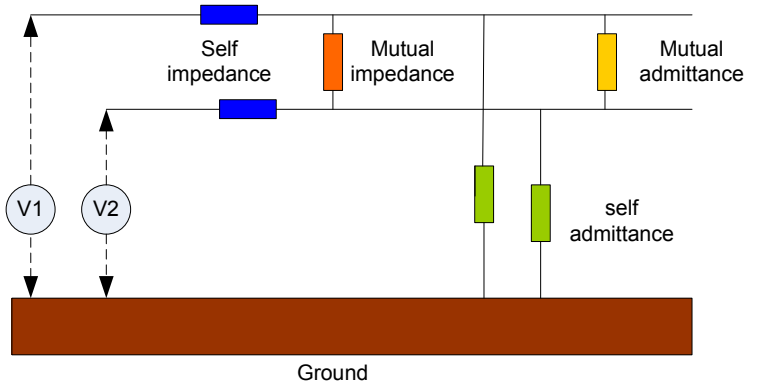

$$\frac{d[V]}{dx} = -[Z].[I]$$

$$\frac{d[I]}{dx} = -[Y].[V]$$

dx is the distance segment over where column vectors V and I is measured (thus per frequency)

Z is the impedance matrix

Y is the admittance matrix

Figure 2.5.2.2 – The components making up the track model used for DC supplied sections of track [15]

The measurements for admittance and impedance are taken relative to ground [15]. For practical measurements of admittance and impedance between the rails and the ground it is very difficult due to the following reasons [15]:

1. The ground conditions differ with depth and the environment, thus the conductivity and permittivity can differ when doing measurements at different locations.

2. The actual rail is made of a ferrous material that may have an influence on the measurements

The modelling approach can be used for time domain analysis by looking at phase variables or as modal variables for frequency domain analysis [18]. For the rail impedance modelling the rail resistance increases and the rail inductance decreases with the increase of the frequency in the track. This is due to the skin effect [15], [18]. Line modelling, like catenary modelling can take the form of a two port/wire model where the one wire is the catenary and the other the return conductor for the sub station. The connection mechanism between the two conductors can be seen as predominantly capacitive [18]. For the modelling of the track feeder line a polynomial can be used to model the resistance [19]:

$$R(f) = C_3.f^3 + C_2.f^2 + C_1.f^1 + C_0 \qquad \Omega/\text{km}$$

$$C_3 = 1.159\times10^{-13}$$

$$C_2 = -7.812\times10^{-9}$$

$$C_1 = 2.245\times10^{-4}$$

$$C_0 = 1.743\times10^{-1}$$

A three part fit for inductance:

$$L(f) = 1.585 \text{ mH/km} \qquad \text{for} \quad f < 16 \text{ Hz}$$

$$L(f) = 1.585 - (4.66\times10^{-7})(f - 16) \text{ mH/km} \qquad \text{for} \quad 200 > f > 16 \text{ Hz}$$

$$L(f) = 1.33\times10^{-3} + 6\times10^{-3}.(2.\pi.f)^{-0.5} \text{ mH/km} \qquad \text{for } f > 200 \text{ Hz}$$

The corresponding traction line model is as follows [19]:

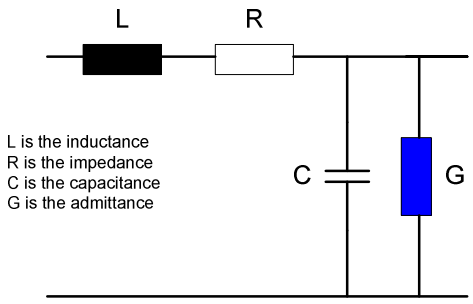

Figure 2.5.2.3 – The traction line model as used for simulation of track sections, the passive components are dependant on the length of the section of interest [19]

For simulation of transmission lines (traction lines), where line effects are insignificant, simple **T** models can be used to analyse traction lines. For transmission effect to be insignificant, the highest frequency of interest is not allowed to complete more than one cycle. For a 6 kHz waveform it is 42.1 km. **T** modelling for one site does have limitations. If the highest frequency of interest's wavelength is shorter than 10 kilometres the **T** model is not valid. DC sub stations are spaced only 20 km apart, thus for T modelling of one site line lengths of longer than 10 km can only be used [18].

2.5.3 Traction interference considerations

Interference between traction power systems and signalling systems can possibly occur due to the following coupling mechanisms [15]:

1. ***Conductive interference*** – when two propagation mediums (signalling and traction) share the same conductor they interfere with each other.
2. ***Inductive interference*** – when changing magnetic flux linkage between two conductors occur.

$$V = L.\frac{dI}{dt}$$

3. ***Electrostatic interference*** – when admittance characteristic capacitive dividers cause voltages to charge and discharge in conductors in close proximity

$$V = C.\frac{dI}{dt}$$

Traction System modelling

The traction system could be modelled as follows [20]:

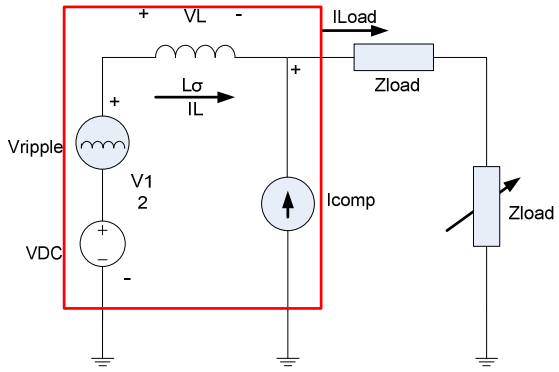

Filter 2.5.3.1 – The model used for traction systems [20]

Icomp is the Norton equivalent circuit for the harmonic filters. The RED region represents the sub station, the variable load represents the frequency dependant elements and the load represents the purely resistive elements in the system [20].

2.6 Capacitor aging

Capacitor selection forms a critical part of design of harmonic filters - using the right material and design geometry would enable the components to operate for years. Reliability of the component is critical. The design of the capacitors are dependant on the environment in which the component is functioning, the voltage applied over the terminals, the shape of the applied wave, the pulse repetition and the duty cycle of the wave shape [36], [37]. The general formulae that applies to capacitor design is, **C = ε A/d**, when the assumption is made that the capacitor operation is linear. The design parameters for capacitors are governed by the area (**A**) of the plate, which is dependant on the clients needs and the separation (**d**) between the plates are dependant on the life span the client wants and the insulation material the manufacturer must use to ensure reliability. The permittivity of the material (**ε**) is the materials ability to insulate the capacitor plates [36].

Factors influencing the life cycle of the capacitor is the operating temperature, the pH value of the solution, the applied voltage. The operation of capacitors at 80% of the rated operating voltage is considered to be optimal in terms of its life cycle. When looking at temperature, for every 8°C the temperature rises above 40°C the life cycle of the capacitor halves [36].

The aging of capacitors can also occur due to the occurrence of electrical discharge. In the case of oil impregnated dielectric capacitors, partial discharge occurs when cavities are left in the dielectric during manufacturing or partial discharge occurs when the gas is formed during capacitor operation [38].

The formation of hydrogen gas during capacitor operation can be seen as a medium with a lower permittivity as that of the oil/paper dielectric, partial discharge in these formed gasses occur, the formation of the hydrogen and the rate of gas generation is dependant on the amount of electrical stress the capacitor is subjected to. Once enough gas has formed, complete breakdown of the dielectric occurs and the capacitor fails. Before total breakdown occurs, the hydrogen causes the total permittivity to reduce, thus reducing the capacitor capacitance. The aging of capacitors therefore influences the capacitor values [38].

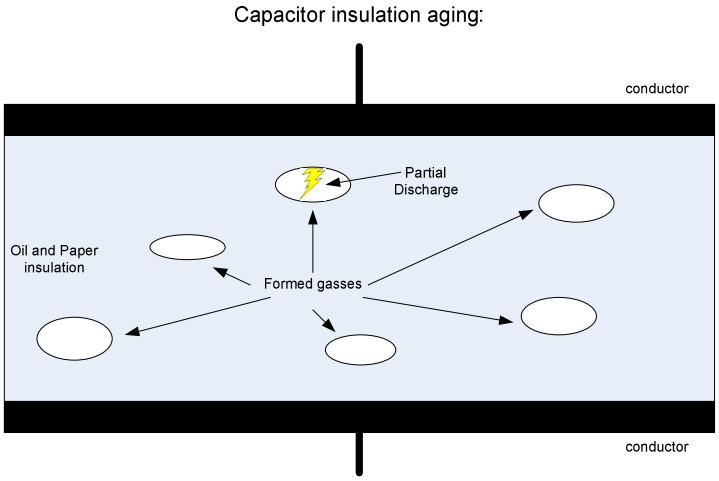

Figure 2.6.1 – The illustration of the partial discharge contributing to the aging of capacitors

Another consideration is the formation of wax around the electrodes due to the insulation oil being under electrical stress. The generated wax around the electrodes promotes the formation of hydrogen gas which in turn promotes partial discharge. The quality of the oil used as the insulation in conjunction with the paper plays an important role in the absorption of the formed hydrogen gas in an attempt to extend the life span of the capacitor [6].

2.7 Conclusion

The chapter dealt with the literature available in an aim to try and get an understanding of what other people have done and to try and quantify the problem at hand. The literature covers methods that are used in theory and practice to measure and quantify harmonics as well as to weigh measurement and modelling methods against each other in an attempt to use and develop methods that best suits the application of this study.

The literature also quantifies why the condition monitoring of passive components are needed, especially capacitors. The chapter also highlights possible scenarios that cause harmonics and that influence harmonics in DC sub stations with passive rectifiers and filters. The possibilities will form the basis of the simulation chapters. The literature also gives a good indication of valid assumptions that can be made when looking at components without compromising the integrity of the measured data.

CHAPTER 3: MODELLING

3.1 Introduction

The modelling of a DC sub station presents the opportunity to get a mathematical representation of the DC sub station. The advantage of having a mathematical model of a system is that quick and relatively accurate validations and calculations can be done to obtain specific data of interest. The efficiency and accuracy of the model is dependant on the need for the model to be simple and the assumptions that were made when the model was developed. It is quite easy to see that the more assumptions are made, the easier the model development becomes, but at the cost of accuracy with regard to actual measured data. The biggest disadvantage of modelling is the fact that it is virtually impossible to cater for all possible operating scenarios.

The assumptions that have been made will be quantified as the development of the model goes on. The first assumptions made are that the DC sub station only generates periodic harmonics and that the diodes act as ideal switches. Various papers have been written in the field of passive rectifier modelling. The work discussed in [32] deals with a passive rectifier supplied by a star and delta secondary from a transformer. The model in [32] investigates commutation and conduction of passive diode rectifiers (12 pulse) and the model outcome is a formula for computing the current output of a passive diode rectifier for one switching period of a set of diodes (commutation and conduction).

The development of the model for the purpose of this project involves adapting the secondary supply topography from the original model and to develop the new model from first principles with the guidance of [32]. The second part of the model deals with expanding the model to include the reactor, wave filters, rail and catenary conditions and locomotive impedances in the time and frequency domain. Changing parameters and investigating the influence it has on the performance of the harmonic filters might enable the model user to better understand wave filter condition monitoring data. The aim of the model is to verify the actual measurements and simulations done later in this document and finally to have a simplified mathematical representation of the sub station.

3.2 Model development

The fundamental difference between the model in [32] and the development of the model specific to this study is the space orientation of the transformer secondary windings. Transnet employs 2 star windings on the secondary windings of the main supply transformer in an aim to get a six phase supply.

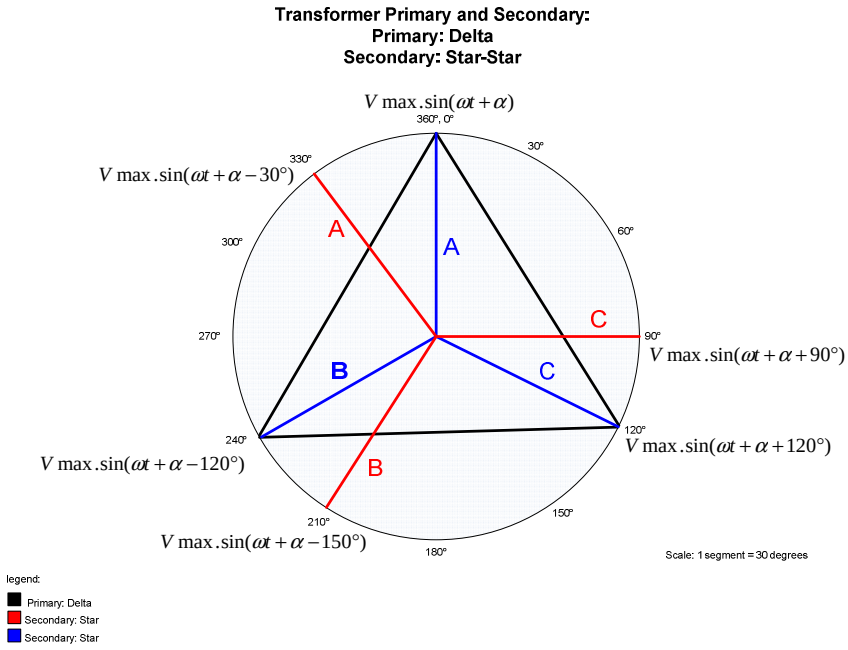

Figure 3.2.1 – The space orientation of the main feeder transformer for a Transnet DC sub station

The space orientation for the transformer secondary winding was chosen in such a way to eliminate certain harmonics. Usually the transformer design aims to reduce doubling in the neutral (triplen harmonics) that cause heating/ageing in motors and transformers. Figure **3.2.1** will serve as the space orientation reference for the development of the model. The convention adopted in figure **3.2.1** is that rotation is clockwise, ω is expressed in radians, ***Vmax*** is the maximum AC voltage (phase to neutral voltage), ***t*** is the time the model is running and the **blue** and **red A, B, C** characters refer to the starting winding for the orientation, thus the **red** windings are **30°** leading to the **blue** winding if the convention is adopted that rotation is clockwise.

A passive 12 pulse rectifier employed by Transnet consists of 2 six pulse rectifiers in series and the advantage as discussed in chapter **2** is that the first generated harmonic is the 12^{th} harmonic (12 pulses) and thus the energy content of the harmonic is relatively low due to a lower amplitude (± 3300/12) as opposed to a 3 pulse rectifier (± 3300/3).

The trade-off between efficiency and cost of implementation brought the design of passive rectifiers in the late 1970's and 1980's to 12 pulse rectifiers.

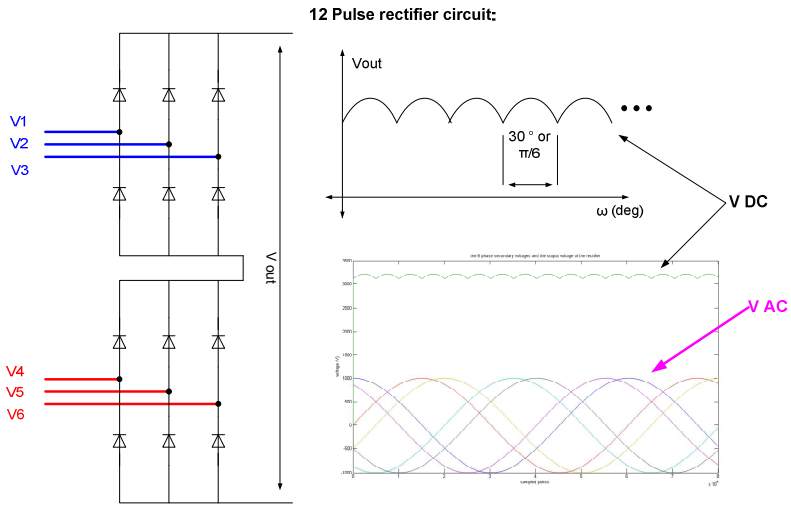

Figure 3.2.2 – The representation of the rectifier topology used by Transnet in the DC sub station

The representation of the blue AC supply lines in figure **3.2.2** is fed from the **blue** star connection in figure **3.2.1** (**A blue** is equal to **V1**, **B** is equal to **V2** and **C** is equal to **V3**). The same applies for the red AC supply in figure **3.2.2** where **A red** is equal to **V4**, **B red** is equal to **V5** and **C red** is equal to **V6**. The **purple** arrow in figure **3.2.2** indicates the various 50 Hz AC waveforms, when looking at the zero x-axis the location of the six waveforms corresponds to the vector locations of the star windings in figure **3.2.1**. The black arrow in figure **3.2.2** indicates the resulting DC voltage where the DC ripple has a period of 30° (360/12 pulses).

The firing/ switching of the diodes will thus not happen at once, due to the fact that the phase voltages did not start at the same time. Before a diode can start conducting the applied voltage over the diode terminals must be equal or greater than the forward biasing voltage (***Vd***). To further explain the diode firing sequence, a simulation was done in Simulink with a circuit similar to that of figure **3.2.2** with a linear load (resistor) and the following assumptions was made:

- The diodes were ideal
- The AC supply voltage was balanced
- Only periodic harmonics will be generated
- Commutation and conduction happens over fixed periods, the assumption builds on the fact that diodes are ideal

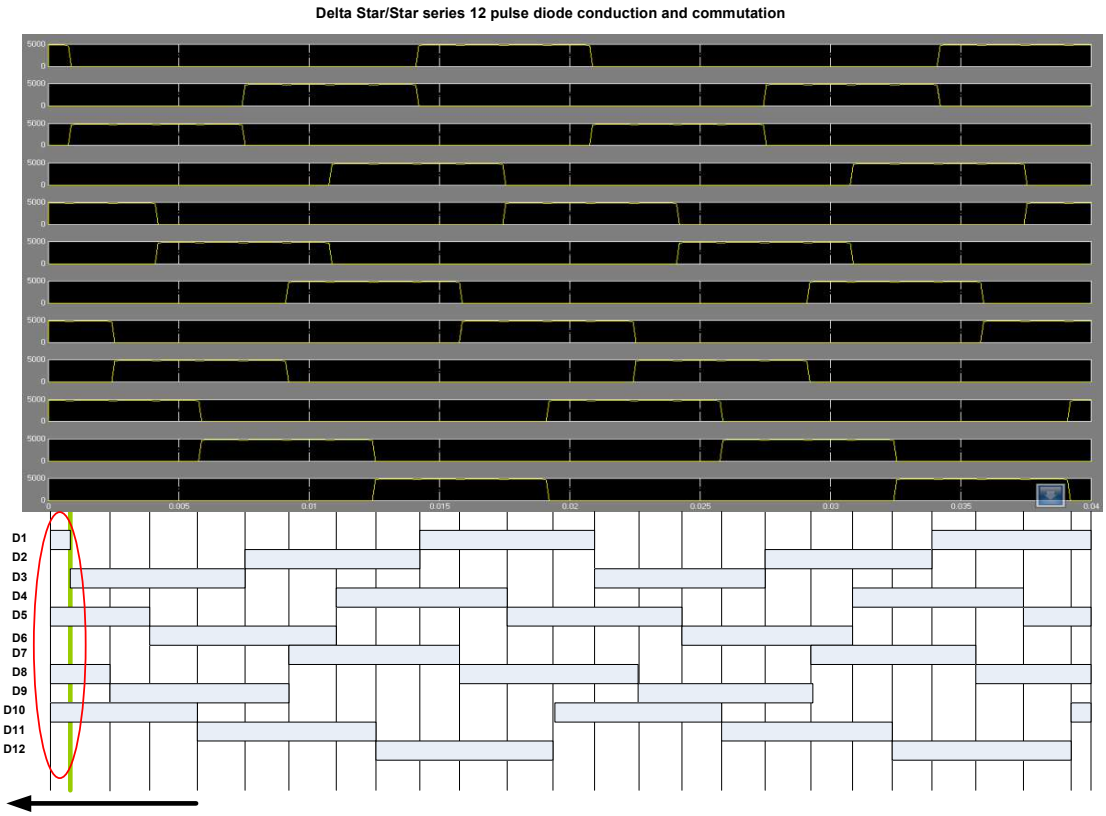

Figure 3.2.3 – The switching sequence of two 6 pulse diode rectifiers in series fed from two star topologies

Figure **3.2.3** illustrates the principle of diode firing (**D1** – **D12**) for the rectifier configuration Transnet employs in DC sub stations. The **red** circle indicates an arbitrarily chosen region of operation for the rectifier. The region could have been chosen anywhere in figure **3.2.3** because the diode firing patterns repeat with only the specific diodes firing that changes. The **red** region will further be used in the derivation of the model. The **green** line indicates the region where commutation goes over into conduction. The **black** arrow indicates the direction of commutation moving over into conduction, the direction of the arrow coinciding with the phase naming convention in figure **3.2.1**.

3.2.1 Derivation of an expression for commutation during diode rectifier operation

The derivation of an expression for commutation during diode rectifier operation is an adaptation of the commutation interval expansion of [32]. Due to the assumptions that were made, the operation of the diode rectifier is of a periodic nature, thus the rectifier operation will have the same characteristics during commutation for multiple instances.

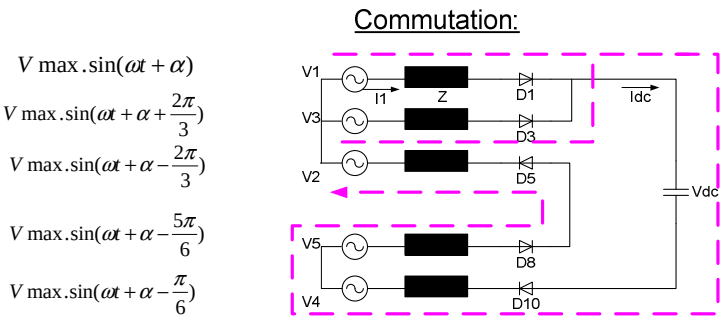

Figure 3.2.1.1 – The commutation circuit and the time dependant voltage waveforms present in the circuit

The commutation circuit in figure **3.2.1.1** only includes the diodes that are present during commutation. These diodes were represented in the **red** region on figure **3.2.3**.

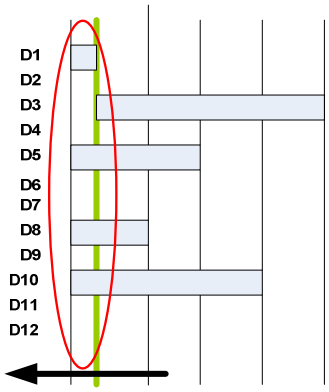

Figure 3.2.1.2 – The region of interest from figure 3.2.3 that indicates what diodes are involved in commutation

In figure **3.2.1.2** the green line indicates where the commutation takes place, thus when two diodes effectively shorts out two voltage sources with each other. During the commutation instance **D1** and **D3** are paralleled. The circuit in figure **3.2.1.1** is populated by the data presented in figure **3.2.1.2**.

Trigonometric Rule 1:

$$\sin(x\pm y)=\sin(x)\cos(y)\pm\cos(x)\sin(y)$$

Trigonometric Rule 2:

$$a.\cos(x)+b.\sin(x)=C.\cos(x+\theta)\_where$$

$$C=\sqrt{a^2+b^2}\_and\_\theta=\tan^{-1}\left(\frac{-b}{a}\right)$$

Trigonometric Rule 3:

$$\int\cos(a.x).dx=\frac{1}{a}.\sin(x)$$

Figure 3.2.1.3 – The summary of the trigonometric rules that were used to simplify the expressions in chapter 3

The derivation of the equivalent commutation expression can be shown as follows:

Writing the equation for comutation:

$$Z.\frac{dI_1}{dt}+3.Z.\frac{dI_{DC}}{dt}=(V1-V2)+(V5-V4)-V_{DC}.....(1)$$

$$(V1-V2)=V\max.\sin(\omega t+\alpha)-V\max.\sin(\omega t+\alpha-\frac{2\pi}{3})$$

Set $(\omega t+\alpha)=y$

$$(V1-V2)=V\max.\sin(y)-V\max.\sin(y-\frac{2\pi}{3})$$

$$=V\max.\sin(y)-V\max[\sin(y)\cos(\frac{2\pi}{3})-\sin(\frac{2\pi}{3})\cos(y)].....(Trig\_rule\_1)$$

$$=V\max[\sin(y)(1-\cos(\frac{2\pi}{3})+\cos(y)(+\sin(\frac{2\pi}{3}))]$$

$$=V\max[\sin(y)(1{,}5)+\cos(y)(+0{,}866)]$$

$$=\sqrt{3}.V\max.\cos(y-\frac{\pi}{3}).....(Trig\_rule\_2)$$

$$(V1-V2)=\sqrt{3}.V\max.\cos(\omega t+\alpha-\frac{\pi}{3})$$

Similarly:

$$(V5-V4)=V\max.\sin(\omega t+\alpha-\frac{5\pi}{6})-V\max.\sin(\omega t+\alpha-\frac{\pi}{6})$$

$$(V5-V4)=-\sqrt{3}.V\max.\sin(\omega t+\alpha)$$

Substituting into (1):

$$Z.\frac{dI_1}{dt}+3.Z.\frac{dI_{DC}}{dt}=\sqrt{3}.V\max[\cos(\omega t+\alpha-\frac{\pi}{3})-\sin(\omega t+\alpha)]-V_{DC}.....(2)$$

Integrating (2):

$$Z.\frac{dI_1}{dt}+3.Z.\frac{dI_{DC}}{dt}=\sqrt{3}.V\max[\cos(\omega t+\alpha-\frac{\pi}{3})-\sin(\omega t+\alpha)]-V_{DC}.....(2)$$

From equation (1), the impedance of the secondary of the feeding transformer is assumed to be inductive; thus the formula is applied to calculate the potential voltage across the inductor.

$$V=L\frac{dI}{dt}$$

The reason for trying to derive a voltage expression for the operation of the diode rectifier during commutation is because of another assumption that the DC bus voltage is considered constant.

The process of integrating equation (2) is summarised below.

$0 \le \omega t \le U$ where U is the commutation angle

$0 \le t \le \frac{U}{\omega}$ for time domain analysis

the following boundary conditions apply:

at $t = 0; I_1 = 0$ and at $U; I_{DC} = I_1$

Figure 3.2.1.4 – The integration parameters and boundary conditions for the commutation interval

The **blue** block, figure **3.2.1.4**, is used to quantify the limits for integration of equation (2). When looking at the **blue** block, it can be seen that the commutation angle is **U** which indicates the condition where diode one and three conduct at the same time. The snubber circuits included in these diodes try and limit these circumstances to a minimum. The parameter of interest in the **blue** block is the time parameter "**t**" because the voltage waveforms are time based. The block refers to the current **I1 = 0** at parameter **t = 0**. When looking at the green line in figure **3.2.1.2** the line represents **t = 0** and the black arrow in figure **3.2.1.2** represents the direction of propagation based on the convention adapted in figure **3.2.1**. At angle **U** the forward bias voltage of **diode 1** is reached and conduction starts, thus at **U** the conduction current is equal to the DC current **I dc**, thus **I dc = I1**.

$LF:$

$$\int_0^{\frac{U}{\omega}} Z.\frac{dI_1}{dt}.dt + \int_0^{\frac{U}{\omega}} 3.Z.\frac{dI_{DC}}{dt}.dt$$

$$\left|Z.I_1(t)\right|_0^{\frac{U}{\omega}} + \left|3.Z.I_{DC}(t)\right|_0^{\frac{U}{\omega}}$$

$$Z.I_1\left(\frac{U}{\omega}\right) - Z.I_1(0) + 3.Z.I_{DC}\left(\frac{U}{\omega}\right) - 3.Z.I_{DC}(0)$$

inserting the boundary conditions:

$$Z.I_{DC}\left(\frac{U}{\omega}\right) - Z.(0) + 3.Z.I_{DC}\left(\frac{U}{\omega}\right) - 3.Z.I_{DC}(0)$$

$$4.Z.I_{DC}\left(\frac{U}{\omega}\right) - 3.Z.I_{DC}(0)$$

Figure 3.2.1.5 – The integration of the left hand side of equation (2) and the inclusion of the boundary conditions and integration parameters from figure 3.2.1.4

The integration of equation (2) entails getting expressions for the DC current and voltage rectified by the 12 pulse passive rectifier by eliminating the differential components of the parameters of interest. By integrating the left hand side of equation (2), figure **3.2.1.5**, the same has to be done on the right hand side of (2).

RF :

$$\left(\sqrt{3}.V\max\right)\left[\int_0^{\frac{U}{\omega}}\cos(\omega t+\alpha-\frac{\pi}{3}).dt-\int_0^{\frac{U}{\omega}}\sin(\omega t+\alpha).dt\right]-\int_0^{\frac{U}{\omega}}V_{DC}.dt$$

$$\left(\sqrt{3}.V\max\right)\left[\frac{1}{\omega}\left|\sin(\omega t+\alpha-\frac{\pi}{3})\right|_0^{\frac{U}{\omega}}-\frac{1}{\omega}\left|\cos(\omega t+\alpha)\right|_0^{\frac{U}{\omega}}\right]-\left|V_{DC}\right|_0^{\frac{U}{\omega}}.....rule(3)$$

$$\left(\sqrt{3}.V\max\right)\left[\frac{1}{\omega}\left|\sin(\omega.\left(\frac{U}{\omega}\right)+\alpha-\frac{\pi}{3})\right|-\frac{1}{\omega}\left|\cos(\omega.\left(\frac{U}{\omega}\right)+\alpha)\right|-\frac{1}{\omega}\left|\sin(\omega.(0)+\alpha-\frac{\pi}{3})\right|+\frac{1}{\omega}\left|\cos(\omega.(0)+\alpha)\right|\right]-V_{DC}\left(\frac{U}{\omega}\right)$$

the assumption is made that $V_{DC}(0)=0$

$$\left(\frac{\sqrt{3}.V\max}{\omega}\right).\left[\left|\sin(U+\alpha-\frac{\pi}{3})\right|-\left|\cos(U+\alpha)\right|-\left|\sin(\alpha-\frac{\pi}{3})\right|+\left|\cos(\alpha)\right|\right]-V_{DC}\left(\frac{U}{\omega}\right)$$

Figure 3.2.1.6 – The integration of the right hand side of equation (2) and the inclusion of the boundary conditions and integration parameters from figure 3.2.1.4

The right hand side of equation (**2**) is integrated in the **green** block, figure **3.2.1.6**, with the integration parameters inserted. The reason for breaking up equation (**2**) in a left and right hand side is to simplify the equation first.

Commutation:

$$4.Z.I_{DC}\left(\frac{U}{\omega}\right)-3.Z.I_{DC}(0)=\left(\frac{\sqrt{3}.V\max}{\omega}\right).\left[\left|\sin(U+\alpha-\frac{\pi}{3})\right|-\left|\cos(U+\alpha)\right|-\left|\sin(\alpha-\frac{\pi}{3})\right|+\left|\cos(\alpha)\right|\right]-V_{DC}\left(\frac{U}{\omega}\right)$$

Figure 3.2.1.7 – The expression for the commutation interval

The combination of the left and right hand sides is summarised in the **black** block, figure **3.2.1.7**. The **black** block is the equation for the commutation of a twelve pulse passive rectifiers fed by a transformer with the same space orientation as utilised by Transnet. The steady state commutation expression in the **black** block thus shows what the aim of the model is. The aim is to get a model that is independent of switching characteristics during steady state.

3.2.2 Derivation of an expression for commutation during diode rectifier operation

The derivation of an expression for conduction during diode rectifier operation is an adaptation of the conduction interval expansion of [32]. Due to the assumptions that were made, the operation of the diode rectifier is of a periodic nature, thus the rectifier operation will have the same characteristics during conduction for multiple instances.

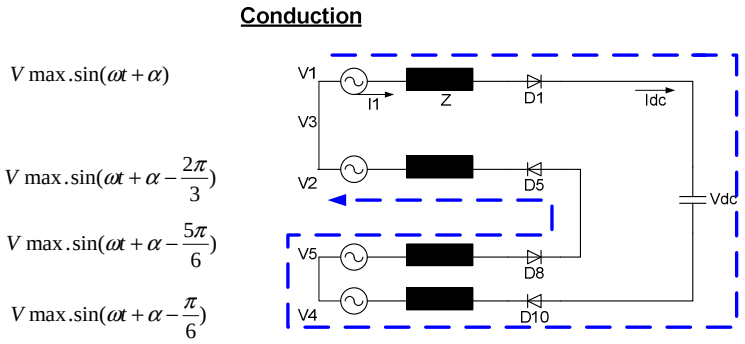

Figure 3.2.2.1 – The conduction circuit and the time dependant voltage waveforms present in the circuit

The main difference between the conduction interval and the commutation interval is the fact that the forward voltage bias has been overcome and **diode 1** is conducting while **diode 3** has stopped conducting as was the case with commutation. The voltage expressions on the left have been derived from the actual orientation Transnet employs with three phase transformers. The impedance "**Z**" is shown in figure **3.2.2.1** and represents the inductance of the wire and the windings of the transformer secondary.

The conduction interval can be formulated as follows:

Writing the equation for conduction:

$$4.Z.\frac{dI_{DC}}{dt}=(V1-V2)+(V5-V4)-V_{DC}\ldots\ldots\ldots\ldots\ldots\ldots(3)$$

Inserting the voltage values into the formulae:

$$(V1-V2)=V\max.\sin(\omega t+\alpha)-V\max.\sin(\omega t+\alpha-\frac{2\pi}{3})$$

Set $(\omega t+\alpha)=y$

$$(V1-V2)=V\max.\sin(y)-V\max.\sin(y-\frac{2\pi}{3})$$

$$=V\max.\sin(y)-V\max[\sin(y)\cos(\frac{2\pi}{3})-\sin(\frac{2\pi}{3})\cos(y)].....(Trig\_rule\_1)$$

$$=V\max[\sin(y)(1-\cos(\frac{2\pi}{3})+\cos(y)(+\sin(\frac{2\pi}{3}))]$$

$$=V\max[\sin(y)(1{,}5)+\cos(y)(+0{,}866)]$$

$$=\sqrt{3}.V\max.\cos(y-\frac{\pi}{3}).....(Trig\_rule\_2)$$

$$(V1-V2)=\sqrt{3}.V\max.\cos(\omega t+\alpha-\frac{\pi}{3})$$

Similarly:

$$(V5-V4)=V\max.\sin(\omega t+\alpha-\frac{5\pi}{6})-V\max.\sin(\omega t+\alpha-\frac{\pi}{6})$$

$$(V5-V4)=-\sqrt{3}.V\max.\sin(\omega t+\alpha)$$

Substituting into (3):

$$4.Z.\frac{dI_{DC}}{dt}=\sqrt{3}.V\max[\cos(\omega t+\alpha-\frac{\pi}{3})-\sin(\omega t+\alpha)]-V_{DC}.....(4)$$

Integrating (4):

$$4.Z.\frac{dI_{DC}}{dt}=\sqrt{3}.V\max[\cos(\omega t+\alpha-\frac{\pi}{3})-\sin(\omega t+\alpha)]-V_{DC}.....(4)$$

The simplification of equation (4) entails solving/simplifying the equations left and right of the equal sign of (4).

$U\le\omega t\le\frac{\pi}{6}$ where U is the conduction angle

$\frac{U}{\omega}\le t\le\frac{\pi}{6.\omega}$ for time domain analysis

Figure 3.2.2.2 – The integration parameters for the conduction interval

The parameters for the integration of (4) are shown in the **blue** block, figure **3.2.2.2**. When the commutation and conduction interval is summed it equates to one switching cycle (360°/12 pulses). The conduction cycle starts as soon as the commutation angle is overcome and stops when one switching cycle is completed, then the cycle repeats itself.

$LF:$

$$\int_{\frac{U}{\omega}}^{\frac{\pi}{6\omega}}4.Z.\frac{dI_{DC}}{dt}.dt$$

$$\left|4.Z.I_{DC}(t)\right|_{\frac{U}{\omega}}^{\frac{\pi}{6\omega}}$$

$$4.Z.I_{DC}\left(\frac{\pi}{6.\omega}\right)-4.Z.I_{DC}\left(\frac{U}{\omega}\right)$$

Figure 3.2.2.3 – The left hand side of equation (4) being integrated with the parameters from figure 3.2.2.2

The conduction interval expression is simpler than the commutation interval expression due to the fact that less diodes and voltage sources contribute to the equivalent circuit shown in **3.2.2.1**.

The right hand side of equation (4) follows:

$$RF:$$

$$\left(\sqrt{3}.V\max\right)\left[\int_{\frac{U}{\omega}}^{\frac{\pi}{6\omega}}\cos(\omega t+\alpha-\frac{\pi}{3}).dt-\int_{\frac{u}{\omega}}^{\frac{\pi}{6\omega}}\sin(\omega t+\alpha).dt\right]-\int_{0}^{\frac{\pi}{6\omega}}V_{DC}.dt$$

$$\left(\sqrt{3}.V\max\right)\left[\frac{1}{\omega}\left|\sin(\omega t+\alpha-\frac{\pi}{3}\right|_{\frac{U}{\omega}}^{\frac{\pi}{6\omega}}-\frac{1}{\omega}\left|\cos(\omega t+\alpha)\right|_{\frac{U}{\omega}}^{\frac{\pi}{6\omega}}\right]-\left|V_{DC}\right|_{\frac{U}{\omega}}^{\frac{\pi}{6\omega}}.....trig\_rule(3)$$

$$\left(\sqrt{3}.V\max\right)\left[\frac{1}{\omega}\left|\sin(\omega.\left(\frac{\pi}{6.\omega}\right)+\alpha-\frac{\pi}{3})\right|-\frac{1}{\omega}\left|\cos(\omega.\left(\frac{\pi}{6.\omega}\right)+\alpha)\right|-\frac{1}{\omega}\left|\sin(\omega.\left(\frac{U}{\omega}\right)+\alpha-\frac{\pi}{3})\right|+\frac{1}{\omega}\left|\cos(\omega.\left(\frac{U}{\omega}\right)+\alpha)\right|\right]-V_{DC}\left(\frac{\pi}{6.\omega}\right)+V_{DC}\left(\frac{U}{\omega}\right)$$

$$\left(\frac{\sqrt{3}.V\max}{\omega}\right).\left[\left|\sin(\frac{\pi}{6}+\alpha-\frac{\pi}{3})\right|-\left|\cos(\frac{\pi}{6}+\alpha)\right|-\left|\sin(U+\alpha-\frac{\pi}{3})\right|+\left|\cos(U+\alpha)\right|\right]-V_{DC}\left(\frac{\frac{\pi}{6}-U}{\omega}\right)$$

Figure 3.2.2.4 – The right hand side of equation (4) being integrated with the parameters from figure 3.2.2.2

The green region, figure 3.2.2.4, shows the partial expression obtained for the conduction interval after integrating the right hand side of equation (4).

Conduction:

$$4.Z.I_{DC}\left(\frac{\pi}{6.\omega}\right)-4.Z.I_{DC}\left(\frac{U}{\omega}\right)=\left(\frac{\sqrt{3}.V\max}{\omega}\right).\left[\left|\sin(\alpha-\frac{\pi}{6})\right|-\left|\cos(\frac{\pi}{6}+\alpha)\right|-\left|\sin(U+\alpha-\frac{\pi}{3})\right|+\left|\cos(U+\alpha)\right|\right]-V_{DC}\left(\frac{\frac{\pi}{6}-U}{\omega}\right)$$

Figure 3.2.2.5 – The conduction circuit and the time dependant voltage waveforms present in the circuit

The expression for the conduction interval has been given in the **black** block, figure **3.2.2.5**. The assumption that the commutation and conduction interval repeats every 30° entails that the start and end of every cycle is the same, thus meaning that the start and end of every cycle has the same values. The start of the commutation cycle and the end of the conduction cycle has the same values.

3.2.3 The expression for one switching cycle

The expression for one switching cycle can be seen as the summation of the results from figure **3.2.1.7** and **3.2.2.5**. The summation of the commutation and conduction expression will enable the formulation of one expression. The expression is independent of the switching variations during steady state operation of the passive rectifier. The result is a DC current equation for a 12 pulse passive rectifier as used by Transnet for the specific transformer topology used.

we are interested in the first Commutation and conduction interval $0 \le \omega t \le \frac{\pi}{6}$

$$4.Z.I_{DC}\left(\frac{U}{\omega}\right) - 3.Z.I_{DC}(0) = \left(\frac{\sqrt{3}.V\max}{\omega}\right)\left[\left|\sin(U+\alpha-\frac{\pi}{3})\right| - \left|\cos(U+\alpha)\right| - \left|\sin(\alpha-\frac{\pi}{3})\right| + \left|\cos(\alpha)\right|\right] - V_{DC}\left(\frac{U}{\omega}\right) \text{...(5)}$$

$$4.Z.I_{DC}\left(\frac{\pi}{6.\omega}\right) - 4.Z.I_{DC}\left(\frac{U}{\omega}\right) = \left(\frac{\sqrt{3}.V\max}{\omega}\right)\left[\left|\sin(\alpha-\frac{\pi}{6})\right| - \left|\cos(\frac{\pi}{6}+\alpha)\right| - \left|\sin(U+\alpha-\frac{\pi}{3})\right| + \left|\cos(U+\alpha)\right|\right] - V_{DC}\left(\frac{\frac{\pi}{6}-U}{\omega}\right) \text{....(6)}$$

Add (5) and (6)

$$4.Z.I_{DC}\left(\frac{\pi}{6.\omega}\right) - 3.Z.I_{DC}(0) = \left(\frac{\sqrt{3}.V\max}{\omega}\right)\left[\left|-\sin(\alpha-\frac{\pi}{3})\right| + \left|\cos(\alpha)\right| + \left|\sin(\alpha-\frac{\pi}{6})\right| - \left|\cos(\alpha+\frac{\pi}{6})\right|\right] - V_{DC}\left(\frac{\frac{\pi}{6}}{\omega}\right) \text{............................(7)}$$

The expression for one switching cycle of the passive rectifier is represented by equation (**7**). The **commutation** interval is represented by (**5**) and the **conduction** interval by (**6**). The various coloured lines in (5) and (6) represent the factors that cancel each other out during the addition of the two expressions.

The calculation of the parameter α has been adapted from the prescribed method in [32].

Calculating α:

Looking at this scenario the circuit for the 12 pulse rectifier looks as follows:

Using: $$V_{D4} = \frac{-3.Z.di_{DC}}{dt} + V_{12} + V_{56} - V_{DC} \text{............}(D4)$$

$$4.Z.\frac{dI_{DC}}{dt} = \sqrt{3}.V\max[\cos(\omega t+\alpha-\frac{\pi}{3}) - \sin(\omega t+\alpha)] - V_{DC} \text{.................}(4)$$

We obtain:

$$\frac{-3.Z.dI_{DC}}{dt} = \frac{-3.\sqrt{3}}{4}.V\max[\cos(\omega t+\alpha-\frac{\pi}{3}) - \sin(\omega t+\alpha)] + \frac{3.V_{DC}}{4}$$ Divide by 4 and multiply by -3

$$\frac{-3.Z.dI_{DC}}{dt} = \frac{-3.\sqrt{3}}{4}.V\max[\cos(\alpha-\frac{\pi}{6}) - \sin(\frac{\pi}{6}+\alpha)] + \frac{3.V_{DC}}{4} \text{......substitute } wt = \frac{\pi}{6}$$

$$\frac{-3.Z.dI_{DC}}{dt} = \frac{-3.\sqrt{3}}{4}.V\max[\cos(\alpha-\frac{\pi}{6}) - \sin(\frac{\pi}{6}+\alpha)] + \frac{3.V_{DC}}{4} \text{........(8)}$$

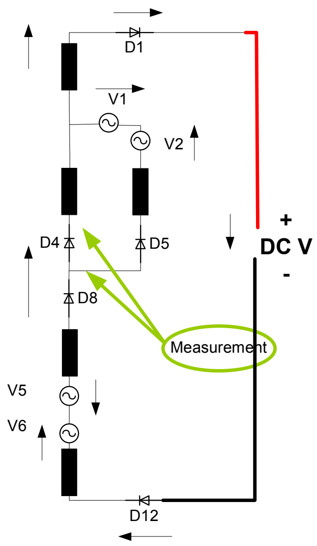

Next we get:

$$(V1-V2) = \sqrt{3}.V\max.\cos(\omega t+\alpha-\frac{\pi}{3}) \text{........substitute } wt = \frac{\pi}{6}$$

$$(V1-V2) = \sqrt{3}.V\max.\cos(\alpha-\frac{\pi}{6}) \text{.......(9)}$$

And:

$$(V5-V6) = V\max.\sin(\omega t+\alpha-\frac{5\pi}{6}) - V\max.\sin(\omega t+\alpha+\frac{\pi}{2})$$

$$= \sqrt{3}.V\max.\cos(\omega t+\alpha-\frac{\pi}{6}) \text{..}(Trig\_rule\_1\&2)$$

$$(V5-V6) = \sqrt{3}.V\max.\cos(\omega t+\alpha-\frac{\pi}{6}) \text{.........substitute } wt = \frac{\pi}{6}$$

$$(V5-V6) = \sqrt{3}.V\max.\cos(\alpha) \text{........(10)}$$

The calculated equations (8) - (10) are substituted into equation (D4):

$$\frac{-3.Z.dI_{DC}}{dt}=\frac{-3.\sqrt{3}}{4}.V\max[\cos(\alpha-\frac{\pi}{6})-\sin(\frac{\pi}{6}+\alpha)]+\frac{3.V_{DC}}{4}$$

constant

$$V_{D4}=\frac{-3.Z.di_{DC}}{dt}+V_{12}+V_{56}-V_{DC}$$

$$V_{12}=\sqrt{3}.V\max.\cos(\alpha-\frac{\pi}{6})$$

$$V_{56}=\sqrt{3}.V\max.\cos(\alpha)$$

Summing we get:

$$V_{D4}=\frac{-3.\sqrt{3}}{4}.V\max.\cos(\alpha-\frac{\pi}{6})+\frac{3.\sqrt{3}}{4}.V\max.\sin(\alpha+\frac{\pi}{6})+\frac{3.V_{DC}}{4}+\sqrt{3}.V\max.\cos(\alpha-\frac{\pi}{6})+\sqrt{3}.V\max.\cos(\alpha)-V_{DC}$$

$$V_{D4}=\sqrt{3}.V\max.[\frac{1}{4}.\cos(\alpha-\frac{\pi}{6})+\frac{3}{4}.\sin(\alpha+\frac{\pi}{6})+\cos(\alpha)]-\frac{V_{DC}}{4}....(11)$$

Trigonometric rule 4:

$$\cos(x\pm y)=\cos(x)\cos(y)\mp\sin(x)\sin(y)$$

As stated the voltage at wt = 30° is zero, thus the voltage over D4 is also zero:

$$0=\sqrt{3}.V\max.[\frac{1}{4}.\cos(\alpha-\frac{\pi}{6})+\cos(\alpha)+\frac{3}{4}\sin(\alpha+\frac{\pi}{6})]-\frac{V_{DC}}{4}$$

$$\frac{V_{DC}}{4.\sqrt{3}.V\max.}=[\frac{1}{4}.\cos(\alpha-\frac{\pi}{6})+\frac{3.}{4}.\sin(\alpha+\frac{\pi}{6})+\cos(\alpha)]$$

Now we apply trigonometric rule 4:

$$\frac{1}{4}.\cos(\alpha-\frac{\pi}{6})=\frac{1}{4}[\cos(\alpha)\cos(\frac{\pi}{6})+\sin(\alpha)\sin(\frac{\pi}{6})].....trig\_rule\_4$$

$$\frac{3}{4}.\sin(\alpha+\frac{\pi}{6})=\frac{3}{4}[\sin(\alpha)\cos(\frac{\pi}{6})+\cos(\alpha)\sin(\frac{\pi}{6})].....trig\_rule\_1$$

$$[\frac{1}{4}.\cos(\alpha-\frac{\pi}{6})+\frac{3.}{4}.\sin(\alpha+\frac{\pi}{6})+\cos(\alpha)]=\cos\alpha[1.5915]+\sin\alpha[0.77452]$$

Applying trig rule 2

$$=(1.7699).\cos(\alpha-0.45292).....rad$$

$$\frac{V_{DC}}{4.\sqrt{3}.V\max.}=(1.7699).\cos(\alpha-0.45292)$$

$$where:$$

$$V_{DC}=3000;$$

$$V\max=1330;.....Transnet\_Data$$

$$0.18395=\cos(\alpha-0.45292)$$

$$\cos^{-1}(0.18395)=\alpha-0.45292$$

$$1.3857928+0.45292=\alpha$$

$$\alpha=1.8387128\_radians$$

The calculated value for alpha can be used in the computation of the current expression for one switching cycle.

Now we can compute the periodic current as presented over one switching cycle:

$$4.Z.I_{DC}\left(\frac{\pi}{6.\omega}\right)-3.Z.I_{DC}(0)=\left(\frac{\sqrt{3}.V\max}{\omega}\right).\left[\left|-\sin(\alpha-\frac{\pi}{3})\right|+\left|\cos(\alpha)\right|+\left|\sin(\alpha-\frac{\pi}{6})\right|-\left|\cos(\alpha+\frac{\pi}{6})\right|\right]-V_{DC}\left(\frac{\frac{\pi}{6}}{\omega}\right).....(7)$$

From our assumption that at 0 and 30° the cycle repeats, if assumed symmetry we get:

$$I_{DC}\left(0,\frac{\pi}{6}\right)=\frac{\left(\frac{\sqrt{3}.V\max}{\omega}\right).\left[\left|-\sin(\alpha-\frac{\pi}{3})\right|+\left|\cos(\alpha)\right|+\left|\sin(\alpha-\frac{\pi}{6})\right|-\left|\cos(\alpha+\frac{\pi}{6})\right|\right]-V_{DC}\left(\frac{\frac{\pi}{6}}{\omega}\right)}{Z}.....(12)$$

The current equation for one switching cycle is expressed in equation (12). Looking at the DC sub station, the main supply transformer and the passive 12 pulse diode rectifier can be expressed as equation (12). The assumption is still made that only periodic harmonics are generated. Expression (12) can now be used to represent a DC current source. The current source and the components contributing to the impedance of the DC sub station are illustrated as follows:

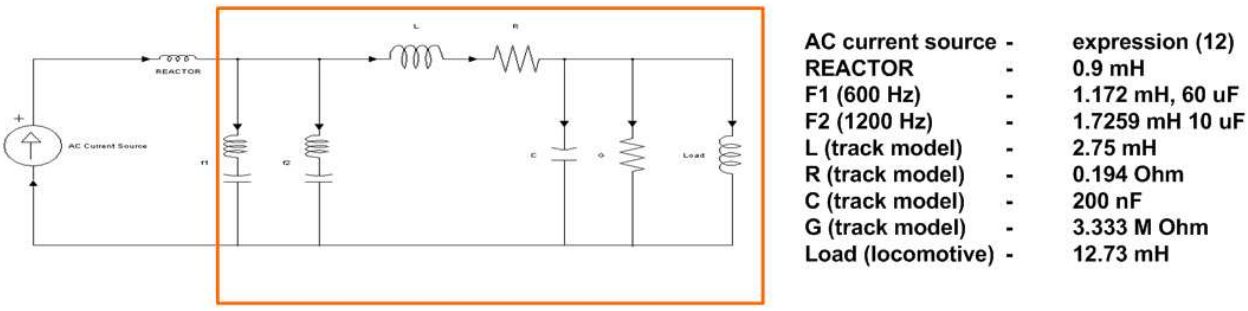

Figure 3.2.3.1 – The representation of the current source [expression (12)] with the rest of the DC sub station circuit (passive components), the orange region represents the impedances of interest

The current through the equivalent impedance of the **orange** region in figure **3.2.3.1** will give a voltage expression for the condition monitoring of the passive harmonic filters in the DC sub station. The values for the passive components in figure **3.2.3.1** were gathered from [42], [43].

3.2.4 The expression for calculating the equivalent impedance of the DC sub station

The calculation of the equivalent impedance of the orange region in figure **3.2.3.1** can be broken into various sub sections.

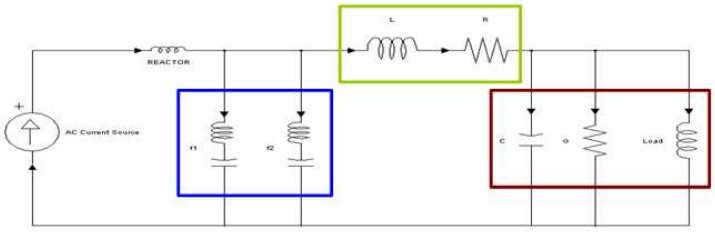

Figure 3.2.4.1 – The circuit used for the computation of the equivalent impedance of the DC sub station, the coloured regions will be computed separately and then added

$$
\begin{aligned}
&blue\_region:\\
&=[(((F1C)^{-1}+(F1L)^{-1})^{-1})^{-1}+(((F2C)^{-1}+(F2L)^{-1})^{-1})^{-1}]^{-1}\\
&green\_region:\\
&=((L)+(R))\\
&burgandy\_region:\\
&((c)^{-1}+(G)^{-1}+(load)^{-1})^{-1}
\end{aligned}
$$

The impedance calculation for the separate regions can now be simplified and the equivalent impedance can be calculated as follows:

$$
\begin{aligned}
&(\{[(((F1C)^{-1}+(F1L)^{-1})^{-1})^{-1}+(((F2C)^{-1}+(F2L)^{-1})^{-1})^{-1}]^{-1}\}^{-1}+\{((C)^{-1}+(G)^{-1}+(load)^{-1})^{-1}+((L)+(R))\}^{-1})^{-1}\\
&where:\\
&(\{[(((\frac{10^6}{\omega\times 60})^{-1}+(\frac{\omega\times 1.172}{10^3})^{-1})^{-1})^{-1}+(((\frac{10^6}{\omega\times 10})^{-1}+(\frac{\omega\times 1.7259}{10^3})^{-1})^{-1})^{-1}]^{-1}\}^{-1}+\{((\frac{10^9}{\omega\times 200})^{-1}+(3.333\times 10^6)^{-1}+\\
&(\frac{\omega\times 12.73}{10^3})^{-1})^{-1}+((\frac{\omega\times 2.75}{10^3})+(0.194))\}^{-1})^{-1}.....(13)
\end{aligned}
$$

The biggest complexity of the expression is the fact that the track model is expressed as the component value per meter. The values used for the track model were taken over a track span of 1km, but the model will not hold for any other distance of track. The computation of the voltage drop across the equivalent impedance follows below:

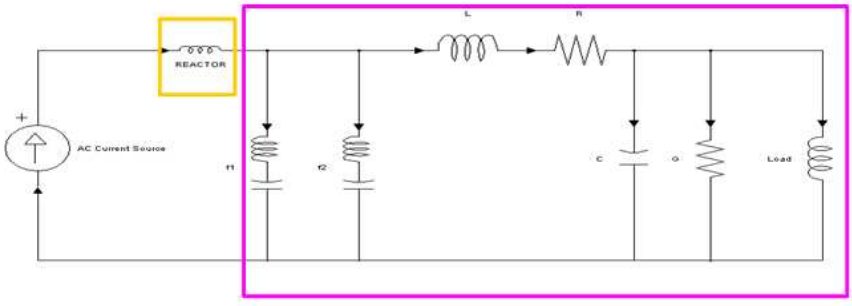

Figure 3.2.4.2 – The DC sub station circuit, where equation (12) serves as the ideal current source, equation (13) serves as the impedance of interest [purple region] and the reactor [yellow region] is in series with the impedance of interest

The reactor (*0.9 mH*) is in series with the equivalent impedance shown in the purple region. The reason for having all the components in the purple region is that the track model components and the locomotive are outside the substation. The filters are parallel to the track model and the locomotive, thus all the components in the purple region form part of the interest and investigation in this study.

The final expression that will be used for the calculation of the voltage waveforms for the condition monitoring of the DC sub station passive harmonic filters is shown below:

$$voltage = \frac{(\{[(((\frac{10^6}{\omega\times 60})^{-1}+(\frac{\omega\times 1.172}{10^3})^{-1})^{-1}+(((\frac{10^6}{\omega\times 10})^{-1}+(\frac{\omega\times 1.7259}{10^3})^{-1})^{-1}]^{-1}\}^{-1}+\{((\frac{10^9}{\omega\times 200})^{-1}+(3.333\times 10^6)^{-1}+(\frac{\omega\times 12.73}{10^3})^{-1})^{-1}+((\frac{\omega\times 2.75}{10^3})+(0.194))\}^{-1})^{-1}}{\left(\frac{\sqrt{3}.V\max}{\omega}\right).\left[\left|-\sin(1.8387128-\frac{\pi}{3})\right|+\left|\cos(1.8387128)\right|+\left|\sin(1.8387128-\frac{\pi}{6})\right|-\left|\cos(1.8387128+\frac{\pi}{6})\right|\right]-V_{DC}\left(\frac{\frac{\pi}{6}}{\omega}\right)}{\omega\times 0.1\times 10^{-3}} \quad .....(14)$$

The aim of the condition monitoring of the DC sub station passive harmonic filters is to find a simple mathematical model for the DC sub station. Equation (14) is only dependant on ω (radians) so its makes it possible to compute voltage values for any value of ω. The parameter ***Vmax*** is the AC supply phase to ground voltage and the parameter ***VDC*** is the assumed constant DC bus voltage. These two parameters are available for all the sub stations and can be fed into equation (14).

3.2.5 Conclusion

The aim of the chapter was to find a simple model that will enable the user of the model to obtain voltage data that can be used for the condition monitoring of the passive harmonic filters in the DC sub station. Expression (14) is the outcome of chapter **3**, but the development of a mathematical model has the following disadvantages:

- The model is limited by the length of the track that is used to compute the values for the track model.
- The model is confined to only one operating scenario. If a fault condition is simulated the model would not be able to accommodate the changes. A new model will have to be generated for every possible operating fault condition.
- The model is more complex than originally thought.

The model for the condition monitoring of the sub station filters does not have a practical implementation possibility due to the fact that the expression is so limited and complex. The model thus serves the purpose of getting a better understanding of the operation of the sub station and in particular the passive switching/conversion of AC to DC. The result: the DC sub station presents much more complex operating combinations and model development restrictions than originally thought. The development of a mathematical model is not feasible.

CHAPTER 4: SIMULATIONS

4.1 Introduction

The simulation structure of the chapter involves the investigation of different scenarios in the sub station. The investigations will serve the purpose of trying to gather harmonic specific information based on the various circumstances.

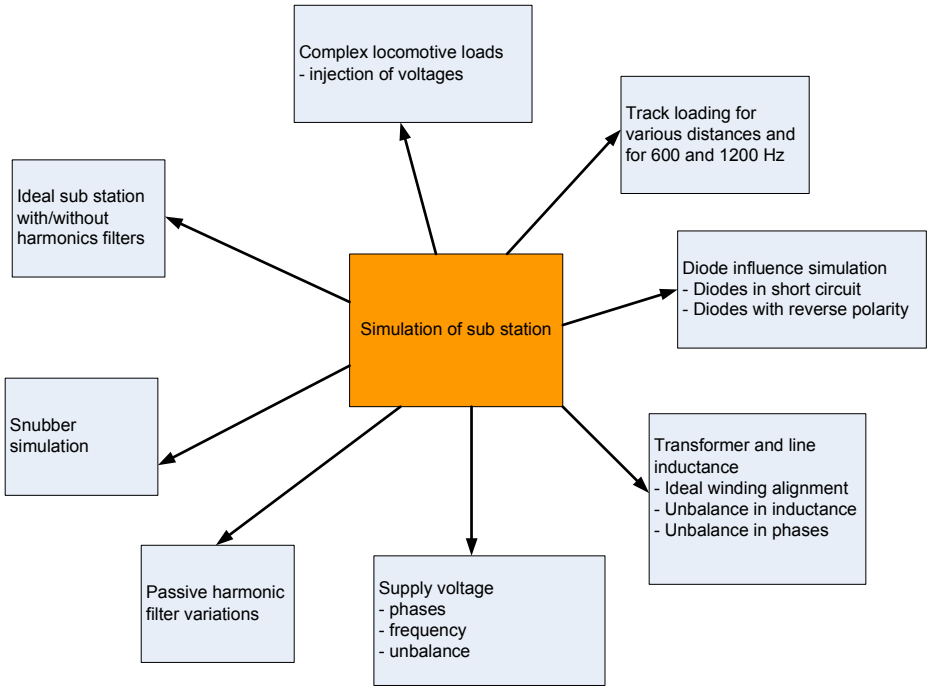

Figure 4.1.1 – The simulation structure of the sub station

The simulations isolates circumstances in order to see the influence these various conditions might have on each other in terms of the **12th** and **24th** harmonic introduced into the DC supply grid. The simulation of all these circumstances is critical because these different scenarios can not be simulated on an actual sub station from a safety perspective and a financial perspective.

The simulations will thus serve as being the reference to actual measured data to try and isolate specific operational circumstances such as un-balanced phases or faulty harmonic filters. For example, when 600 Hz voltage amplitudes are measured; the measured values can be used to diagnose problem conditions in the sub station.

The main aim is to do condition monitoring of the DC sub station harmonic filters, but if the results are inconclusive (between a working filter and a malfunctioning filter) the study will try and give the data user other options that may have an influence on the **600** and **1200** Hz harmonics, thus trying to diagnose the harmonic sources.

The conclusion of the chapter (section **4.11**) will summarize all the investigated harmonic sources for **600** and **1200** Hz frequency bands with the aim of helping to diagnose the condition of the sub station influencing the performance of the harmonic filters.

4.2 Simulation background

The simulation of the ideal DC sub station is done using **MATLAB SIMULINK** where the simulation is solved using differential equations, ODE solvers. There are various ODE solvers that have specific purposes, but the best all round solver is the **ODE45** solver. In the case of the simulations in this chapter the **ODE45** solver used too much of the computer's memory, so a moderately stiff or "relaxed" solver was used, namely the **ODE15** solver.

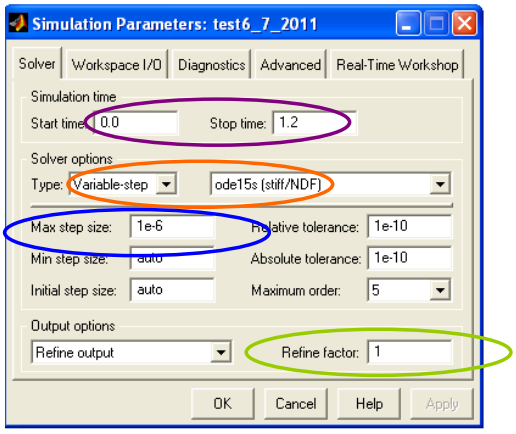

Figure 4.2.1 – The screenshot of the solver used for the simulation

In figure **4.2.1** the purple region shows the simulation time. The reason for making the simulation **1.2** seconds is that **1** second of data is needed for ease of use and the first **0.2** seconds of the simulation the sub station has not reached steady state, thus the first **0.2** seconds of data is discarded from the computation of the FFT.

The **orange** region shows that the **ODE15** solver uses variable step sizes in the computation of the differential equations. The model decides the optimal step size for every differential equation it computes based on the complexity of the equation.
The variable step poses a problem when the FFT of the data is computed because of the variable time step being converted to a variable frequency step. When the FFT is done the data must be interpolated by X-axis data with a fixed step size, thus converting the data to ultimately have fixed frequency steps. Having **1** second of data simplifies the interpolation process.

The **blue** circled area indicates the maximum step size the solver is allowed to take, thus ensuring that data would not be lost. The maximum step size relates to a minimum sampling frequency.

The **green** circled area indicates that the model is not allowed to "filter" the solver solutions in an effort to restrict data from further being rounded by the solver.

The sub station that is simulated is shown in figure **4.2.2**.

Representation of a DC sub station used for simulation

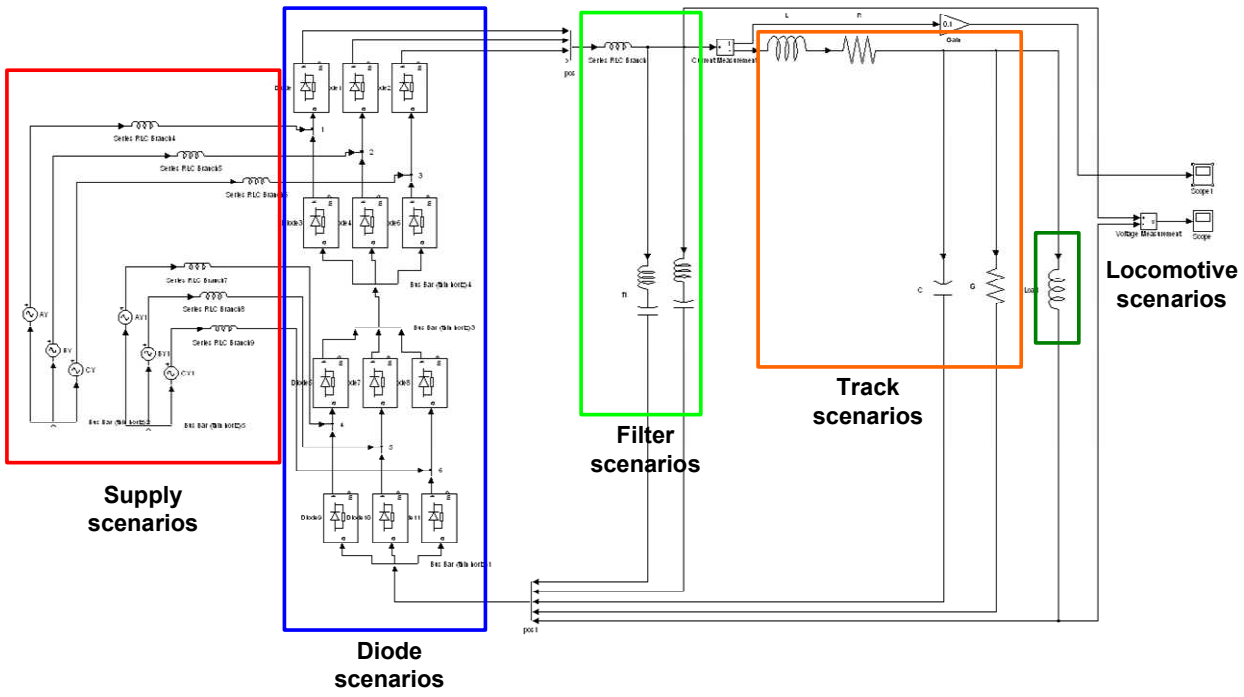

Figure 4.2.2 – The Simulink schematic for the DC sub station

A rail section is considered as being about 20 km long and the sections are fed from either side by a DC sub station. For the purpose of the document an arbitrary distance of 1 km from the sub station was chosen and the sub station was isolated, thus only one sub station feeds the section.

The reason for isolating the sub station is because of the fact that sub stations influence each other when harmonics are generated. Every colour region in figure **4.2.2** shows a region a simulation is going to be conducted in.

4.3 Simulation of an ideal sub station

4.3.1 The frequency simulation of the ideal sub station

The simulation of an ideal sub station will serve as the bench mark for operating failures of various components of the DC sub station during operation. The aim is to eventually measure the sub station conditions and have a **600** and **1200** Hz threshold for the condition monitoring of sub station harmonic filters. The threshold is the voltage measurements for the ideal sub station with / without the harmonic filters. Throughout the section the graphed data is representative of the DC sub station simulation of figure **4.2.1.** The simulation parameter of interest is the DC bus voltage, thus the output of the station.

The reason for choosing the voltage measurement is because it can be realised in practice via measurement coils on the rails or on a moving rail vehicle. The disadvantage is that the parameters outside the sub station have potential differences across the components, which will influence the measurements if they are made at the end of a rail section. To eliminate the problem of voltage drops across measurement influencing the overall voltage measurements the measurements have to be made at the exit of the sub station.

The ideal sub station was simulated and voltage simulation of the sub station is presented in this section of the document.

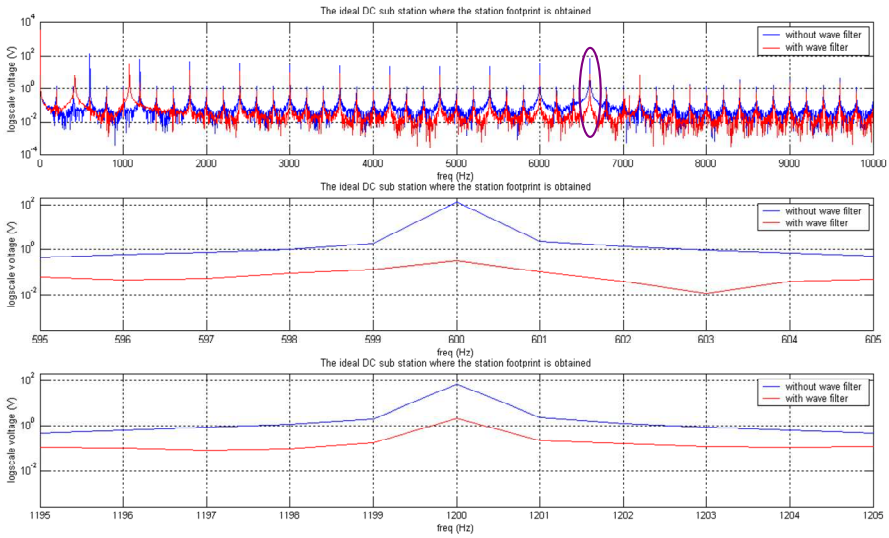

Figure 4.3.1.1 – The simulation of the ideal DC sub station with and without the harmonic filters, the top figure illustrates the simulated data for a 10 kHz spectrum, the middle figure illustrates the zoomed area around the 12th harmonic and the bottom figure illustrates the zoomed area around the 24th harmonic.

The graphed data for the ideal sub station clearly shows the impact the filters have on the generated **12th** and **24th** harmonic, granted that the filters are assumed to be "perfect" or 100% efficient. The purple circled area on the top figure in figure **4.3.1.1** indicates amplitude higher than the harmonics lower in frequency - this is not characteristic of what harmonic theory teaches us. The only possible reason for this is that resonance occurs at that frequency.

The simulation of the DC sub station has the primary focus of zooming in on the **12th** and **24th** harmonics, where the data without the harmonic filters serves as the worst case threshold and the data with the harmonics filters in place as the best scenario. So when a DC sub station's DC bus voltage is measured it will be possible to quantify the whether the harmonic filters are effectively suppressing the harmonics (**12th** and **24th**) and possible reasons for the reduced efficiency such as blown rectifier diodes, AC supply unbalance and even blown filter components or filter components being out of specification.

In order to quantify the upper and lower bounds of the ideal sub station the amplitudes of the **12th** and **24th** harmonics are measured. The measured values are given as follows:

	with harmonic filter	without harmonic filter
600 Hz	0.3295 V	133.2263 V
1200 Hz	2.16 V	63.38 V

Table 4.3.1.1 – The amplitude values for the simulated ideal DC sub station

The **12th** and **24th** harmonic amplitude values are summarised in table **4.3.1.1** and the red column shows the amplitude values for the simulated sub station without harmonic filters. The green area indicates the various amplitude values for the simulated sub station when the harmonic filters are present. The red column values will indicate the upper bound of respective harmonic amplitudes and the green column will be used as the lower bound of the respective harmonic amplitudes. These limits/bounds will be used to asses the efficiency of the harmonic filters at the **12th** and **24th** harmonics.

The rest of chapter **4** deals with the influence of various operating conditions on the efficiency of the harmonic filters, thus giving the data user a reference framework for assessing measured data and finding possible factors (operating fault conditions) influencing the efficiency of the harmonic filters.

4.3.2 The time domain simulation of the ideal sub station

This section of the document deals with the time domain analysis of the ideal sub station. The aim of the section **4.3.2** is to show the difference between the time domain simulations and the frequency domain simulations for the same sub station instance. In various instances the time domain simulations can be used to visually see a waveform containing noise and even oscillations, but it is difficult to accurately analyse the “nature” or source of the noise. The advantage of the frequency spectrum is that the waveform can easily be compared to a noiseless footprint and the source of the noise can be seen where the ideal footprint differs from the actually measured footprint.

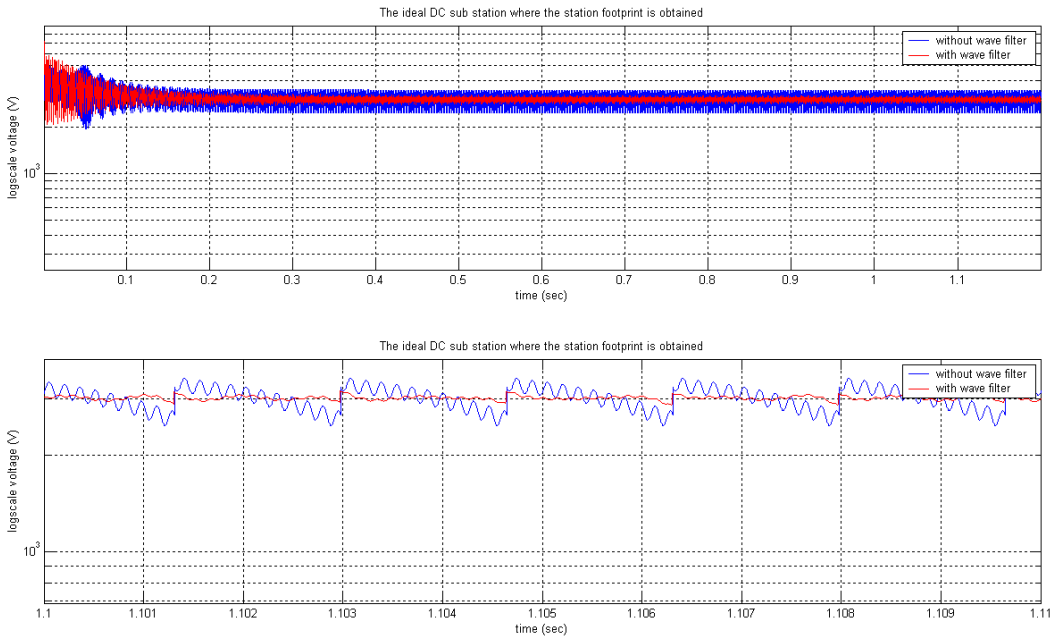

Figure 4.3.2.1 – The time domain simulation of the ideal DC sub station where the figure on the top is the data for the duration of the simulation and the figure at the bottom is a zoomed view of the time signal during steady state

The data in figure **4.3.2.1** illustrates the problem with time domain signal analysis. To do analysis, the time duration of one cycle of a periodic waveform must be known in order to compare similar looking waveform data. Figure **4.3.2.1** has the advantage of indicating when steady state begins, thus the inrush currents etc of the big inductors have stabilised. In the case of the figure above the steady state starting time can be taken as **0.2** seconds. Most of the assumptions made throughout the literature and the modelling process rely on the fact that the generated harmonics are periodic, thus originating from steady state time waveforms.

4.4 Investigation based on snubber operation

Power electric converter devices such as diodes are confronted by various types of stresses relating to the switching capabilities of the device. Snubbers are used to relieve the stresses from over voltages and over currents during turn on and turn off of the devices.

The switching stresses can be reduced by the snubber as follows: [44]

- The snubber limits the voltage applied over the device during turn off transients
- The snubber limits the current transients during turn on
- The snubber limits the rise of current (di/dt) during turn on
- The snubber limits the rise of voltage (dv/dt) during turn off
- The snubber is used to condition or shape the switching trajectory during turn on and turn off

The snubber topology used for Transnet applications is the un-polarized RC snubber. The snubber is responsible for limiting over voltages, because of the reverse current snap-off in the presence of stray inductances.

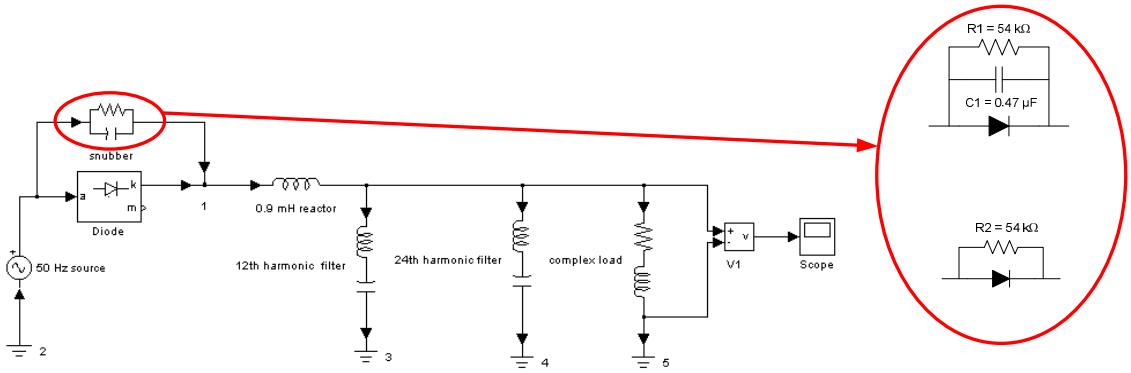

Figure 4.4.1 – The circuit diagram and setup of the snubber test with the two snubber scenarios in red

The values used for the setup was chosen based on the actual component values used in Transnet installations. The complex load was gathered from the 50 Hz impedance of a locomotive and track [39].

simulation parameters:	
snubber C	0.47 µF
snubber R	54 kΩ
reactor L	0.9 mH
12th harmonic filter L	1.759 mH
12th harmonic filter C	10 µF
24th harmonic filter L	1.172 mH
24th harmonic filter C	60 µF
complex load R	4 Ω
complex load L	10 µH
diode forward voltage V	10 V
diode inductance Lon	0 H
diode resistance Ron	0.253 Ω
source frequency Hz	50 Hz

Table 4.4.1 – The values used for the simulation of the snubber efficiency

The following results were obtained from SIMULINK simulations.

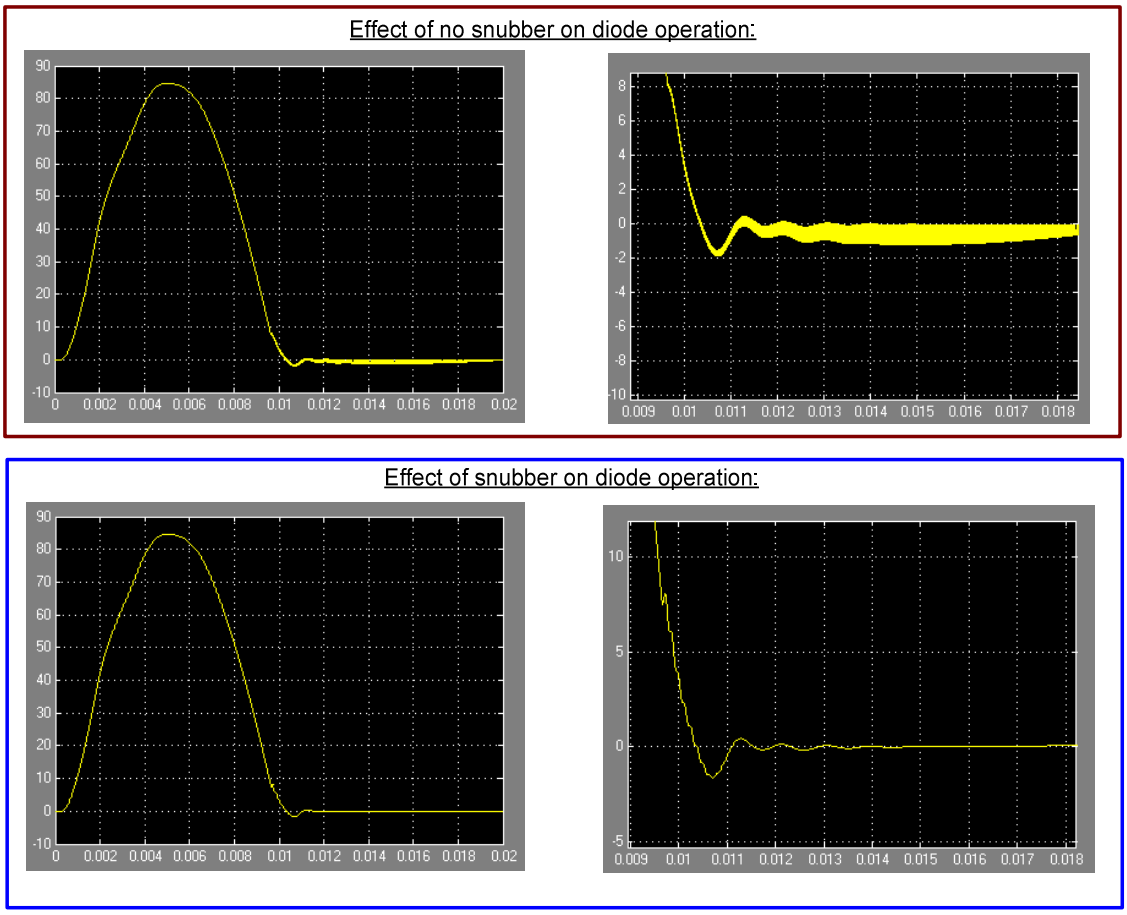

Figure 4.4.2 – The impact of the snubber circuit is evident on the damping of the oscillations, the diode without a snubber is blocked in burgundy and the diode equipped with the snubber used in Transnet is blocked with blue. The X-axis of the graphs is time in seconds and the Y-axis is the voltage across a complex load.

The simulation results in **figure 4.4.2** shows the effect the snubber had on the damping of the recovery of the diode voltage for one switching cycle. The voltage measurement was used because the snubber is utilised to damp voltage (dv/dt) and over voltages.

The aim of the experiment was to prove that the diode operating with a snubber has, as close as possible, linear operation in terms of harmonic production. The outcome of the experiment is thus that for the purposes of the document, the diode operation can be assumed ideal in terms of harmonic production.

4.5 Simulation of supply fluctuations and unbalance

DC sub stations are often confronted by un-balanced AC supplies from the supplier. The term un-balanced refers to voltage harmonics present in one or more of the three AC supply phases, this scenario is often realised when equipment such as variable speed drives are supplied of energy on the same grid. The generated harmonics from utilities on the same grid mitigates towards the DC sub station and these harmonics find their way into the DC supply grid. The types of voltage fluctuations investigated in this section deals with voltage dips on a single phase, phase shifts encountered on a single phase and finally high frequency voltage sources introduced on a single phase.

The section presented investigates the different possibilities that influence supply balance of the AC grid.

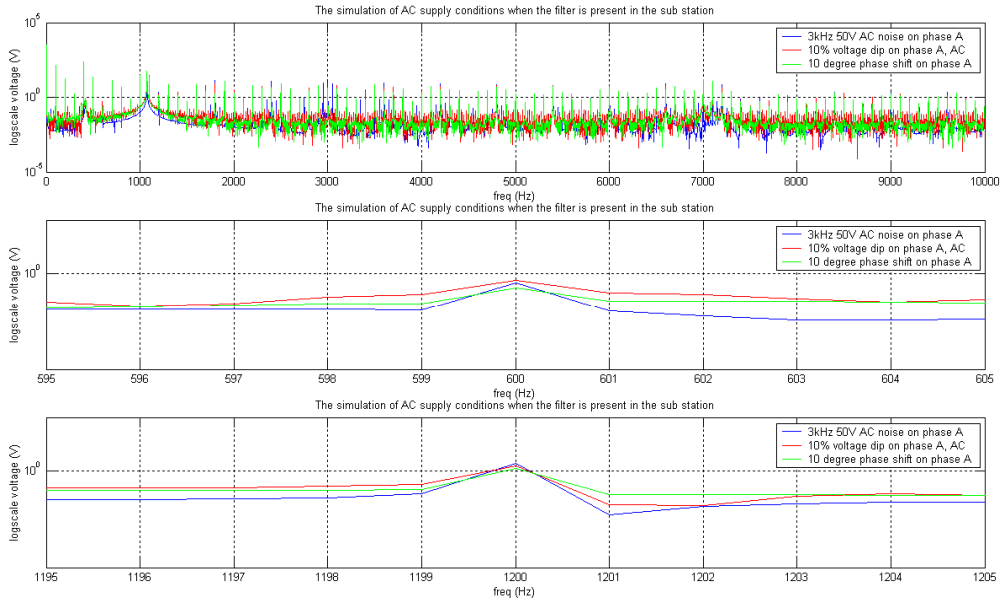

Figure 4.5.1 – The graphs for the simulated voltage fluctuations on one phase of the ideal DC sub station, the top graph illustrates frequency spectrum of the simulation data, the middle graph shows the zoomed voltage data for 600 Hz of the top graph and the bottom graph shows the zoomed voltage data for 1200 Hz for the top graph. The simulations were done while the harmonic filters were active.

A **3 kHz** interference source (**BLUE** graph) was included in the simulation of the ideal sub station to try and isolate the interference source to investigate the effects the interference source would have on the ideal DC sub station harmonics.

The interference source presented a **50V** amplitude at **3 kHz** on the secondary of the ideal sub station and was present on one phase, thus phase **A** star (AY) and phase **A1** star (AY1). The problem with these harmonics is that they are often in the **3 – 100 kHz** range. As mentioned in **Chapter 2**, the high frequency harmonics severely influences transformer saturation which leads to non-linear characteristics of the transformer, thus making the system vulnerable for resonance and other harmonics that can be generated.

Voltage dips (**RED** graph) in energy supply grids is a very common occurrence, due to the fact that various utilities are present on the same grid that provide large amounts of energy to complex loads, thus inrush current and voltage sags on the AC grid is possible. The simulation of the voltage dip is aimed to see the influence on the passive rectified AC to DC bus. The voltage dip simulated is **10%** of the supplied 1330 VAC. A **10%** voltage dip on the supplied AC phases is considered as being quite severe and most under voltage detectors would detect **10%** fluctuations.

Phase shifts (**GREEN** graph) can sometimes be attributed to the manufacturing process of the transformers. The quality of the transformer in part comes down to the tolerances between the phases. In practice there are rules governing the tolerances between phases. A 10 degree phase shift on a phase is possible but probably highly unlikely. The phase shift will be smaller in practice for a working sub station.

The summary of the simulated data for 600 and 1200 Hz is summarised in the following table:

Sub station conditions:	**value: 600 Hz**	**value 1200Hz:**
ideal with harmonic filter	**0.3295 V**	**2.16 V**
10 % VAC dip on phase A with harmonic filter	0.532 V	1.718 V
10 degree phase shift on phase A with harmonic filter	0.251 V	1.358 V
3kHz 50V AC noise on phase A with harmonic filter	0.425 V	2.210 V
ideal without harmonic filter	**133.2263 V**	**63.38 V**

Table 4.5.1 – The summary of the supply fluctuations when the harmonic filters are included in the sub station simulations

The data in table **4.5.1** shows that the most severe supply fluctuation condition is the **10 %** voltage dip, secondly is the **3** kHz source and lastly is the **10** degree phase shift. The table also shows that the harmonic amplitude for the **10** degree phase shift is lower than the ideal sub station with harmonic filter (**green** block).

When looking at the voltage dip and the phase shift we expect harmonics to be generated in the order of 100 Hz and 100 Hz multiples, when only one phase has been simulated for having supply fluctuations. If more phases have been simulated with supply fluctuations, the result will be a lower frequency and its harmonics.

The following figure illustrates the principle where different phased harmonics influence each other.

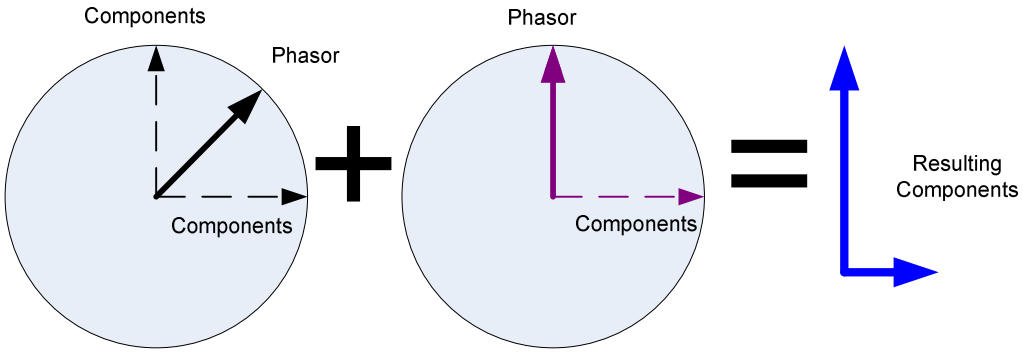

Figure 4.5.2 – The summation of subtraction of components can be seen as breaking the phasors into components and subtracting or adding components.

The voltage dip and the generated 600 and 1200 Hz component is added to the 600 and 1200 Hz component of the ideal sub station (figure **4.5.2**). The phases are of such nature that components of the harmonics are added. The result is a 600 and 1200 Hz harmonic component higher that the 600 and 1200 Hz component for the ideal sub station. The voltage dip amplitudes, in comparison to the ideal sub station amplitudes indicate that voltage dips would have an influence on the performance of the harmonic filters, due to the fact that the filters may not be able to completely suppress the additional harmonic energy.

The reason for the phase shift being lower than the ideal sub station harmonic at 600 Hz can be due to the phase difference between the ideal sub station 600 Hz component and the phase shift 600 Hz component. The harmonics actually subtract from each other, thus the lower resulting amplitude. The phase difference of 10% on one phase actually has a positive influence on the performance of the harmonic filters.

The **3** kHz **50** V source influence on the 600 and 1200 Hz components can be attributed to inter-harmonics or the influence that higher order harmonic have on harmonics below the fundamental component (**3** kHz). A possible reason for that is that the **50** V component is quite large in relation to the other components at **3** kHz. The injected noise source has a negative influence on the performance of the harmonic filters.

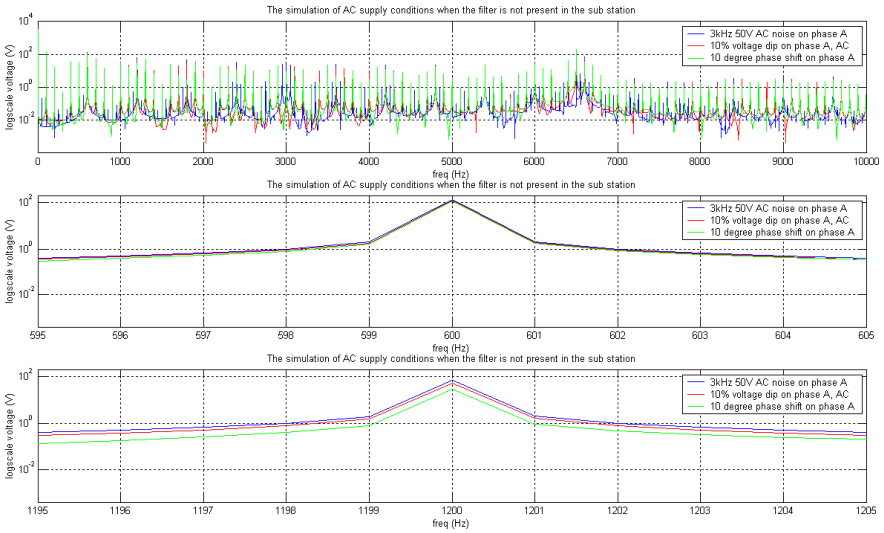

Figure 4.5.3 – The graphs for the simulated voltage fluctuations on one phase of the ideal DC sub station, the top graph illustrates frequency spectrum of the simulation data, the middle graph shows the zoomed voltage data for 600 Hz of the top graph and the bottom graph shows the zoomed voltage data for 1200 Hz for the top graph. The simulations were done while the harmonic filters were <u>not</u> active.

The top graphs in figure **4.5.1** clearly show the impact the harmonic filters have on the absorption of the harmonics compared to figure **4.5.3**. The aim of figure **4.5.3** is to investigate the influence the supply fluctuations have on the sub station when the harmonic filters are not present.

The summary of the simulated data for 600 and 1200 Hz voltage amplitudes are shown in the following table:

Sub station conditions:	**value: 600 Hz**	**value 1200Hz:**
ideal with harmonic filter	**0.3295 V**	**2.16 V**
10 % VAC dip on phase A without harmonic filter	122.470 V	51.529 V
10 degree phase shift on phase A without harmonic filter	111.530 V	28.700 V
3kHz 50V AC noise on phase A without harmonic filter	133.583 V	66.644 V
ideal without harmonic filter	**133.2263 V**	**63.38 V**

Table 4.5.2 – The summary of the supply fluctuations when the harmonic filters are excluded from the sub station

The voltage data for the supply fluctuation simulations are shown in table **4.5.2**. In comparison to table **4.5.1** the amplitude values are large, and this indicates the impact the harmonic filters have on the respective frequency bands. Figure **4.5.2** illustrates the principle why the voltage dips and phase shift produces higher and lower harmonic amplitudes respectively compared to the ideal simulated sub station without harmonic filters.

The main difference between the **600** Hz results and the **1200** Hz results is the scenarios that are the most severe, in figure **4.5.1** the highest amplitude was that of the voltage dip, in figure **4.5.3** the highest amplitude was the **3** kHz noise source. The reason for this is because, the **1200** Hz component is more likely influenced by the **3** kHz interference source than the **600** Hz components because it is the closest. The amplitude of the interference source is large in relation to the other harmonics at **3** kHz and the possibility exists that sub-harmonics exist.

4.6 Simulation of the influence of transformer secondary winding inductance

The simulation of the transformer secondary winding inductance characteristics is important because transformer design flaws and tolerances that are out of specification play a very important role in the balance of the supply to the passive rectifier. The aim of this section is to investigate the influence additional inductance on one phase has on the ideal sub station. The frequency spectrum of the simulated voltage data has been graphed and is presented in figure **4.6.1**.

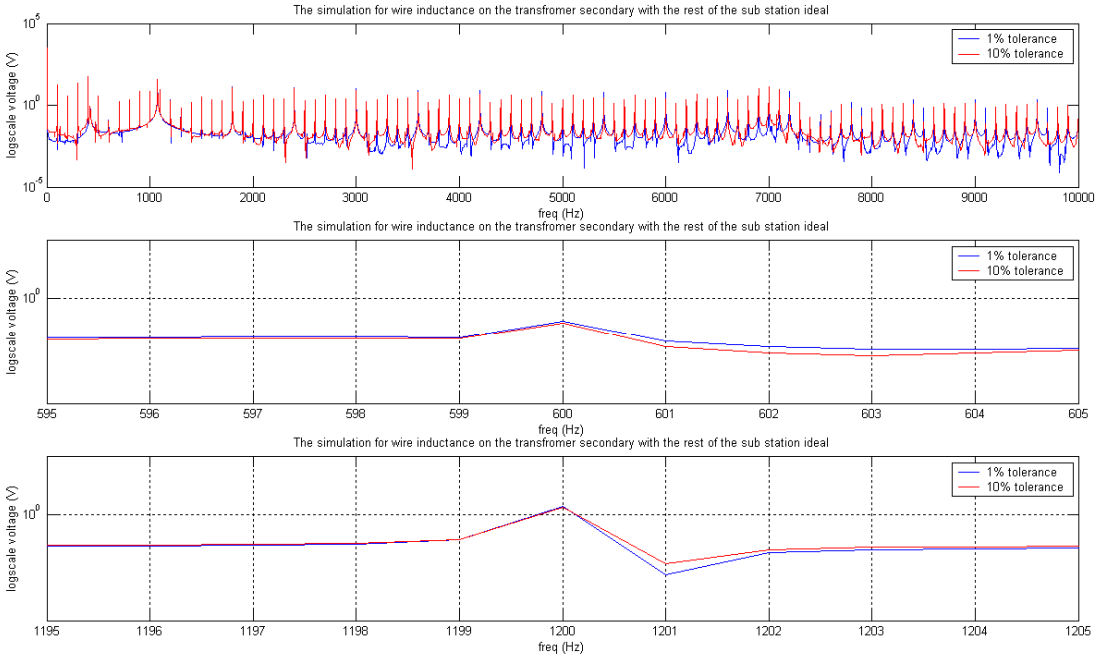

Figure 4.6.1 – The voltage frequency spectrum for the ideal sub station with harmonic filters where the transformer inductance has been changed for one phase, the top graph indicates the total frequency spectrum, the middle graph the 600 Hz zoomed components and the bottom graph the 1200 Hz zoomed components.

The generated harmonics on the top graph in figure **4.6.1** shows the influence a **1%** (**BLUE** graph) and **10%** (**RED** graph) tolerance of the **0.1** mH transformer secondary inductance has on the frequency spectrum. The **10%** tolerance inductor frequency amplitudes are larger than the **1%** tolerance inductor for the lower frequency band (**0 – 2 kHz**). The increased amplitudes are attributed to the **10%** tolerance inductor attributing to a larger un-balance in the phases than the **1 %** tolerance inductor variation.

The following table summarises the obtained amplitude values for 600 and 1200 Hz:

Sub station conditions:	**value: 600 Hz**	**value 1200Hz:**
ideal with harmonic filter	**0.3295 V**	**2.16 V**
wire inductance 1% tolerance	0.124 V	2.150 V
wire inductance 10% tolerance	0.110 V	1.967 V
ideal without harmonic filter	**133.2263 V**	**63.38 V**

Table 4.6.1 – The summary of the simulated inductor tolerance influence on the supply balance and the generated harmonics at 600 and 1200 Hz

The data form table **4.6.1** shows the influence the variation of the inductor value has on one phase on a DC sub station. The **1200** Hz components are very close to the simulation values of the ideal sub station.

From figure **4.5.2**, the principle is shown where harmonic components “add” together if they have the same frequency value. In the case of the inductor tolerance simulation, the harmonic components subtracted. These components are the following:

- The generated **600** and **1200** Hz components from the rectifier
- The generated harmonics from the un-balance caused by the inductor tolerance

The simulation of the influence the tolerance of the secondary wire inductance has on the harmonics generated in the sub station supply circuit follows:

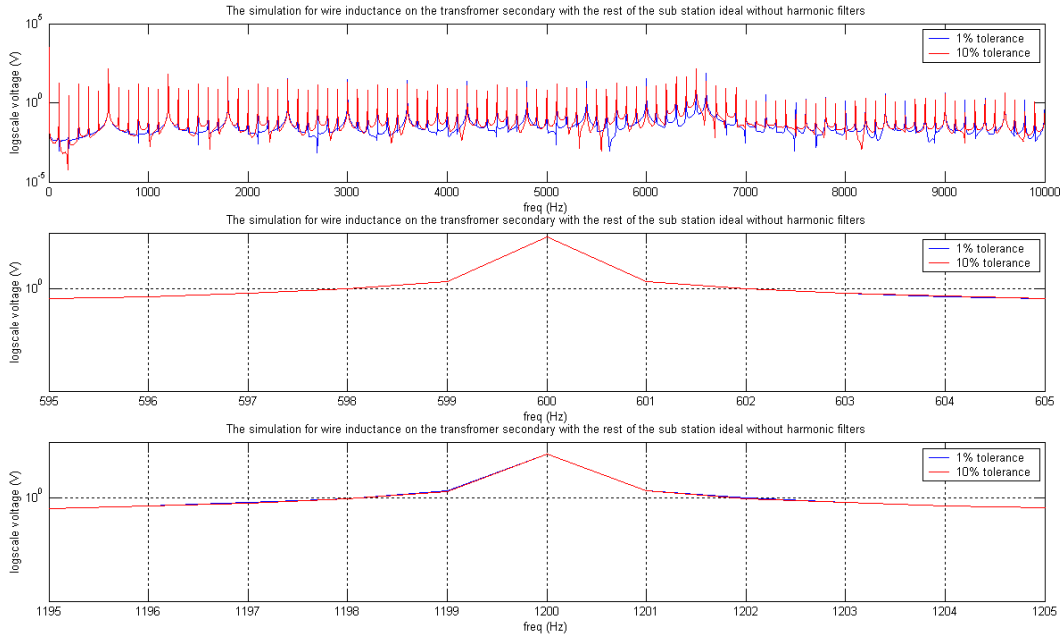

Figure 4.6.2 – The voltage frequency spectrum for the ideal sub station without harmonic filters where the transformer inductance has been changed for one phase, the top graph indicates the total frequency spectrum, the middle graph the 600 Hz zoomed components and the bottom graph the 1200 Hz zoomed components.

The simulation results presented in figure **4.6.2**, the top figure, shows that the **10%** tolerance graph (**red** graph) harmonics are dominant compared to the **1%** inductance tolerance (**blue** graph) between **0** and **3** kHz. The amplitude difference between the **blue** and **red** graph can be attributed to the degree of unbalance in the AC supply to the passive rectifier circuit.

The summary of the inductor tolerance simulations are tabled below in table **4.6.2**.

Sub station conditions:	**value: 600 Hz**	**value 1200Hz:**
ideal with harmonic filter	**0.3295 V**	**2.16 V**
wire inductance 1% tolerance without filters	133.577 V	66.524 V
wire inductance 10% tolerance without filters	133.807 V	64.063 V
ideal without harmonic filter	**133.2263 V**	**63.38 V**

Table 4.6.2 – The summary of the simulated inductor tolerance influence on the supply balance and the generated harmonics at 600 and 1200 Hz with the harmonic filters are excluded from the simulations

The measured amplitude values for 600 and 1200 Hz are very close to the values obtained for the ideal sub station without filters (**red** blocks). The unbalance caused by the inductor tolerance is not large enough to have a large harmonic influence on the 600 and 1200 Hz frequency components.

4.7 Simulation based on diode operation and failure states

The investigation of the failure modes of a diode that makes up the passive rectifier circuit converting AC/DC in the sub station is very important. In practice, various scenarios have been documented where a diode has been installed with reverse polarity, a diode shorts after failure and a diode becomes open circuit after failure. The investigation of the project does not deal with the condition monitoring of the diodes, but when these diodes fail or is installed incorrectly it might have an influence on the generation of harmonics. These circumstances might have an influence on the performance of the harmonic filters.

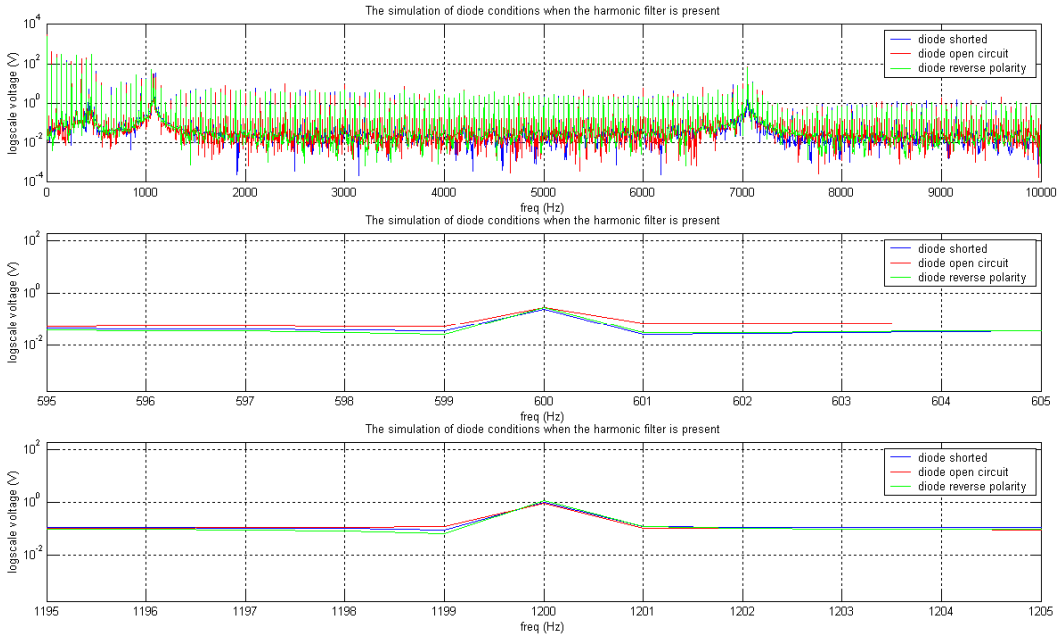

Figure 4.7.1 – The voltage data for various diode operating conditions when the sub station harmonic filters are installed, the top figure illustrates the complete spectrum of the diode scenarios, the middle figure illustrates the zoomed 600 Hz components and the bottom figure illustrates the 1200 Hz components

The diode simulation voltage data is shown in figure **4.7.1** and compared to the figures in section **4.6** the generated harmonics are more - the harmonics are multiples of **50** Hz.

The reason for this is because the “faulty” diode has to switch one of the phase voltages every half cycle, either positive or negative half of a **50** Hz AC supply voltage. With passive rectifiers each diode is responsible for switching once every **50** Hz. The **50** Hz harmonics apply to all the diode operation scenarios.

The summary of the simulated diode operating conditions data is presented in table **4.7.1** below.

Sub station conditions:	**value 600 Hz:**	**value 1200Hz:**
ideal with harmonic filter	**0.3295 V**	**2.16 V**
shorted diode with harmonic filter	0.247 V	0.990 V
diode open circuit with harmonic filter	0.291 V	0.899 V
diode reverse polarity with filter	0.280 V	1.142 V
ideal without harmonic filter	**133.2263 V**	**63.38 V**

Table 4.7.1 – The summary of the simulated diode operating conditions and the generated harmonics at 600 and 1200 Hz while the harmonic filters are included

The simulated voltage amplitudes indicate that the amplitudes for the diode operating conditions are lower than the ideal sub station simulation amplitude. The lower amplitudes can be attributed to the harmonic phases having components 180° out phase with respect to the ideal sub station harmonic components. The result: harmonic components that subtract from each other.

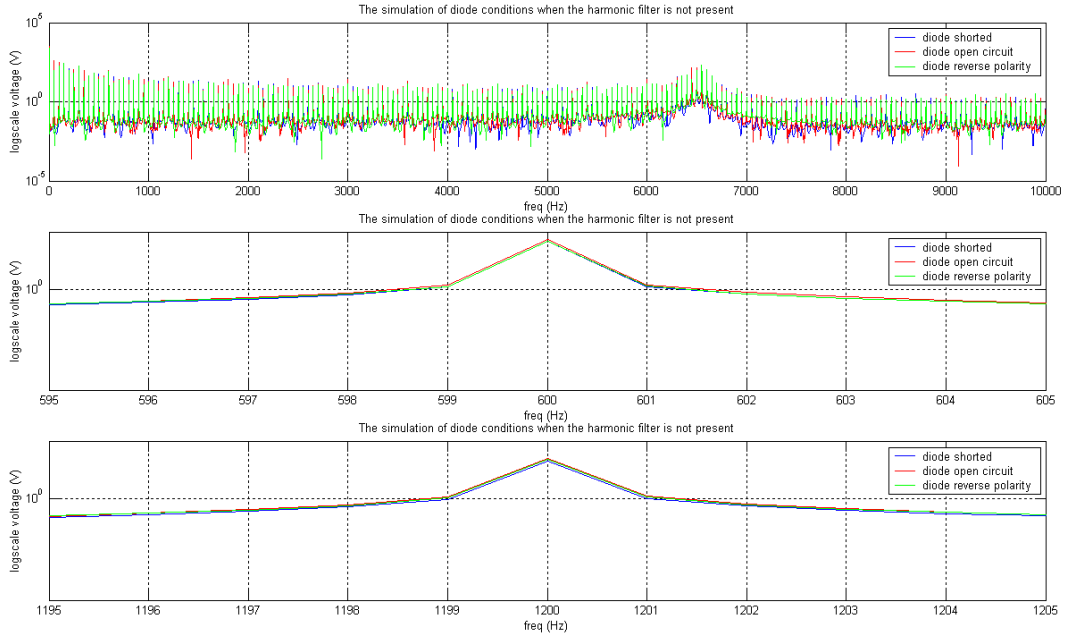

Figure 4.7.2 – The voltage data for various diode operating conditions when the sub station harmonic filters are not installed, the top figure illustrates the complete spectrum of the diode scenarios, the middle figure illustrates the zoomed 600 Hz components and the bottom figure illustrates the 1200 Hz components

The data presented in figure **4.7.2** illustrates the influence the harmonic filters have on the generated harmonic amplitudes in comparison to figure **4.7.1**.

The summary of the results is presented in table **4.7.2** below.

Sub station conditions:	**value 600 Hz:**	**value 1200Hz:**
ideal with harmonic filter	**0.3295 V**	**2.16 V**
shorted diode without harmonic filter	83.844 V	31.514 V
diode open circuit without harmonic filter	99.150 V	38.778 V
diode reverse polarity without filter	87.022 V	35.425 V
ideal without harmonic filter	**133.2263 V**	**63.38 V**

Table 4.7.2 – The summary of the simulated diode operating conditions and the generated harmonics at 600 and 1200 Hz while the harmonic filters are included

The harmonic amplitudes for the diode operating conditions indicate that the amplitudes are lower than that of the ideal sub station without harmonic filters. The amplitudes´ values are relatively close to each other with the biggest amplitude being the open circuit scenarios. This is due to the snubber circuits still being present during the reverse polarity simulation and during the shorted diode simulation there is still continuity through the short (lowest amplitude).

4.8 Simulation of track impedance and the effect on sub station harmonics

The track impedance has been characterised in [42] where the investigation looks at the quantifying track components such as inductance and capacitance and the influence the distance away from the sub station has on the equivalent track impedance. The model includes the influence of the feeder supply (VDC positive), the impedance to earth from the rail, the impedance of the rail and finally the impedance between the two rails.

The figure below, figure 4.8.1 illustrates the equivalent track impedance model.

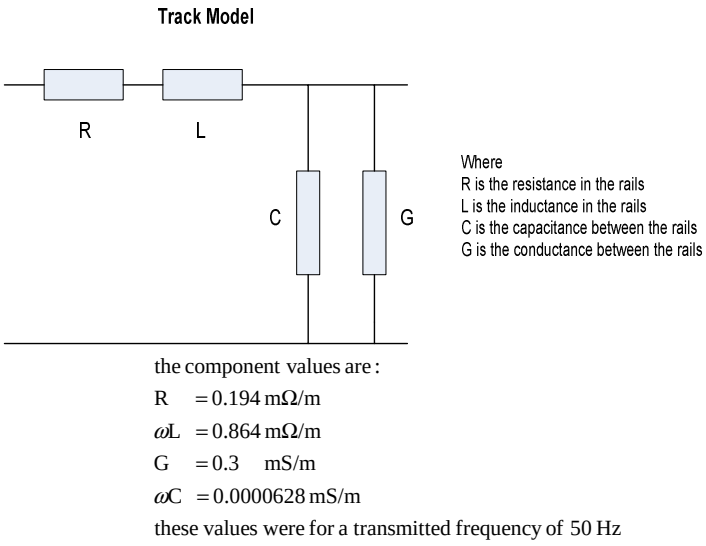

Figure 4.8.1 – The equivalent track impedance model for railway lines being fed from DC sub stations

The component values illustrated in figure **4.8.1** is expressed per meter, due to the fact that the model is dependant on the distance the train is from the source, the DC sub station. The model introduces an additional parameter to the investigation of this document, namely distance from the sub station. In practice, this would not be feasible due to the fact that the condition monitoring rail bound trolley or similar will not be able to measure the distance from the sub station in order to factor in the track model into the measured amplitude values. The assumption is thus made that the condition monitoring measurement will always be done at the same distance from the sub station.

4.9 Simulation of locomotive impedance and the effect on sub station harmonics

Traction locomotives consist of various components that present complex impedances, the components range from induction motor sets to inverter drives responsible for the speed control of the locomotive. One of the components that can be considered as having a substantial influence on the overall impedance of the locomotive is the motor sets. Three assumptions are made regarding the impedance of the locomotive:

- The locomotive impedance is made up of mostly inductive reactance
- The induction motors do not operate in saturation
- The locomotives used in Transnet have the same impedance

The importance of assuming that the motor operation is linear is that the inductance present in the motor is constant. The reason for making the assumption that all the locomotives in Transnet have the same impedance is because it is actually presented as a design guideline to locomotive manufacturers, where the guideline specifies minimum locomotive consist **50** Hz impedance.

The 50 Hz impedance of the sub station was tested by Transnet and the data gathered is presented as follows [43]:

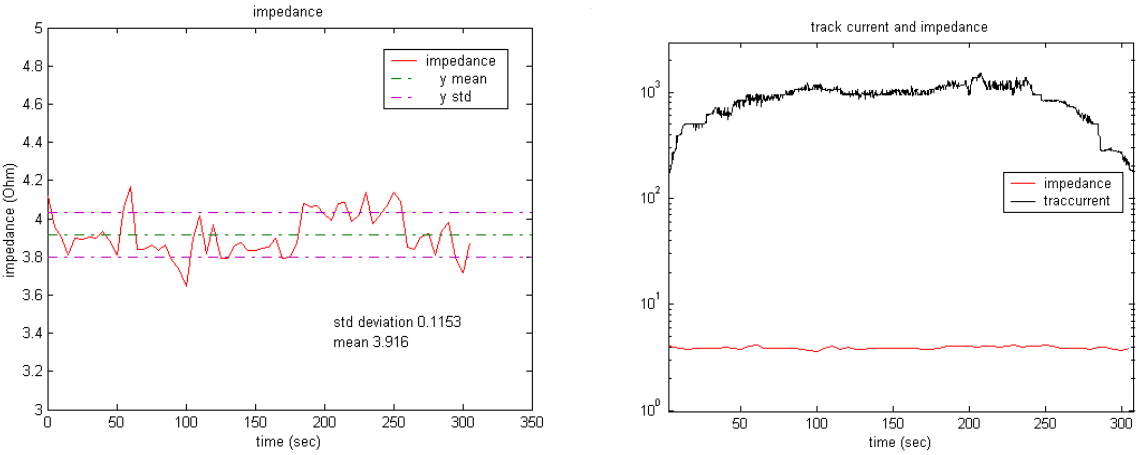

Figure 4.9.1 – The measurement of the impednace at 50 Hz of a locomotive [43]

The results obtained from figure **4.9.1** can be used to find the impedance of the locomotive at **600** and **1200** Hz. The assumption was made that the induction motors on the locomotive presents the dominant impedance of the locomotive. Actual inductance, capacitance and resistance values of the locomotive have not been measured.

$X_{Loco} \approx 4\Omega$ at 50 Hz

thus for 600 Hz:

$X_{Loco} = 2.\pi.f.L$.....[4.9.1]

f is the frequency that increased and the assumption is made that L stays constant

$$X_{Loco} = 4\times(\frac{600}{50})$$

$X_{Loco} = 48\Omega$ for 600 Hz

The same principle is applied for 1200 Hz:

$X_{Loco} = 96\Omega$ for 1200 Hz

The inductnace can be calculated from (4.9.1):

$$L = \frac{X_{loco}}{2.\pi.f}$$

$L = 0.01273H$

$L = 12.73mH$

The above formulae present a way of calculating the **600** and **1200** Hz impedance of the locomotive. The assumptions made have a linear effect on the increase of the locomotive impedance.

The results for the locomotive simulations while the sub station harmonic filters are present are shown in figure **4.9.2**.

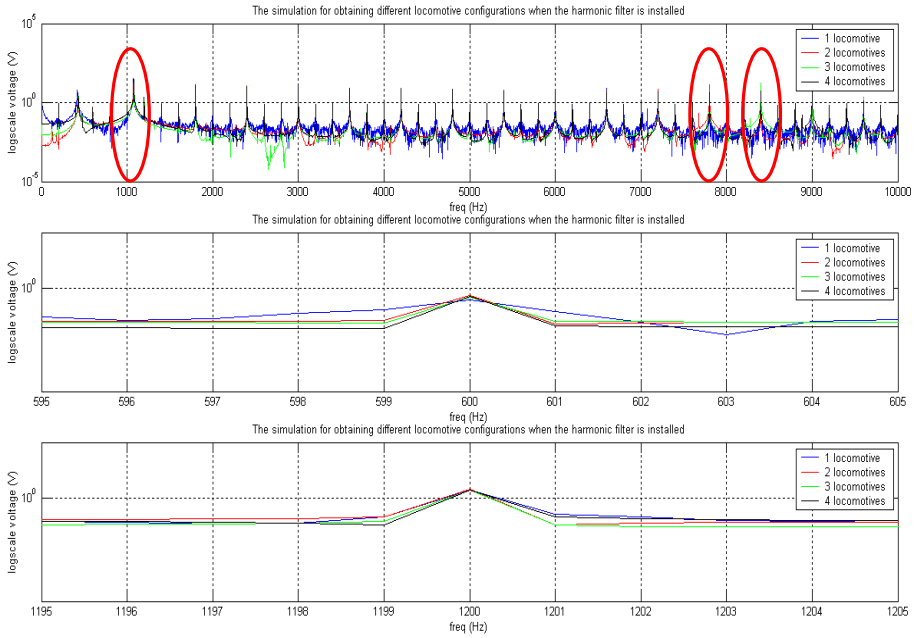

Figure 4.9.2 – The simulated data for various locomotive scenarios while the harmonic filters are installed, the top figure shows the simulated frequency spectrum, the middle figure illustrates the 600 Hz zoomed spectrum and the bottom figure shows the 1200 Hz zoomed spectrum

The influence of the locomotive inductance is expected to have resonance at different frequencies, due to the inductance having a dominant influence on the sub station supply circuit. The top figure in figure **4.9.2** confirms that resonance is present at various frequencies for the various numbers of locomotives in the simulation. The **red** circled areas indicate resonance.

The summary of the 600 and 1200 Hz amplitudes for the sub station with harmonic filters are given below in table **4.9.1**.

Sub station conditions:	**Value: 600 Hz**	**value 1200Hz:**
ideal with harmonic filter	**0.3295 V**	**2.16 V**
1 locomotive fed by sub station with filters	0.3295 V	2.16 V
2 locomotive fed by sub station with filters	0.513 V	2.263 V
3 locomotive fed by sub station with filters	0.445 V	2.199 V
4 locomotive fed by sub station with filters	0.463 V	2.081 V
ideal without harmonic filter	**133.2263 V**	**63.38 V**

Table 4.9.1 – The amplitude values for the locomotive simulation with the harmonic filters included in the sub station

The data presented in table **4.9.1** does not show any definite "patterns" based on the number of locomotives in the simulation, for instance, **2** locomotives have the highest amplitudes for **600** and **1200** Hz. The only reason for the amplitudes is that the different locomotives have a resulting inductance that causes resonance at different frequencies, where the higher harmonics can be seen as closer to their respective resonance frequencies. The only constant in the data is the fact that the amplitudes for the various locomotives are higher than the amplitude for one locomotive while the sub station is equipped with harmonic filters.

The simulation of the influence that locomotives have on the sub station DC supply voltage circuit when the harmonic filters are excluded can be shown in figure **4.9.3**.

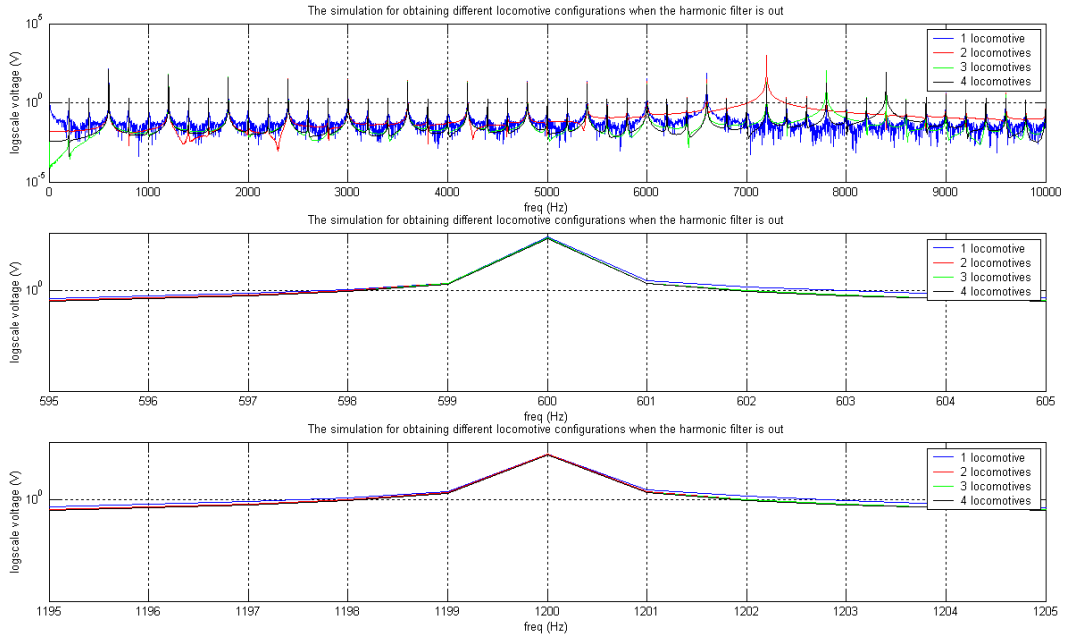

Figure 4.9.3 – The simulated data for various locomotive scenarios while the harmonic filters are disabled, the top figure shows the simulated frequency spectrum, the middle figure illustrates the 600 Hz zoomed spectrum and the bottom figure shows the 1200 Hz zoomed spectrum

The top figure in figure **4.9.3** illustrates the resonance various locomotive numbers per locomotive consist has on the frequency spectrum. The resonance of a **2** locomotive consist is the most severe between **7** and **8** kHz. The effect of resonance in the simulated scenarios for figure **4.9.2** and **4.9.3** differs because the harmonic filters have been excluded for figure **4.9.3**, thus indicating that the inductance and capacitance of the filters play a role with resonance.

The measured amplitude values form the simulations are summarized in table **4.9.2** below.

Sub station conditions:	**Value: 600 Hz**	**value 1200Hz:**
ideal with harmonic filter	**0.3295 V**	**2.16 V**
1 locomotive fed by sub station without filters	133.225 V	66.380 V
2 locomotive fed by sub station without filters	127.004 V	63.494 V
3 locomotive fed by sub station without filters	122.577 V	60.702 V
4 locomotive fed by sub station without filters	119.440 V	59.120 V
ideal without harmonic filter	**133.2263 V**	**63.38 V**

Table 4.9.2 – The amplitude values for the locomotive simulation with the harmonic filters excluded in the sub station

The amplitude values in table **4.9.2** indicate that all the values for the number of locomotives in the locomotive consist are lower than the value for the ideal sub station without harmonic filters. This can be attributed to the summation of harmonics that are out of phase with each other, resulting in lower amplitude values.

4.10 Filter components

The investigation of the influence harmonic filter components has on the performance of the harmonic filters forms the core of the document. The condition monitoring of sub station harmonic filters will largely focus on the components that are subjected to ageing. The harmonic filters employed by Transnet consist of inductors and capacitors. The component that is affected by ageing the most is the capacitor in the harmonic filter.

Filter capacitors in Transnet is monitored in terms of the tolerance it has based on the original value, thus 4 simulations was run, where the **shorted** capacitor and the **20%** tolerance is the worst case scenarios. When the harmonic filter capacitors are outside the specified tolerance (**10%)** the filter can be seen to have a poor efficiency with regard to absorbing the designated frequency component energies. The filter cut off frequencies shift away from the designed **600** and **1200** Hz frequencies, resulting in reduced performance and increased harmonic pollution.

The simulation results are shown in figure **4.10.1** below.

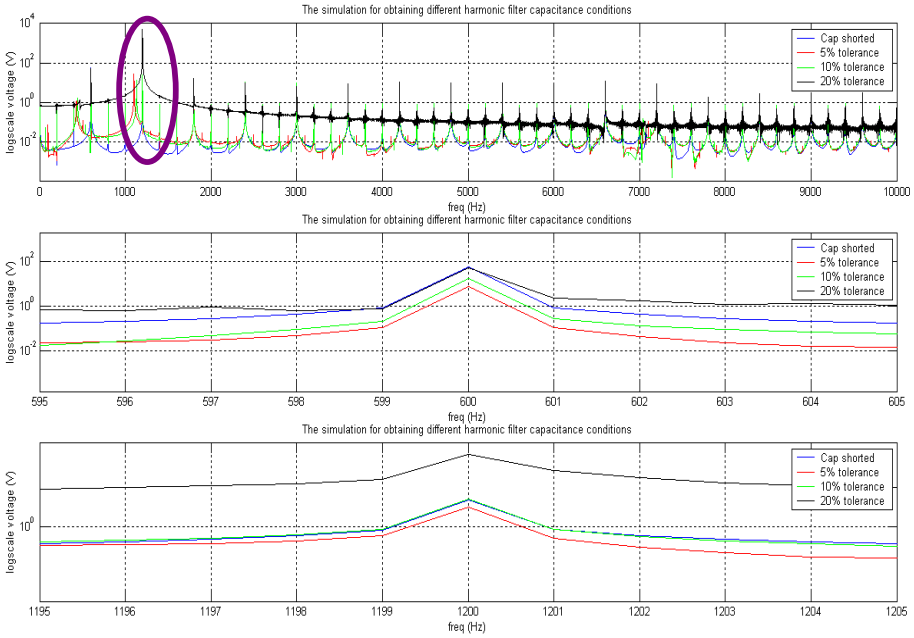

Figure 4.10.1 – The simulation investigating the influence of harmonic filter components on the performance of the filter, the capacitor operating conditions have been simulated, the top figure shows the frequency spectrum, the middle figure shows the 600 Hz zoomed components and the bottom figure illustrates the 1200 Hz components

The data shown in figure **4.10.1** shows the influence the capacitors tolerances have on the performance of the harmonic filters. In practice **5** and **10%** tolerances are still seen to be viable. In figure **4.10.1** the **purple** circled region illustrates the drift of the frequencies as soon as the tolerance of the capacitors exceeds the allowed **10%** value.

A clear indication that the **5** and **10%** tolerance rule has merit can be seen when looking at the **black** graph in the top figure.

The amplitude values for the **600** and **1200** Hz frequency regions are summarised in table **4.10.1** below.

Sub station conditions:	**value: 600 Hz**	**value 1200Hz:**
ideal with harmonic filter	**0.3295 V**	**2.16 V**
harmonic filter capacitor shorted	58.385 V	22.733 V
harmonic filter capacitor 20% tolerance	54.7 V	5897.935 V
harmonic filter capacitor 10% tolerance	17.269 V	25.520 V
harmonic filter capacitor 5% tolerance	7.858 V	10.022 V
ideal without harmonic filter	**133.2263 V**	**63.38 V**

Table 4.10.1 – The summary of the 600 and 1200 Hz amplitudes for the simulation of the influence of capacitor tolerances and short circuit on the sub station

The amplitude values in table **4.10.1** shows that for **600** Hz the two worst case simulations (shorted capacitor and **20%** tolerance) the values are reasonably close. In the case of the **1200** Hz amplitudes, the **20%** tolerance had very high amplitude values for unexplained reason apart from the possibility of resonance. Although the **5** and **10%** tolerance capacitance is seen as being within specification, it can clearly be seen that the performance of the filters will be drastically reduced based on the amplitude values for 600 and 1200 Hz.

4.11 Conclusion

The condition monitoring of DC sub stations entails building a reference framework of operating scenarios in order to accurately diagnose faulty equipment that contribute to the 12^{th} and 24^{th} harmonics in the supply grid. The ideal condition monitoring scenario would be if the filters were installed and works properly (best case) and when the filters are not included in the sub station (worst case). This is not always the case and when measured values at 600 and 1200 Hz are not conclusive with regard to the best and worst case, a reference framework must exist where operating scenarios as broken diodes or out of specification filter capacitors have been simulated.

The advantage of the simulations is the fact that scenarios can be simulated that would not have been possible in practice due to safety and financial reasons. The disadvantage is that it is almost impossible to simulate all the possible operating scenarios, thus a complete reference for all operating conditions will probably not be possible. For this chapter, the ideal sub station was simulated to obtain the benchmark for the sub station testing with and without harmonic filters. The sub station was simulated with only one “fault” condition at a time, to try and quantify the condition in terms of 600 and 1200 Hz.

The simulation of the sub station was done in **MATLAB SIMULINK** and the data was simulated in the time domain, with the **FFT** done afterwards. Various differential solvers were tried and the optimal solution was found to be the **ODE15** solver from **SIMULINK**.

A tabled reference framework for the simulation of the sub station with operating scenarios is presented in table **4.11.1**.

Sub station conditions:	**value: 600 Hz**	**value 1200Hz:**
ideal with harmonic filter	**0.3295 V**	**2.16 V**
harmonic filter capacitor shorted	58.385 V	22.733 V
harmonic filter capacitor 20% tolerance	54.7 V	5897.935 V
harmonic filter capacitor 10% tolerance	17.269 V	25.520 V
harmonic filter capacitor 5% tolerance	7.858 V	10.022 V
1 locomotive fed by sub station without filters	133.225 V	66.380 V
2 locomotive fed by sub station without filters	127.004 V	63.494 V
3 locomotive fed by sub station without filters	122.577 V	60.702 V
4 locomotive fed by sub station without filters	119.440 V	59.120 V
1 locomotive fed by sub station with filters	0.330 V	2.216 V
2 locomotive fed by sub station with filters	0.513 V	2.263 V
3 locomotive fed by sub station with filters	0.445 V	2.199 V
4 locomotive fed by sub station with filters	0.463 V	2.081 V
shorted diode with harmonic filter	0.247 V	0.990 V
diode open circuit with harmonic filter	0.291 V	0.899 V
diode reverse polarity with filter	0.280 V	1.142 V
shorted diode without harmonic filter	83.844 V	31.514 V
diode open circuit without harmonic filter	99.150 V	38.778 V
diode reverse polarity without filter	87.022 V	35.425 V
wire inductance 1% tolerance with filters	0.124 V	2.150 V
wire inductance 10% tolerance with filters	0.110 V	1.967 V
wire inductance 1% tolerance without filters	133.577 V	66.524 V
wire inductance 10% tolerance without filters	133.807 V	64.063 V
10 % VAC dip on phase A without harmonic filter	122.470 V	51.529 V
10 degree phase shift on phase A without harmonic filter	111.530 V	28.700 V
3kHz 50V AC noise on phase A without harmonic filter	133.583 V	66.644 V
10 % VAC dip on phase A with harmonic filter	0.532 V	1.718 V
10 degree phase shift on phase A with harmonic filter	0.251 V	1.358 V
3kHz 50V AC noise on phase A with harmonic filter	0.425 V	2.210 V
ideal without harmonic filter	**133.2263 V**	**63.38 V**

Table 4.11.1 – The summary of the various operating scenarios for the DC sub station, the RED region is the ideal sub station without harmonic filters and the GREEN region is the ideal sub station when the harmonic filters is included

The amplitude value for the **20%** capacitor tolerance **1200** Hz component is large and will cause a sub station trip/failure. When amplitudes are measured in practice it is possible to have more than one scenario on table **4.11.1**, an example of such situations follows.

EXAMPLE:

The measurements have been conducted on a DC sub station and the value of **0.45 V** for **600** Hz and **2.2 V** for **1200** Hz was measured. The values do not clearly indicate that the sub station filters are working, thus looking at table **4.11.1**, the following possibilities can be read from the table:

Sub station conditions:	**value: 600 Hz**	**value 1200Hz:**
3 locomotive fed by sub station with filters	0.445 V	2.199 V
4 locomotive fed by sub station with filters	0.463 V	2.081 V
3kHz 50V AC noise on phase A with harmonic filter	0.425 V	2.210 V

The three possibilities are in the region of the measured values for 600 and 1200 Hz, but the test vehicle has known impedances at these frequencies. The result might be that a **3** kHz interference source is present on one of the phases.

The simulation scenario such as the 3 kHz interference source is hypothetical and illustrates the principle of operation for the document. The aim of the simulation chapter is to verify the model results. The verification of the model is not possible due to the complexity of the model as stated in chapter 3. The actual measurement will be used to verify that the assumptions made for simulation did not have an influence on the simulations compared to the actual measurements.

CHAPTER 5: ACTUAL TESTING

5.1 Introduction

The actual testing of the DC sub station involves the measurement of the voltage harmonics at the output of the DC sub station. In general DC sub stations employed by Transnet are old, 20 years and older. The aim of the chapter is summarised below.

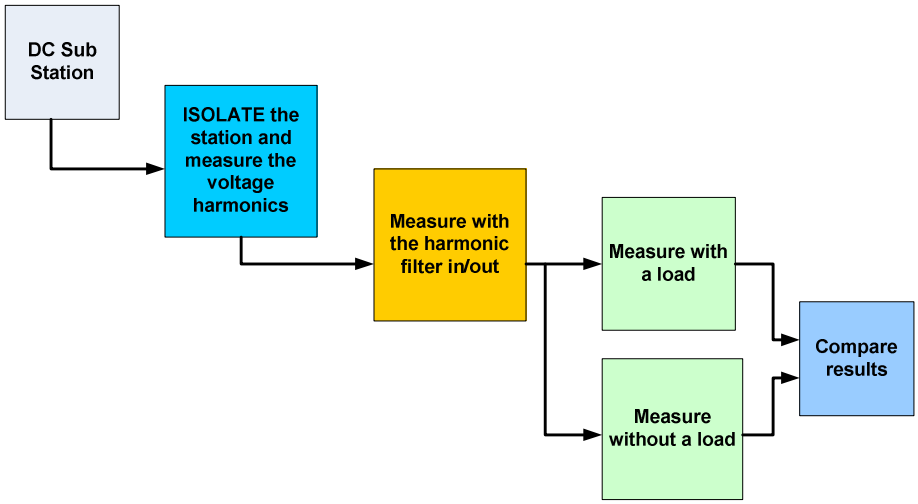

Figure 5.1.1 – The aim of the actual measurements chapter, the process runs from the top (left) to the bottom (right)

The way the energy is transferred in the DC supply grid is by means of parallel sub stations, thus having a common DC bus voltage. The sub stations contribute to the energy demand in ratios proportional to the distance from the presented load. From a harmonic mitigation perspective having all the DC sub stations in parallel means that a “sick” sub station injects harmonics into the entire grid. The condition monitoring of a sub station might be influenced by the neighbouring sub stations. The isolation of the adjacent sub stations is cumbersome and not advised because occupation of the lines are also needed, the same constraints the old harmonic filter monitoring has.

The actual measurements on the sub station will give great insight into how many factors influence the sub station harmonics and their amplitudes.

5.2 Test procedure

The voltage measurement data will be used to obtain amplitudes per frequency interval of the DC sub station for various operating scenarios. The aim of the experiment is to obtain voltage harmonic data to validate the results of the simulation chapter, chapter **4**. Validating the simulated data will verify the assumptions made in terms of component operation and linearity. The validation of the data will also verify the assumption that a DC sub station can be isolated from the DC supply grid, thus the reason for measuring the DC sub station voltage harmonics.

5.2.1 Test setup

The test setup for the DC sub station can be illustrated as follows:

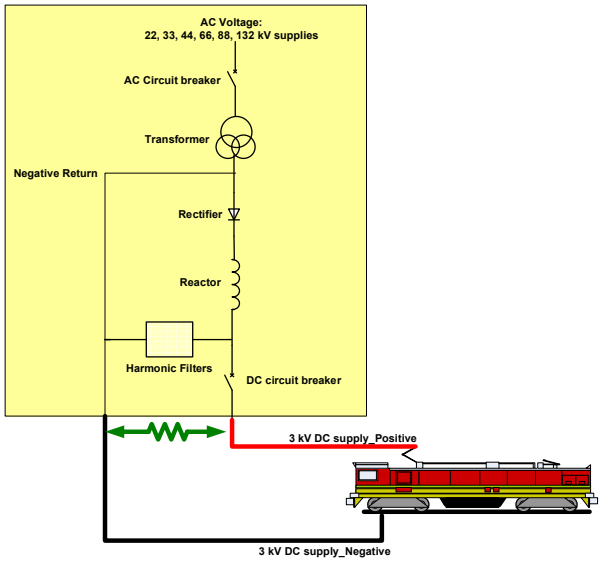

Figure 5.2.1 – The proposed test setup for the DC sub station

For the measurement of the voltage harmonics (**green** lines) a potential divider is proposed, where the voltage measurement has a **600:1** ratio , thus a **3000 VDC** waveform will be represented by an **5V VDC** waveform. The ratio is realised using linear elements such a high MΩ rated carbon resistors. To isolate the voltage measurement a fibre optic measurement device is proposed and the assumption is made that the fibre optic measurement device is linear. To ensure that the voltage measurement data is sufficient, the Nyquist sampling criteria is used where the bandwidth of the fibre optic channel is at least **10 kHz** if a frequency reach of the harmonic data is set at **5 kHz**.

The data acquisition device used will consist of a National Instrument USB-9229 and a laptop. The USB-9229 has to comply with the following:

- Channel to channel isolation
- Channel to ground isolation
- At least 30 V reach for the measure waveform (USB-9229 has a 60 V reach)
- 1 voltage sampling channel
- 24-bit resolution to ensure accurate measurement even at low voltages, thus a 24 bit 10V reach for the measurement channels has a 0.00000059604V/segment resolution.
- At least 10 kHz sampling rate in order to effectively measure 5 kHz without aliasing
- Anti aliasing filters to reduce possible waveform distortion

A laptop with National Instruments Labview software shall be used and software shall be developed for the acquisition and saving of the data. The following data structure shall be used:

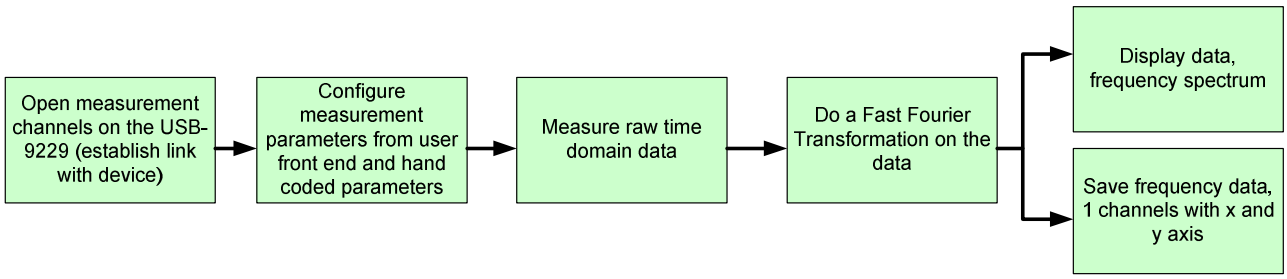

Diagram 5.2.1 – The conceptual representation of the data acquisition software

The validation of simulations with regard to actual measured data is important, because the simulation data plays the role of being a reference for DC sub station operating conditions that can not be realised during normal train operation, such as shorted and faulty diodes and supply unbalance. The most important measurement is to get the lowest and highest readings for the condition monitoring of the filters by measuring the same sub station with and without harmonic filters. In practice this is obtained by taking out the series fuse for the filters.

The following figures are used to illustrate the installation and preparation of the sub station for measurements.

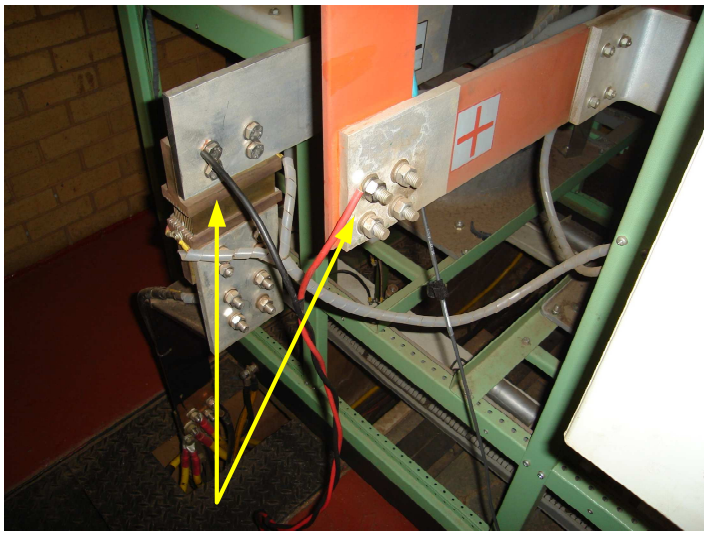

Figure 5.2.2 – The installation of the potential divider in the DC sub station, the yellow arrows indicate the connections, where the red wire is on the positive bus bar and the black wire on the negative bar

The measurements in the sub station were done by using optic fibre in an attempt to make the measurements as safe as possible.

Figure 5.2.3 – The fibre optic setup for the sub station where the yellow numbers indicate the various components used

The yellow numbers used in figure **5.2.3** indicates the following:

1. The potential divider used to step the voltage down from **3330** VDC to **5** VDC to be able to measure the voltage harmonics.
2. The fibre optic transmitter consisting of a battery, a DC to DC converter and the transmitter, the transmitter has a bandwidth of **25** MHz and a reach of **10**V peak to peak.

The optic fibre was tested at the maximum sampling frequency of **25** kHz and there was no distortion or attenuation of the supplied waveform at maximum expected measurement voltage. The test waveform was supplied by a calibrated frequency generator. The results obtained indicate that the fibre optic transceiver does not introduce a factor into the actual measurements.

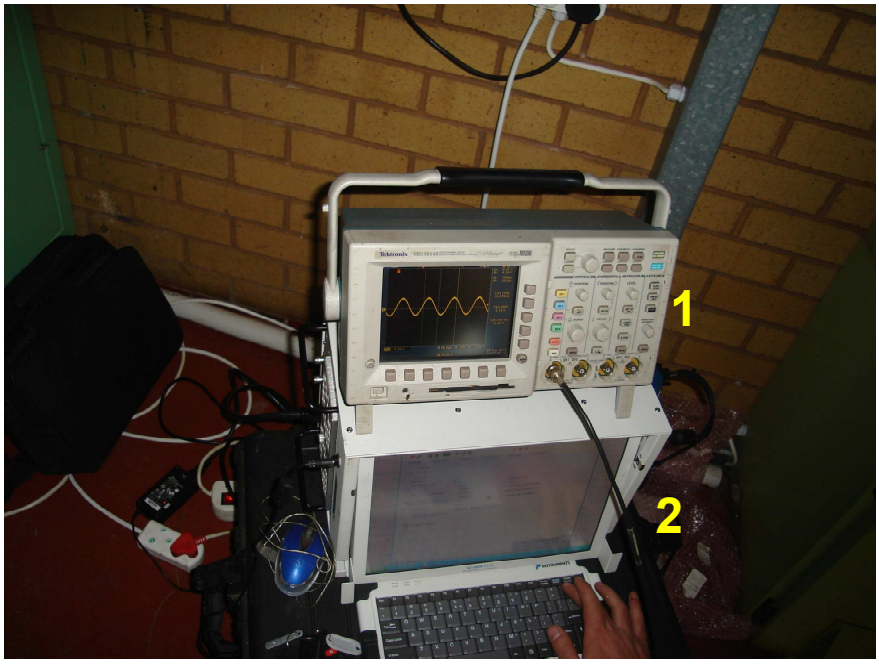

Figure 5.2.4 – The measurement devices used for the acquisition of the voltage data, the yellow numbers indicate the equipment used

The equipment used in figure **5.2.4** is the oscilloscope used for verifying the measurements and for measuring the initial testing conducted on the fibre optic devices. The second device is used for data acquisition, the National Instruments DAQ. The DAQ is equipped with a Windows XP operating system with National Instruments Labview installed on it, thus the program written for data acquisition for this specific study is loaded onto the machine and data is captured. The program can be found in **Appendix A**.

Figure 5.2.5 – The components that make up the harmonic filter, the photo on the left is the inductors, the middle photo is the series fuse and the photo on the right is the capacitor

The problems generally encountered with the measurement of DC sub station components is that there is no guarantee that the components are within specification when taking into account that the most recent surveys were done 1 year ago. The present topology of filter connection sees that the filters are paralleled to the main line which is live, thus the tolerance of the components could not be tested without disrupting the train traffic.

5.2.2 The Sub station test procedure

The proposed test setup for the sub station under test is that is totally isolated from the grid by opening the section breakers on either side of the sub station. This will ensure that adjacent sub stations do not interfere with the measurements. The sub station under test, after complete isolation, will be subjected to a load (10E max 600A), thus ensuring linearity and eliminate possible saturation of the sub station equipment because the sub station can deliver 1200 A.

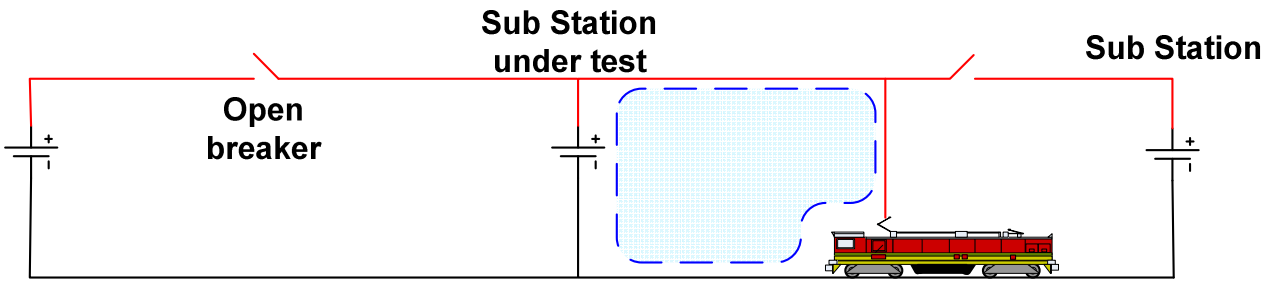

Figure 5.2.2.1 – The isolation principle of the DC sub station

The isolation of the DC sub station is aimed to get the same test setup as was used for the simulation setup. The isolation of the sub station also ensures that adjacent sub station does not influence the sub station under test. The problems encountered during testing at Savannah was that the sub stations were not switched off due to excessive traffic thus the sub stations influenced each other. To further complicate the measurements, the Savannah tests consisted of 6 and 12 pulse sub stations with filters in and out. Nolte test sites sub station could however be isolated and measured properly with and without harmonic filters.

The installation of a potential divider (3330VDC to 5 VDC) is done on the positive and negative bus bars, which is done by loosening one bolt per bar. The isolation of the measurements will be done using fibre and the fibre is driven from batteries, thus completely isolating the operator from the cage.

The proposed testing at two sub stations was as follows:

- Wave filters functioning: (Nolte and Savannah test station)

    1. loco panto down to get the sub station footprint
    2. loco panto up (600A consumption)

- Wave filters out: (Nolte test station)
  The sub station is isolated completely by disconnecting the fuse of the filter. This method is the least invasive to the installation.

    1. loco panto down
    2. loco panto up

The aim of measuring the sub station with and without the presence of the locomotive (load) is to investigate the harmonic being generated in the DC supply grid. In chapter **4** the assumptions were made that the DC supply grid is considered to be lossless and to operate in the linear region of the components, thus the components only generate periodic harmonics and the AC supply is balanced. The measurement of the DC sub station that is isolated will give actual data to evaluate the assumptions made during simulation.

In the case of Savannah station it is not possible to evaluate the no load situation, because the sub stations are in parallel loads very far away is able to absorb energy from the sub station, thus there is no guarantee that the sub station under test is supplying energy to a load.

5.3 Measurement results

The measurement of the sub stations, Nolte and Savannah, is summarised in this section of the chapter. The obtained results for the Nolte sub station test were chosen as being the closest to the simulation scenarios due to the sub station isolation from the grid as well as the fact that the sub station passive filters are within specification based on the most recent survey.

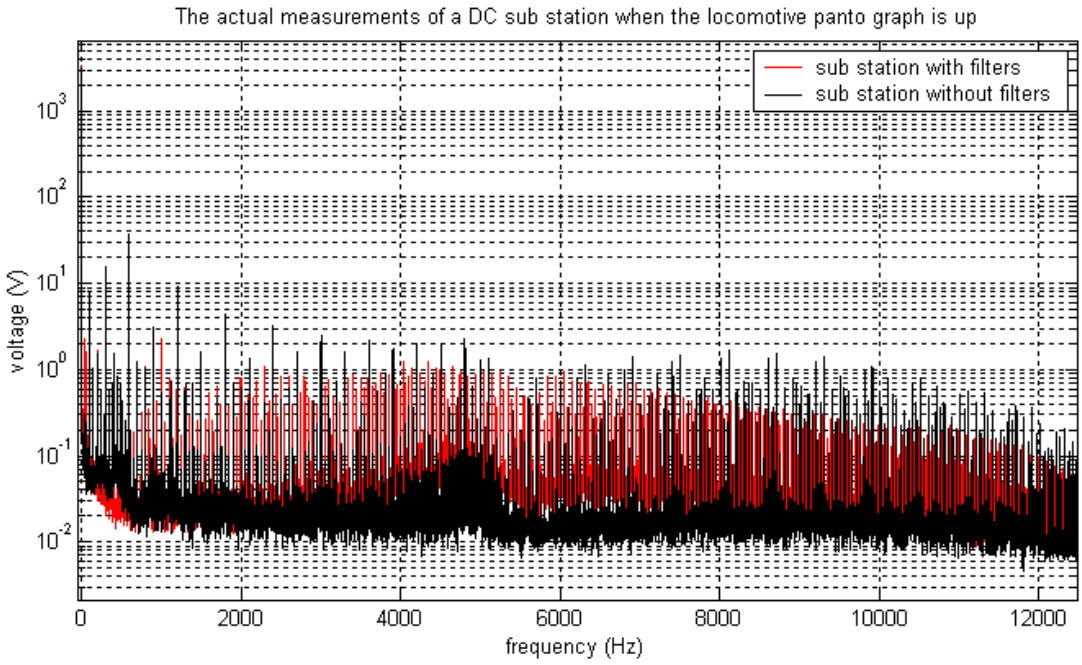

Figure 5.3.1 – The actual result measured at Nolte sub station when the locomotive is presented as a load

The measured scenario in figure **5.3.1** was used as the baselines or thresholds for simulation in chapter **4**. The **red** line indicates the sub station when the filters are present and the **black** line illustrates the sub station without filters. The measurements were made at Nolte sub station after being isolated from the DC supply grid. Effectively the values gathered here will serve as the calibration constants for the data in table **4.11.1.** The comparison between figure **5.3.1** and figure **4.3.1.1** should be made and the first observation that can be made is that the harmonics are more in the case of figure **5.3.1**. This can be expected because the model did not compensate for all the harmonic sources present in the DC supply circuit.

The second observation that can be made is that figure **4.3.1.1** has a definite point of resonance between **6** and **7** kHz but figure **5.3.1** does not have a definite point of resonance over the measured frequency spectrum. The zoomed data for the parameters of interest of figure **5.3.1** is shown below:

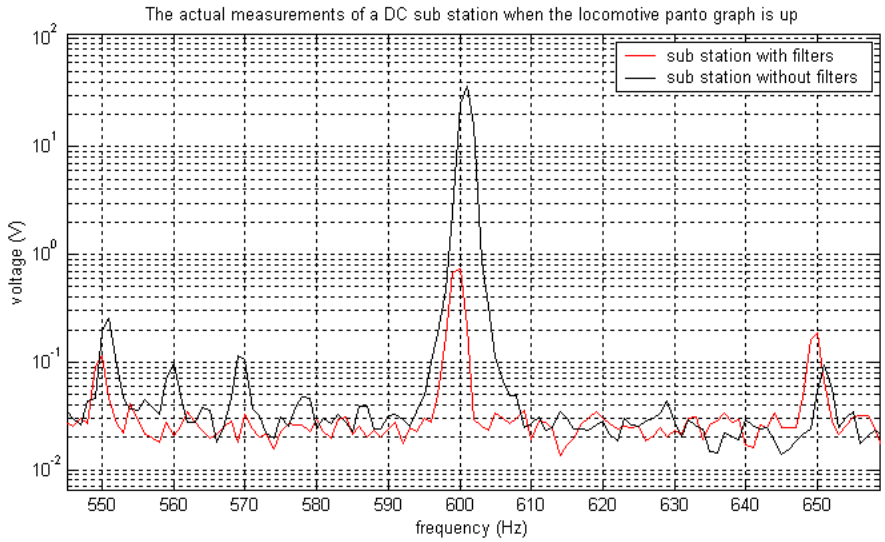

Figure 5.3.2 – The 600 Hz zoomed graph for the sub station measurement when the locomotive presents a load to the sub station

The measured sub station data in figure **5.3.2** already rejects the assumption that the AC supply is balanced, the graphs indicate a drift in the frequency. The **red** graph illustrates the sub station with harmonic filters and the **black** graph represents a sub station without harmonic filters when a locomotive presents a load to the DC supply circuit. The 1200 Hz zoomed area of figure **5.3.1** is presented below:

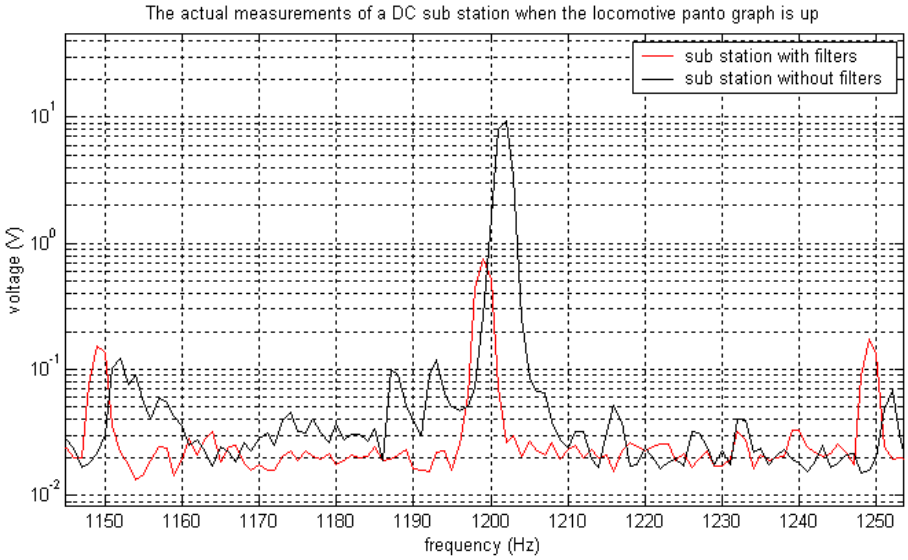

Figure 5.3.3 – The 1200 Hz zoomed graph for the sub station measurement when the locomotive presents a load to the sub station

The data in figure **5.3.3** emphasises that the sub station experienced frequency drift on the AC supply grid. The **red** graph illustrates the sub station with harmonic filters and the **black** graph represents a sub station without harmonic filters when a locomotive presents a load to the DC supply circuit.

	with filters		**without filters**	
NOLTE site	**600 Hz**	**1200 Hz**	**600 Hz**	**1200Hz**
load	1.02234784 V	1.07001403 V	51.80848 V	13.10679 V

Table 5.3.1 – The summarised results of the amplitudes at 600 and 1200 Hz for the actual measurement of Nolte DC sub station

The **yellow** sections in table **5.3.1** show the amplitude values of the actual measurements done when the sub station harmonic filters were present when a locomotive presented a load. The **yellow** region measured amplitudes for 600 and 1200 Hz are the same, this might be that the filter design consideration was to limit the actual harmonic voltage to a maximum of 1 V, thus the 600 Hz passive filter has to absorb more energy. The **orange** regions in table **5.3.1** shows the amplitudes measured for the various frequencies of interest when the harmonic filter was disabled in the sub station when a locomotive presented a load. The passive filter influence can be seen when comparing the **yellow** and **orange** regions with each other. The actual amplitudes measured in table **5.3.1** appear higher than the values on the graphs due to the fact that the graphed data was measured as peak hold root mean squared while the table data has been converted to peak values because the simulation results in chapter **4** is represented as peak values. The tabled values for the 600 and 1200 Hz components have been taken at the peak of the harmonic, although frequency drift was evident. The aim is to get the maximum value of the harmonic and not the specific value at 600 and 1200 Hz. In chapter **4** one operating condition was simulated at a time while keeping the sub station ideal, the actual measurements actually have various operating conditions playing a role.

The measured data used to evaluate the assumption made that the DC sub station can be considered as lossless when the load is not present is graphed in the section below.

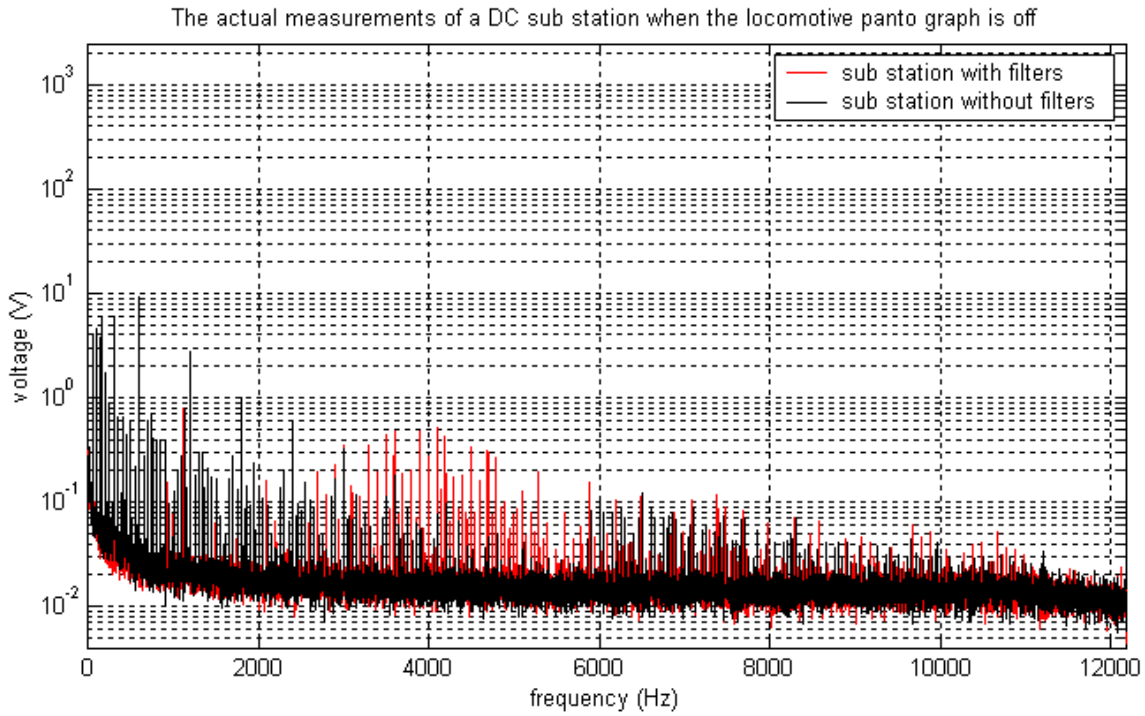

Figure 5.3.4 – The spectrum of the data obtained when the harmonic filter are included and excluded when the sub station is not presented with a load while being isolated

The **red** graph illustrates the sub station with harmonic filters and the **black** graph shows the sub station without harmonic filters. The main difference between figures **5.3.4** and **5.3.1** is that figure **5.3.4** sees a reduction in the harmonic amplitudes and density. A further observation can be made that resonance or a harmonic source exists around **4** kHz. Great care has been taken to eliminate aliasing in an attempt to eliminate the generation of false data/harmonics during sampling.

The main verifications from figure **5.3.4** with regard to figure **5.3.1** is the following:

- The generated harmonics increased with the introduction of a load (locomotive) that was assumed to be purely inductive due to the large motors. The locomotive might, in part, be responsible for the generation of more harmonics than was initially expected when the assumption was made that the load is purely inductive.
- The components that make up the rail actually act as a load even when a locomotive is not present.

- The components in the DC supply circuit operate in or very close to saturation. The fact that non periodic harmonics are generated when energy is supplied to a load (even marginal amounts with regard to normal operation) is indicative of components operating in saturation. The assumption made that the components are linear does not hold in practice based on the results obtained in figure **5.3.1** and **5.3.4**.

The zoomed graphs of figure **5.3.4** are discussed below.

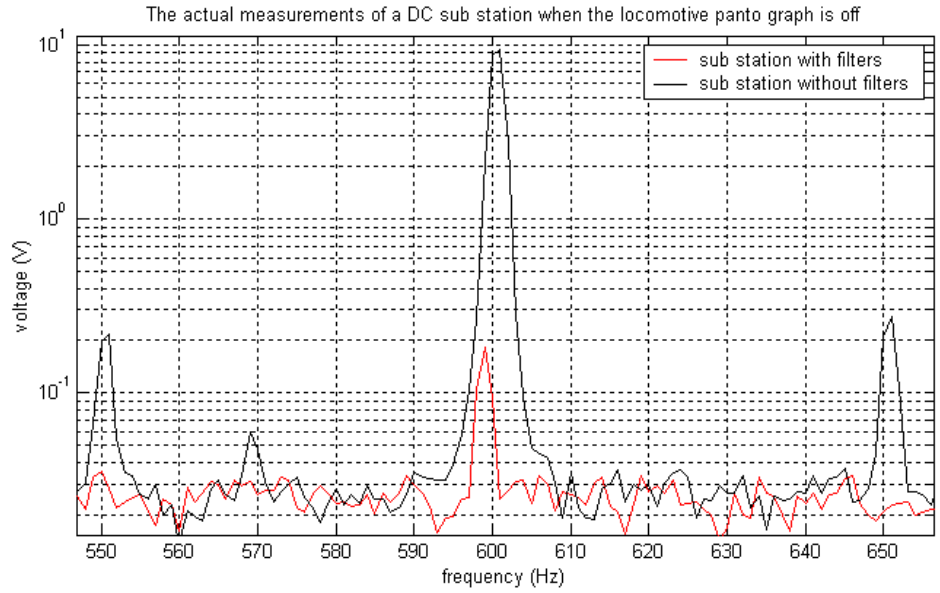

Figure 5.3.5 – The 600 Hz zoomed graph for the sub station measurement when no loads are presented to the sub station

The **red** graph on figure **5.3.5** indicates the sub station equipped with harmonic filters when the DC supply grid is not presented with a load from a locomotive. The **black** graph illustrates the measurements taken when the harmonic filters were disconnected and the sub station was not presented with a locomotive as a load. The **red** graph illustrates that the DC sub station was subjected to frequency drift on the AC supply grid. The disadvantage of measuring the sub station while frequency drift is present is that the efficiency of the passive filters actually reduce due to the filters´ inability to adapt to frequency drift, thus the filter cut-off frequency (600 Hz) no longer correlates with the actual measured frequency peak. The reason for the **black** graph being close to 600 Hz and the red graph is further is because the measurement times differ and the frequency drift changes regularly.

The **black** graph clearly shows that the harmonics of the passive rectifiers are present even when the sub station is not feeding a load. This can in part be due to the parasitic capacitances, the rail model contributing to the circuit in terms of a load and saturation of the components even during sub station idling.

The 1200Hz zoomed graph of figure 5.3.4 is presented in the following figure.

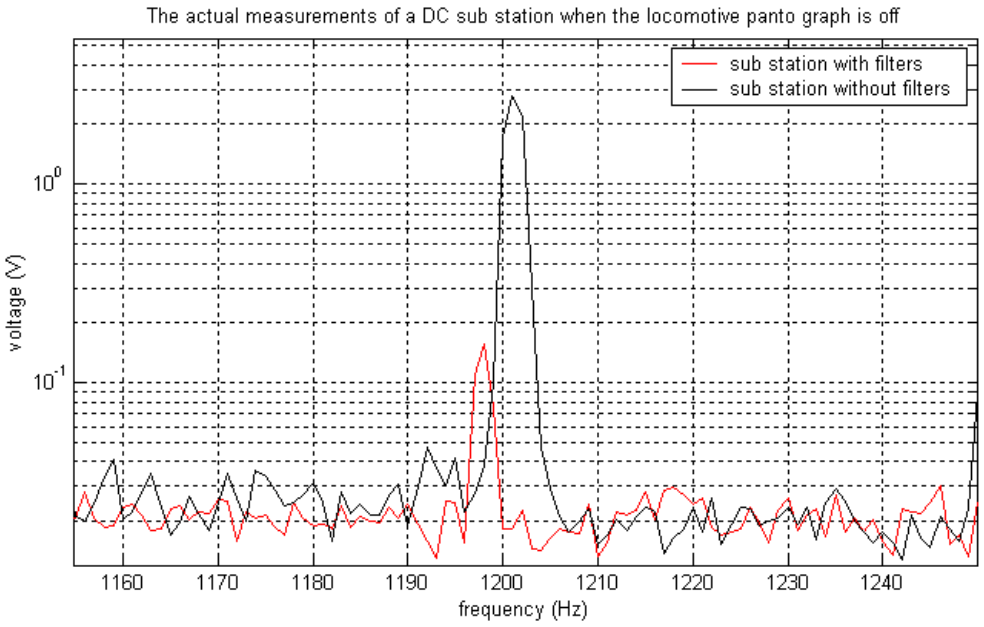

Figure 5.3.6 – The 1200 Hz zoomed graph for the sub station measurement when no loads are presented to the sub station

The red graph illustrates the sub station without a locomotive as a load when the passive harmonic filters are enabled. The frequency drift is once again evident and when looking at the data in figure 5.3.5 and 5.3.6 it is evident that the drift is less at 600 Hz than at 1200 Hz, while in theory the drift is supposed to be twice the amount for 1200 Hz than for 600 Hz.

frequency drift	
theory	actual
600 Hz	599 Hz
1200 Hz	1198 Hz

Table 5.3.2 – The table showing the extend of the frequency drift of the measured data at Nolte DC sub station

The summary of the measured data for the DC sub station at Nolte when the locomotive was not used as a load is presented below.

	with filters		without filters	
NOLTE site	**600 Hz**	**1200 Hz**	**600 Hz**	**1200Hz**
no load	0.25685994 V	0.22206504 V	13.2703 V	3.906082 V

Table 5.3.3 – The summarised results of the amplitudes at 600 and 1200 Hz for the actual measurement of Nolte DC sub station under no load conditions

The **yellow** region in table **5.3.3** shows the results for the sub station measurements when the sub station had no load from a locomotive while the harmonic filters were installed. The sub station was completely isolated, thus the only load present was the impedance of the track. The **orange** region indicates the peak of the measured amplitudes when the harmonic filters were disabled and the locomotive did not present a load to the sub station. The influence of the harmonic filters can be seen when comparing the **yellow** and **orange** region with each other. The amplitude values in table **5.3.2** is significantly larger than the values in table **5.3.3** and can be attributed to the fact that the locomotive was used as a load, the energy demand on the sub station increased and the amplitudes of the generated harmonic increased accordingly.

5.4 Conclusion

The measurement of the DC sub stations presented some problems with regard to filter tolerance information and changing sub station operating conditions, due to un-availability of documents, safety of the person and cost implications if a sub station is damaged. The other consideration was that DC sub stations are paralleled, and one faulty sub station with regards to harmonics influences the whole DC supply grid in that region. The aim of measuring the sub station is to obtain threshold data (sub station with and without harmonic filters) to calibrate the table (**4.11.1**) gathered in chapter **4** in an attempt to compensate for the factors that were not included in the simulations such as parasitic capacitance and non linear operation of components that were simulated as linear.

The actual measurements of two sub stations, Savannah and Nolte is summarised in the following table.

	with filters		without filters	
	600 Hz	**1200 Hz**	**600 Hz**	**1200Hz**
NOLTE site				
load	1.02234784 V	1.07001403 V	51.80848 V	13.10679 V
no load	0.25685994 V	0.22206504 V	13.2703 V	3.906082 V
SAVANNAH site				
load	27.8076 V	11.5362 V		
load	21.2898 V	11.9616 V		
no load	19.8198 V	3.76884 V		
no load	25.077 V	3.4191 V		
	load 1loco with filters			
	load 1loco no filters			

Table 5.4.1 – The summarised results of the amplitudes at 600 and 1200 Hz for the actual measurement of Nolte and Savannah DC sub stations when the harmonic filters are enabled and disabled.

The results obtained from Nolte sub station is considered as being the closest to ideal due to the sub station being completely isolated. The measurement at Savannah sub station was used to quantify the influence other sub stations has on the generated harmonics. Savannah sub station was not isolated from the DC supply grid. The grid is fed by sub stations employing either 6 or 12 pulse passive rectifiers.

The **green** region in table **5.4.1** indicates the lower threshold (sub station with filters) and the **red** region shows the maximum threshold (sub station without filters). When looking at the results for Savannah compared to the results of Nolte there is no relation to each other. The possibility exists that although a locomotive was not close to Savannah sub station; energy was still consumed from the sub station from locomotives even 10 km away. The obtained results for Savannah thus only show the enormity of the problem at hand - daily operation of the DC supply grid involves sub stations influencing each other due to load sharing.

The Savannah sub station results do however indicate that the distance to the load/locomotive does not have such a big impact on the measurements at the exit of the sub station. The potential drop over the track components such as the inductance and conductance is marginal due to it being paralleled with the impedance of the locomotive which is very small with regard to the equivalent track components. The influence of the locomotive is thus dominant regardless of the distance from the sub station, because the measured harmonic amplitudes are almost similar with the locomotive close to the sub station and far from the sub station.

The distance observation might be explained due to the DC grid having almost unlimited energy at its disposal from DC sub stations in the region supplying the same grid. Another possibility might be that the 6 pulse rectifier harmonic components is additive to the 600 Hz harmonic from the 12 pulse rectifier and finally that the harmonic filters in Savannah is out of specification and does not absorb the 12^{th} and 24^{th} harmonic properly anymore. The most recent survey report indicated that the harmonic filters are with specification, but the report is almost 1 year old.

Because the DC sub station at Nolte was completely isolated, the voltage drops over components were evident due to adjacent sub stations not supplementing it with energy. These actual measured results will be compared to the simulation results in chapter **6**.

CHAPTER 6: CONCLUSION AND FUTURE WORK

6.1 Introduction

The possibility of doing condition monitoring of DC sub station passive harmonic filters has been investigated in this document. The primary aim of the investigation is to measure the voltage harmonics at 600 and 1200 Hz in an attempt to make an informed decision whether the passive harmonic filters are still operational, within specification, outside specification and faulty. The secondary aim of the investigation is to diagnose possible faulty sub station components (such as diodes etc) that influence the efficiency of the filter operation. All DC sub station 600 and 1200 Hz components are thus classified based on an ideal sub station footprint for various operating conditions.

The ideal sub station has been classified in terms of literature and the assumptions made during the formulation of the ideal sub station is intended to make the simulation and modelling simpler without losing critical data. The investigation aim was to simulate operating conditions and to calibrate the simulation results with results obtained from actual measurements of a DC sub station considered as being ideal.

The investigation presented various hurdles with regard to the actual measurements of the DC sub station. The DC supply grid topology entails that the DC sub stations are parallel to each other in an attempt to share the load presented by the locomotive. The problem with this, however, is that sub station harmonics influence each other. To measure a sub station in isolation entails taking occupation of a 20 km section of track, disrupting train operation. Simulating actual operating fault conditions on actual sub stations was not allowed due to safety and cost reasons.

The aim was to measure the sub station while in service feeding the grid with the nearest load to the sub station being the measurement locomotive. The old method involves taking the sub station out of service and measuring the passive components in isolation. The ideal method entails measuring the sub station filters without entering the sub station and taking it out of service. During the investigation the voltage was measured without taking the filters out of service but the sub station was still entered for instrumentation.

6.2 Investigation findings

The ideal is to have a model, simulation and actual measurements that are the same, but in the case of the condition monitoring of passive harmonic filters the results did not match. The simulations and model were simplified by making assumptions based on literature and will be discussed later in this section.

The aim of the model development was to obtain a mathematical model describing the operation of the ideal DC sub station based on the same assumptions made for the simulations. The model was not intended to be used for the calculation of harmonic amplitudes for all the simulated operating fault conditions, as the process would have taken much longer than the object based simulation of the sub station using SIMULINK. If the approach of using the model for calculating operating conditions was adapted, a new formulation for every operating condition would have had to be formulated. The model does serve the purpose of understanding the operating principle of the DC sub station from a mathematical perspective.

The realisation is made that the sub station cannot be measured in practise by measuring the voltage harmonics at the exit of the sub station by means of a load presented by a locomotive. The main differences between theory and practise are as follows:

- The assumption was made that the components operate in their linear region, this is not the case.
- The assumption was made that the sub station is always supplied by a balanced three phase AC supply. The assumption was discredited during actual measurements.
- The load presented to the sub station by means of a locomotive cannot be considered as being purely inductive. The new fleet of locomotives employ active motor speed drives.
- The influence of the DC sub stations on each other was underestimated; locomotives in other DC sub station feeding sections influenced each other. The influence was evident at Savannah DC sub station.

The DC sub station used for actual measurement can be seen as close as possible to the ideal sub station simulated in chapter **4** of this document. The actual measured results can be compared to the simulated results as follows:

sub station condition	value simulated	value measured	simulated/measured (unit-less)
load with filter 600 Hz	**0.3295 V**	**0.25685994 V**	**1.283**
load with filter 1200 Hz	**2.16 V**	**0.22206504 V**	**9.727**
load without filter 600 Hz	**133.2263 V**	**13.2703 V**	**10.04**
load without filter 1200 Hz	**63.38 V**	**3.906082 V**	**16.226**

Table 6.2.1 – The summary of the simulated and actual measured results for the parameters of interest (600 and 1200 Hz) with the blue region representing the factor between the simulation and measurement results

The results summarised in table **6.2.1** in the blue region indicates that there is no clear factor difference between the simulation results and the actual measured results. The findings of the actual measurements and the simulation results are thus inconclusive. The only pattern that can be seen is that the 1200 Hz component factors for the sub station with and without filters are bigger than the 600 Hz component factors. The observation indicates that other factors than was thought to be dominant plays a role with regard to the higher components. The indication in figure **4.3.1.1** in comparison to figure **5.3.1** clearly shows dominant resonance in the simulations while the same result was not present during actual measurements, thus indicating that other components than what was thought as being dominant had an influence on the data. The simulated voltage harmonic amplitudes are larger than the actual measurements, indicating that the generated harmonics in practice are attenuated due to voltage drops over various components, thus discrediting the assumption made that components are lossless.

The objective of the investigation was to obtain a table such as table **4.11.1** that is calibrated with actual measurements and gives the measurement technician the ability to diagnose the sub station 600 and 1200 Hz components in an attempt to monitor the efficiency and operating status of passive harmonic filters. By obtaining the actual measured amplitudes from a table and diagnosing potential faulty sub station components, the technician can keep the sub station filters efficient and prolong the lifetime of the harmonic filter components by limiting harmonic amplitudes caused by faulty components. The investigation does not, however, give a conclusive factor for the calibration of table **4.11.1** that is populated from the simulation of critical operating conditions. The result is that it will not be possible to use the prescribed method of measurement to enable diagnosis of DC sub stations based on only measured voltage harmonics.

The outcome of the study is thus that the field of harmonic filter condition monitoring has too many unknown parameters influencing the measurements in comparison to the known parameters used for simulations. Possible reasons for the many unknown parameters is that the DC sub station cannot be isolated from the grid, the grid is comprised of the complex locomotive, the complex track sections and finally the complex AC supply grid. Making assumptions based on any of the mentioned complex "circuits" proved to be a big underestimation. The result is that the DC sub station is more complex than originally quantified and an almost infinite amount of factors can critically influence the 600 and 1200 Hz generated harmonic components.

6.3 Future work and implementation possibilities

The field of condition monitoring of DC sub station passive harmonic filters is a great concern for Transnet due to the introduction of power harmonic penalties for harmonics by utilities. Until this particular study was started the condition monitoring of passive harmonic filter components has been neglected and the harmonic filter component measurement method outdated.

The investigation covered the acquisition of voltage harmonics, but the possibility of measuring harmonic impedance by means of measuring voltage and current harmonics should be pursued. With the constraints of not being able to enter the DC sub station without taking occupation and measuring the components, other data acquisition possibilities should be investigated in an attempt to accurately do condition monitoring of the DC sub station filters. This entails the possible development of a measurement trolley that will serve as a load with known impedance.

The obtained results also indicate that further investigation needs to be done in the field of parasitic components that influence the generated harmonics of the DC sub station employed by Transnet. Known parasitic components will ensure that more unknown sub station parameters are quantified and the result will be more accurate simulations and mathematical models.

Currently the investigated method for doing condition monitoring of DC sub station passive harmonic filters cannot be used due to fact that to many unknown factors influence the measured results in comparison to the ideal simulated sub station. The investigation does, however, serve the purpose of a starting point for future work highlighting possible constraints of doing condition monitoring of passive harmonic filters in future.

The condition monitoring of passive harmonic filters opens up the possibility of monitoring the filter components more efficiently and finally ensuring that even passive harmonic filters, with proper monitoring and maintenance, can efficiently suppress 600 and 1200 Hz harmonics for prolonged periods of time.

REFERENCES

[1] S. Perera, V.J. Gosbell, B. Sneddon, *"A study on the identification of major harmonic sources in power systems"*

[2] S.J. Ranade, W. Xu, *"An overview of harmonics modelling and simulation"*, Chapter 1,

[3] R.P. Bingham, *"Harmonics – Understanding the facts"*,

[4] Hammond Power Solutions Inc, *"Zero Sequence Harmonics"*, page 1 – 3, Literature code HPS – TA 15

[5] W.M. Grady, R.J. Gilleskie, *"Harmonics and how they relate to power factor"*, Proc. of the EPRI Power Quality Issues & Opportunities Conference (PQA '93), San Diego, CA, November 1993

[6] Q. Su, K. Strunz, *"Stochastic Polynomial – Chaos – Based Average Model of Twelve – Pulse Diode Rectifier for Aircraft Applications"*, 2006 IEEE COMPEL Workshop, Rensselaer Polytechnic Institute, Troy, NY, USA, July 16 – 19, 2006, page 64 – 68

[7] K.W Louie, P. Wilson, R.A. Rivas, A. Wang, P. Buchanan, *"Discussion on Power System Harmonic Analysis in the Frequency Domain"*, 2006 IEEE PES Transmission and Distribution and Exposition Latin America, Venezuela

[8] W.M. Grady, S. Santoso, *"Understanding Power System Harmonics"*, September 1, 2001

[9] Dr. J. Kang, *"Multi – Pulse Rectifier Solutions for Input Harmonic Mitigation"*, Doc WP. AFD.02, December 1, 2005

[10] J. Pou, *"The DQ transformation – Appendix A"*, Technical University of Catalonia, page 193 – 196

[11] S. Srianthumrong, H. Akagi, *"A DC Model for Transient Analysis of a Series Active filter Integrated with a double series Diode Rectifier"*, IEEE PCC, Osaka, 2002, page 74 – 79

[12] K. Chaijarurnudomrung, K.N. Areerak, K.L. Areerak, *"Modelling of Three – phase Controlled Rectifier using a DQ – Method"*, Latest trends on applied mathematics, simulation, modelling, ISSN 1792 – 4332, ISBN 978 – 960 – 474 – 210 – 3, page 93 – 97

[13] S. Rosado, R. Burgos, F. Wang, D. Boroyevich, *"Large – and Small – Signal Evaluation of Average Models for Multi – pulse Diode Rectifiers"*, 2006 IEEE COMPEL Workshop, Rensselaer Polytechnic Institute, Troy, NY, USA, July 16 – 19, 2006, page 89 – 94

[14] Y. Hsiao, K. Lin, *"Analysis of Signals Characterization of Circuits on the Traction Power Systems*", WSEAS Transactions on Circuits and Systems, Issue 6, Volume 7, June 2008, page 569 – 578, ISSN 1109 – 2734

[15] P.C. Coles, M. Fracchia, R.J. Hill, P. Pozzobon, A. Szelag, "*Identification of Catenary Harmonics in 3 kV DC Railway Traction Systems*", IEEE, ISBN 0 – 7803 – 1772 – 6 – 94, 1994, page 825 – 828

[16] J. Li, S. Huang, J. Zhao, X. Daozhi, "*Simulation for Probabilistic Harmonic Currents of Electrical Railway Traction Substation*", IEEE, ISBN 0 – 7803 – 745 9 – 2 – 02, 2002, page 2511 – 2515

[17] G.F. Christoforidis, A.P. Sakis Meliopoulos, "*Parameters affecting the harmonic distortion in a converter substation*", IEEE Transactions on Power Delivery, Vol 6, No 4, October 1991, page 1727 – 1734

[18] P.C. Coles, M. Fracchia, R.J. Hill, P. Pozzobon, G. Sciutto, "*Modelling and simulation of supply current interference in traction systems arising from multi – level converters in high – power locomotive drives*", The European Power Electronics Association, 1993, page 24 – 28

[19] R.J. Hill, M. Fracchia, P. Pozzobon, G. Sciutto, "*A frequency domain model for 3 kV DC traction DC – side resonance identification*", IEEE Transactions on Power Systems, Vol 10, No 3, August 1995, page 1369 – 1375

[20] R.H. Wilkinson, C. Putter, J.H.R. Enslin, "*DC – side harmonic compensation in DC traction applications*", IEEE, ISSN 0 – 7803 – 3019 – 6 – 96, 1996, page 827 – 832

[21] P. Pozzobon, "*Transient and Steady – State Short – Circuit Currents in Rectifiers for DC Traction Supply*", IEEE Transaction on Vehicular Technology, Vol 47, No 4, November 1998, page 1390 – 1404

[22] A. Prudenzi, "Estimation of Electrical Traction Load Harmonic Impact on Distribution Networks", IEEE, ISSN 0 – 7803 – 7989 – 6 – 03, 2003, page 1166 – 1171

[23] S.H. Hosseini, F. Shahnia, M. Sarhangzadeh, E. Babaei, "*Power Quality Improvement of DC Electrified Railway Distribution Systems Using Hybrid Filters*", page 1273 – 1277

[24] L. Zhou, Q. Fu, X. Li, C. Liu, "*A Novel Multilevel Power Quality Compensator for Electrified Railway*", IEEE IPEMC, ISSN 978 – 1 – 4244 – 3557 – 9 – 09, 2009, page 1141 – 1147

[25] A. Sikora, B. Kulesz, "*Influence of Diode Commutation Processes on Rectifier Transformers Operation"*, IEEE XIX International conference on Electrical Machines – ICEM 2010, Rome, ISSN 978 – 1 – 4244 – 4175 – 4 – 10 , 2010

[26] K.L. Lian, B.K. Perkins, P.W, Lehn, "*Harmonic Analysis of a Three – Phase Diode Bridge Rectifier based on Sampled Data Model*",

[27] S. Fassbinder, "*Power Quality Application Guide – Harmonics Passive Filters*", Leonardo Power Quality Initiative, Copper Development Association – IEE endorsed provider, section 3.3.1, June 2003, page 1 – 8

[28] F. Zheng Peng, H. Akagi, A. Nabae, "*A New Approach to Harmonic Compensation in Power Systems – A Combined System of Shunt Passive and Series Active Filters*", IEEE Transactions on Industry Applications, Vol 26, No 6, November – December 1990, ISSN 0093 – 9994 – 90 – 1100 – 0983, page 983 – 989

[29] Dr. S.A. Qureshi, G. Murtaza Hashmi, "*Power Factor Improvement in Harmonically Polluted Power System and Design of Harmonic filter*", Australasian Universities Power Engineering Conference (AUPEC 2004), 26 – 29 September, Brisbane Australia

[30] I. Daut, H.S. Syafruddin, R. Ali, M. Samila, H. Haziah, "*The Effects of Harmonic Components on Transformer Losses of Sinusoidal Source Supplying Non – Linear Loads*", American Journal of Applied Sciences, ISSN 1546 – 9236, 2006 Science Publication, page 2131 – 2133

[31] Y. Liu, Z. Wang, "*Modelling of Harmonic Sources – Magnetic Core Saturation*",

[32] T. Rechberger, "*Experimental Analysis of the Line Side Behaviour of an Uncontrolled 12 – Pulse Rectifier with Capacitive DC – Smoothing Compared to Analytical Analysis*",

[33] K.M. Hink, "*Harmonic Mitigation of 12 – pulse Drives with Unbalanced Input Line Voltages*", page 1- 6

[34] D.A. Rendusara, A. von Joanne, P.N. Enjeti, D.A. Paice, "*Design Considerations for 12 – Pulse Diode Rectifier Systems Operating under Voltage Unbalance and Pre – Existing Voltage Distortion with Some Corrective Measures*", IEEE Transactions on Industry Applications, Vol 32, No 6, November – December 1996, ISSN 0093 – 9994 – 96, page 1293 – 1303

[35] Y. Nishida, M. Nakaoka, "*A New Harmonic Reducing Three – Phase Diode Rectifier for High Voltage and High Power Applications*", IEEE, ISSN 0 – 7803 – 4067 – 1 – 97, 1997, page 1624 – 1632

[36] W.J. Sarjeant, F.W. MacDougall, D.W. Larson, I. Kohlberg, "*Energy Storage Capacitors: Aging and Diagnostic Approaches for Life Validation*", IEEE Transactions on Magnetics, Vol 33, No 1, ISSN 0018 – 9464 – 97, January 1997

[37] G.C. Montanari, D. Fabiani, "*The Effect of Non – sinusoidal Voltage on Intrinsic Aging of Cable and Capacitor Insulating Materials*", IEEE Transactions on Dielectrics and Electrical Insulation, Vol 6, No 6, ISSN 1070 – 9878 – 99, December 1999

[38] M. Pompili, C. Mazzetti, R. Bartnikas, "*Partial Discharge Behaviour in Switching-Surge-Aged Oil-Paper Capacitor Bushing Insulation*", ISSN 1070-9878/1, 2002 IEEE, page 104 – 111

[39] C.F. Schecckle, "*Traction Power Supplies Handbook*", South African Transport Services Electrical Engineering Department, specification CEE.0172.86, December 1986

[40] Dr. W. le Roux (2010), "*readsections.vi*", LABVIEW 8.6, National Instruments, development of the program was done for Transnet EMC, the program can be found on request to Wiehan.LeRoux@transnet.net

[41] Suriadi, "*ANALYSIS OF HARMONICS CURRENT MINIMIZATION ON POWER DISTRIBUTION SYSTEM USING VOLTAGE PHASE SHIFTING CONCEPT"*, Thesis submitted in fulfilment of the requirements for the degree of Master of Science, June 2006

[42] B.M. Steyn, "*ELEKTROMAGNETIESE MODELLE VIR SPOORBAANSTELSELS VAN DIE SUID-AFRIKAANSE VERVOERDIENSTE*", Master of Science investigation, Randse Afrikaanse Universiteit, Novemeber 1987, chapter 8, page 142

[43] P.G. Breedt, W. le Roux, H.J. Fourie, B.M. Steyn, " *19E AC and DC EMC signal acceptance testing*", Technology Management, Transnet, BBB 6800 version 1, July 2011, page 24 – 29

[44] N. Mohan, T.M. Undeland, W.P. Robbins, "*POWER ELECTRONICS – Converters, Applications, and design*", second edition, John Wiley and Sons Inc, 1995, Chapter 27, page 669 – 693

APPENDIX

In Chapter **4** the MATLAB code for the SIMULAINK simulation that has been done. The SIMULINK simulation data is time based and the frequency data was needed. Every operating condition from chapter **4** has been graphed using the template below

```
clear;
%THE PROGRAM COMPUTES THE FFT OF THE CONTINIOUS SAMPLED DATA
load vnf.mat;
load vwf.mat;
% for Vnf where nof stands for no filter
    vx = vnf(:,1);
    vy = vnf(:,2);
    %[vx,vy] = unique(vx);
    xi = 0.2:1/40000:1.2;
    vyi = interp1(vx,vy,xi);
    vY = fft(vyi);
    vYY = abs(vY(1:10000))./3.6338e+004;
    frek = 0:1:9999;
% for Vwf where nof stands for with filter
    v1x = vwf(:,1);
    v1y = vwf(:,2);
    %[vx,vy] = unique(vx); % the function eleimates doubles
    x1i = 0.2:1/40000:1.2; %need one second of data to ensure that the frequency
spacing will be exact, thus 40kHz
    v1yi = interp1(v1x,v1y,x1i);
    v1Y = fft(v1yi);
    v1YY = abs(v1Y(1:10000))./3.6338e+004; %FFT only half the data is used the rest is
mirrored
    frek1 = 0:1:9999;
subplot(3,1,1);
semilogy(frek,vYY);
hold on;
semilogy(frek1,v1YY,'-r');
grid on;
title('The ideal DC sub station where the station footprint is obtained');
xlabel('freq (Hz)');
ylabel('logscale voltage (V)');
legend('without wave filter','with wave filter');
```

```
subplot(3,1,2);
semilogy(frek,vYY);
hold on;
semilogy(frek1,v1YY,'-r');
axis([595 605 0 2e2]);
grid on;
title('The ideal DC sub station where the station footprint is obtained');
xlabel('freq (Hz)');
ylabel('logscale voltage (V)');
legend('without wave filter','with wave filter');
subplot(3,1,3);
semilogy(frek,vYY);
hold on;
semilogy(frek1,v1YY,'-r');
axis([1195 1205 0 2e2]);
grid on;
title('The ideal DC sub station where the station footprint is obtained');
xlabel('freq (Hz)');
ylabel('logscale voltage (V)');
legend('without wave filter','with wave filter');
```

The code has further been adapted for graphing the various simulation outputs, but the code above serves as the template. The object based programming code of the data acquisition software is shown below. The programming was done in LABVIEW 8.6 from National Instruments.

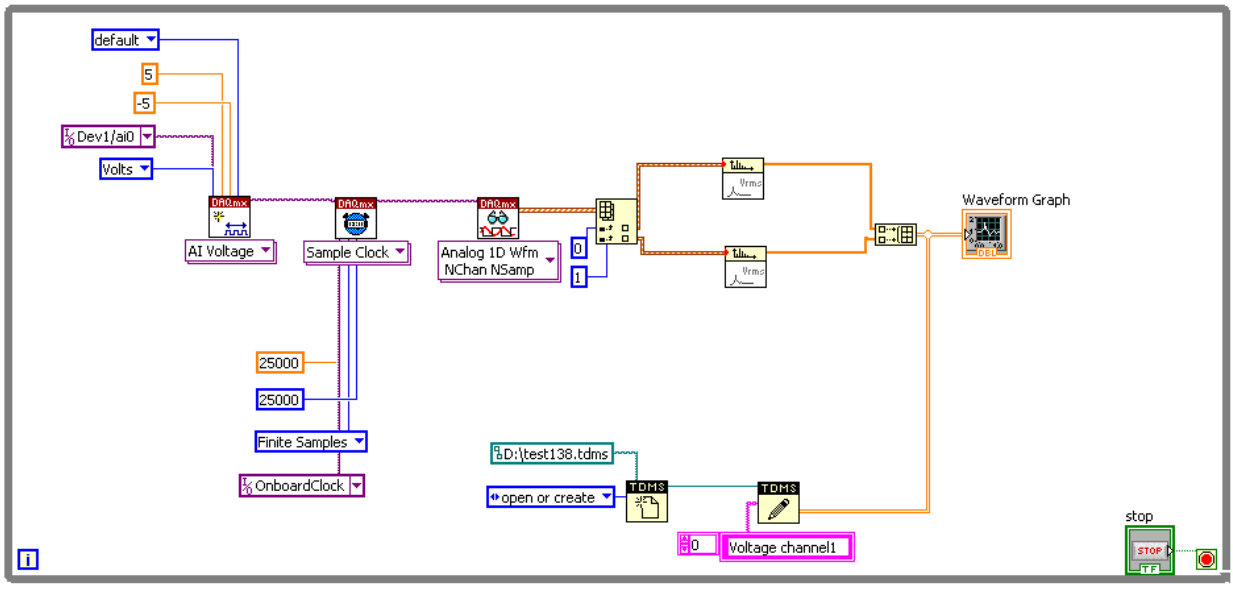

The display of the program is simple. The data is sampled, stored and then displayed as a frequency spectrum during the recording process. The method of sampling used is peak hold and the sampling frequency is 25 kHz. The saved file extensions are *.tdms* and the extraction of the data is done via a "*readsections.vi*" [40]. Once conversion from .tdms to .txt is done the data is graphed with MATLAB.

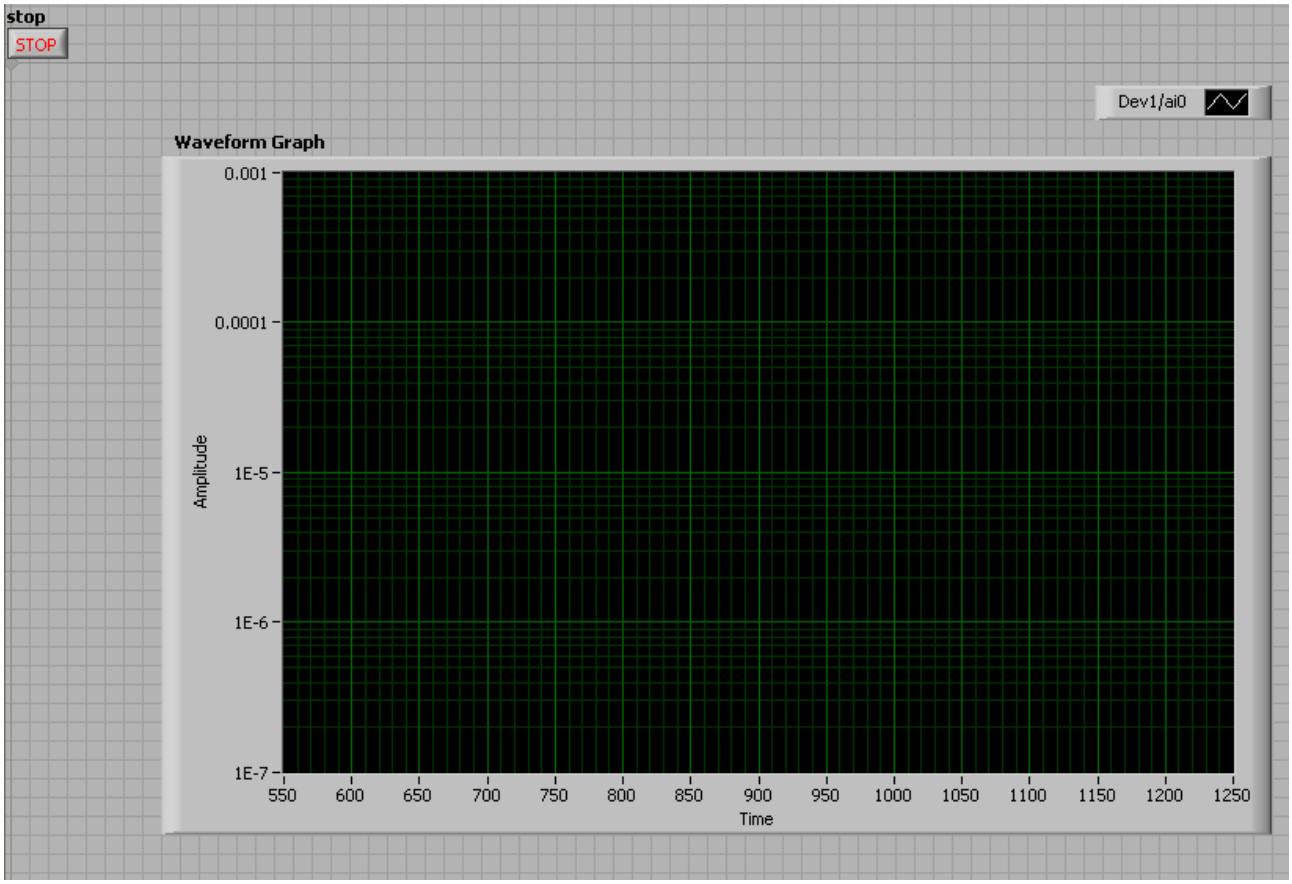

The MATLAB code used for the graphing of the actual measured data follows:

```
clear;
%the graphing of the data for the actual measurements
load toets131PD.txt;
load toets132PD.txt;
load toets133PD.txt;
load toets134PD.txt;
load toets135PD.txt;
load toets136PD.txt;
load toets137PD.txt;
x = 0:1:12499;
%the no load testing with and without filters
```

```
%panto af
PD11 = (toets131PD.*6938.4)'; %with filters with 6938.4 the PD multiplication factor
PD1 = PD11(:,1);
PD51 = (toets135PD.*6938.4)'; %without filters
PD5 = PD51(:,1);
%panto op
PD21 = (toets132PD.*6938.4)'; %with filters
PD2 = PD21(:,1);
PD61 = (toets136PD.*6938.4)'; %without filters
PD6 = PD61(:,1);
figure (1);
semilogy(x,PD1,'-r');
hold on;
semilogy(x,PD5,'-k');
hold off;
grid on;
title('The actual measurements of a DC sub station when the locomotive panto graph is
off');
xlabel('frequency (Hz)');
ylabel('voltage (V)');
legend('sub station with filters','sub station without filters');
figure (2);
semilogy(x,PD2,'-r');
hold on;
semilogy(x,PD6,'-k');
hold off;
grid on;
title('The actual measurements of a DC sub station when the locomotive panto graph is
up');
xlabel('frequency (Hz)');
ylabel('voltage (V)');
legend('sub station with filters','sub station without filters');
```